## LICENCE TO McMASTER UNIVERSITY

This Thesis has been written
[Thesis, Project, Report, etc.]

by Michelle Susanne Larson for
[Full Name(s)]

Undergraduate course number 4K06 at McMaster University

under the supervision/direction of Drs. J.H Crocket and W.A. Morris.

In the interest of furthering teaching and research, I/we hereby grant to McMaster University:

1. The ownership of 6 copy(ies) of this work;
2. A non-exclusive licence to make copies of this work (or any part thereof) the copyright of which is vested in me/us, for the full term of the copyright, or for so long as may be legally permitted. Such copies shall only be made in response to a written request from the Library or any University or similar institution.

I/we further acknowledge that this work (or a surrogate copy thereof) may be consulted without restriction by any interested person.

J.H Crocket
Signature of Witness, Supervisor

M. Larson
Signature of Student

W.A. Morris

29 April 94
date

(This licence to be bound with the work)

# GEOPHYSICAL RESPONSE OF SULFIDE-POOR PGM-BEARING MAFIC-ULTRAMAFIC ROCKS

# Geophysical response of sulfide-poor PGM-bearing mafic-ultramafic rocks: example of the Boston Creek Flow, Abitibi greenstone belt, Ontario

By

**Michelle Susanne Larson**

A Thesis

Submitted to the Faculty of Science

in Partial Fulfilment of the Requirements

for the Degree

Honours Bachelor of Science

McMaster University

April, 1994

Bachelor of Science 1994
Honours Geology Specialist

McMaster University
Hamilton, Ontario

TITLE: Geophysical response of sulfide-poor PGM-bearing mafic-ultramafic rocks: example of the Boston Creek Flow, Abitibi, Ontario.

AUTHOR: Michelle Susanne Larson

SUPERVISORS: Drs. W.A. Morris and J.H. Crocket

NUMBER OF PAGES: 123, i-ix

## Abstract

Sulfide-poor platinum-group element (PGE) mineralization occurs within the Archean Boston Creek Flow ferropicrite, Abitibi greenstone belt, Canada. The PGE mineralization ($\Sigma$PGE+Au = up to 1000 ppb) is manifest as metre-scale platinum-group mineral-bearing pods of disseminated chalcopyrite and pyrite ($<1$ modal%) within titaniferous magnetite-rich gabbroic rock at the base of its central gabbroic layer. This mineralization is distinct in character from well known PGE mineralization associated with massive Fe-Ni-Cu sulfides at the base of komatiite flows at Kambalda, Western Australia and elsewhere. Exploration strategies presently used to search for PGE in mafic and ultramafic volcanic rock terrains are based on the geological and geophysical characteristics of sulfide-rich PGE mineralization. Consequently, refinements in exploration strategies are required if economic concentrations of sulfide-poor PGE mineralization are to be discovered in volcanic terrains.

To begin development of such exploration criteria, ground-based magnetic and VLF surveys were conducted over the PGE mineralization along a single cross-section through the BCF. Drill core samples were collected along this transect to characterize the volume magnetic susceptibility and natural remanent magnetization (NRM) of the mineralization. Magnetic highs ranging in intensity from 64000 to 65000 nT were recorded for the base of the gabbroic layer, including mineralized outcrops. Susceptibilities of up to 9700 cgs and high remanence values with variable directions were determined. VLF, as expected, was not useful in identifying the mineralized horizons. The peridotite at the base of the flow appears to be the only conductive rock in the BCF.

The magnetic highs associated with the base of the gabbroic layer define a positive anomaly that appears to be podiform in outline and up to ten metres in maximum dimension. This result suggests that the titaniferous magnetite-rich rock is itself podiform, like the enclosed PGE mineralization. This magnetic anomaly is not extensive enough to be evident on a regional scale aeromagnetic map as a separate anomaly within the BCF, and is not evident through VLF techniques. The rocks hosting the PGE mineralization is defined by the paleomagnetic results but this is not a practical field method.

The geophysical characterization of the PGE mineralization host rocks, and of the BCF in general, demonstrates the potential of detailed magnetic and susceptibility mapping, together with petrographic and petrologic studies, in the search for economic PGE concentrations of sulfide-poor PGE mineralization in other volcanic and possibly plutonic rocks as well. Specifically, the results suggest that podiform magnetic anomalies within titaniferous magnetite-rich pyroxenites and gabbroic rocks may have potential use in the exploration for economic sulfide-poor PGE mineralization. Although the paleomagnetic methods used in this study are probably not of direct use in exploration, they were able to distinguish the different lithologies in the BCF. This substantiates the results of the susceptibility measurements in characterizing PGE mineralized, titaniferous magnetite-bearing rocks. The results of the paleomagnetic study also show that the NRM of the Ghost Range intrusive complex is not primary and therefore the Archean apparent polar wander path as it is currently defined is incorrect.

## Acknowledgements

The research was funded by a Natural Sciences and Engineering Research Council of Canada Strategic grant to Drs. J.H. Crocket and M.E Fleet.

Assistance and support from Drs. Bill Morris, Jim Crocket and Dave Good was greatly appreciated. Thanks Bill, I've never done field work in a BMW - it was quite an experience! Ken Versteeg, Scott Smith, Edna Meuller and Susanne Manning were also very helpful, especially when all I had was visions of spinifex and platinum-group metals dancing in my head. I am grateful for Mike Bersch's assistance at the University of Alabama with my probe work. Special thanks go to my parents for putting up with me (especially the past four years). Most of all, I am deeply indebted to Bill Stone for his unending patience and friendship. Without his help and understanding this work would not have been possible with out me loosing all my hair or having fun.

## Table of Contents

## List of Figures

## List of Tables

# Chapter 1

## General Introduction

### *1.1 Purpose*

Platinum-group elements (PGE) are generally associated with high concentrations of Fe-Ni-Cu sulfides. Therefore, in a sulfide-poor environment, a geologist is likely to miss a potentially PGE mineralized horizon. On the basis of little or no sulfide present in outcrop, one would literally *walk right over* the mineralization. However, once a sulfide-poor body is known to possess PGE, certain lithologic and structural features can be used to identify potentially mineralized sites. PGE mineralization is often hosted within thick, differentiated mafic to ultramafic flows or layered intrusions, such as the Salt Chuck Intrusion, Alaska (Postle et al., 1986). Typically, the mineralization is stratabound, and may be associated with large concentrations of primary titaniferous magnetite. Large scale magnetic anomalies may therefore be associated with these types of deposits. From an exploration point of view, it is critical to be able to distinguish geophysically between a rock rich in titaniferous magnetite and a serpentinized peridotite, for example. Both rock types would have a large positive magnetic anomaly associated with them. A question addressed in this thesis is whether or not rock types hosting PGE mineralization associated with high concentrations of titaniferous magnetite can be distinguished from strongly magnetic, unmineralized rocks based on their geophysical signatures alone.

The main purpose of this project was to test for any magnetic and/or electromagnetic responses which could be important in delineating PGE mineralized horizons within a

FIGURE 1. Regional geology of the Boston Creek area (modified after Stone et al., in review).

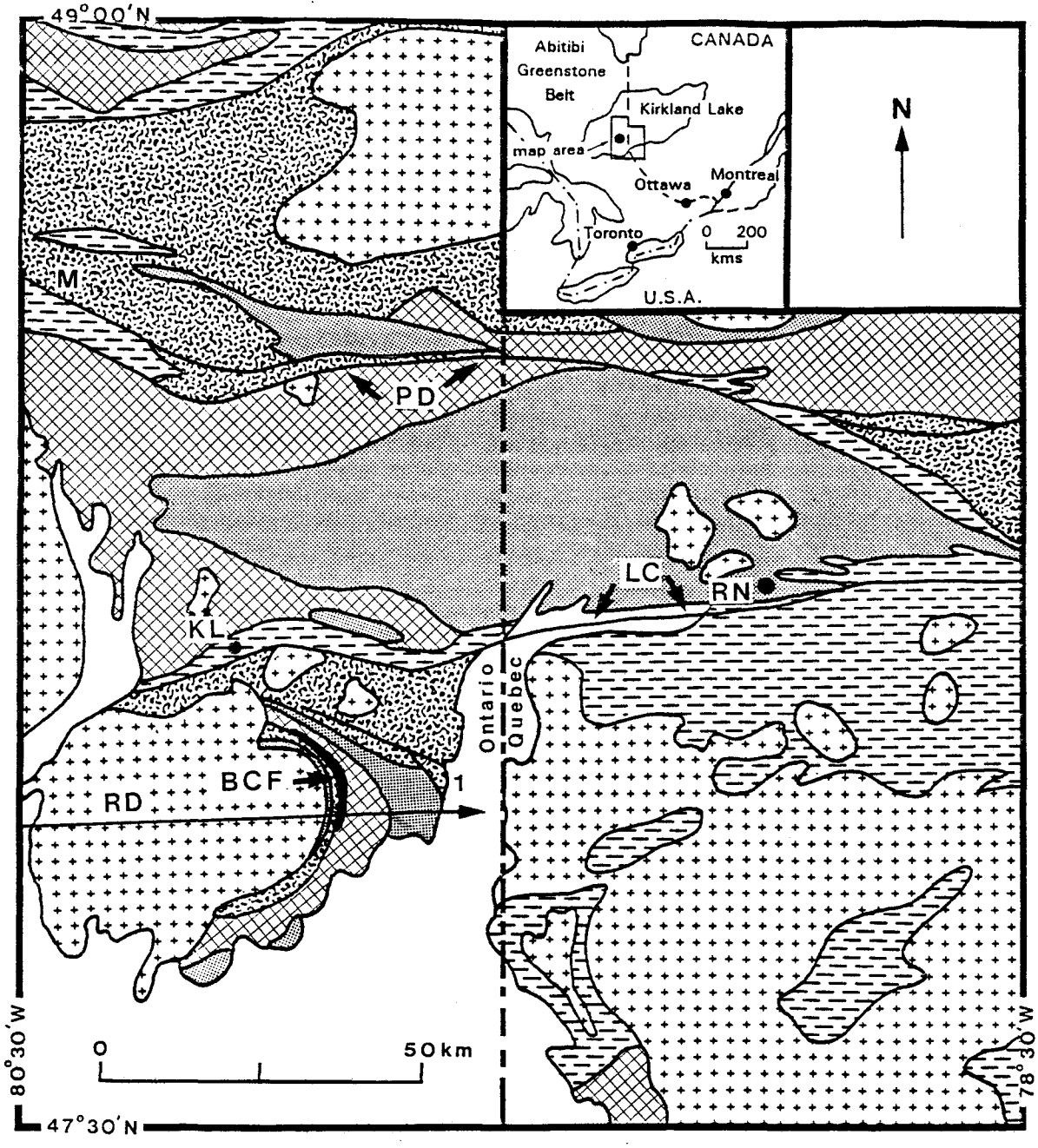


LEGEND

Proterozoic

Intrusive rocks and sedimentary rocks

Archean

Felsic Intrusions

Metasedimentary rocks

Intermediate - felsic calc - alkalic metavolcanic rocks

Mafic metavolcanic rocks

Mafic - ultramafic, tholeiitic and komatiitic metavolcanic rocks

EXPLANATION

| | |
|---|---|
| M | Munro Township |
| KL | Kirkland Lake |
| RN | Rouyn - Noranda |
| 1 | Lincoln - Nipissing fault zone |
| LC | Larder - Cadillac fault zone |
| PD | Porcupine - Destor fault zone |
| RD | Round Lake dome |
| BCF | Boston Creek Flow |
| → | plunge direction |

FIGURE 2. Boston Creek Flow road access and study area location.

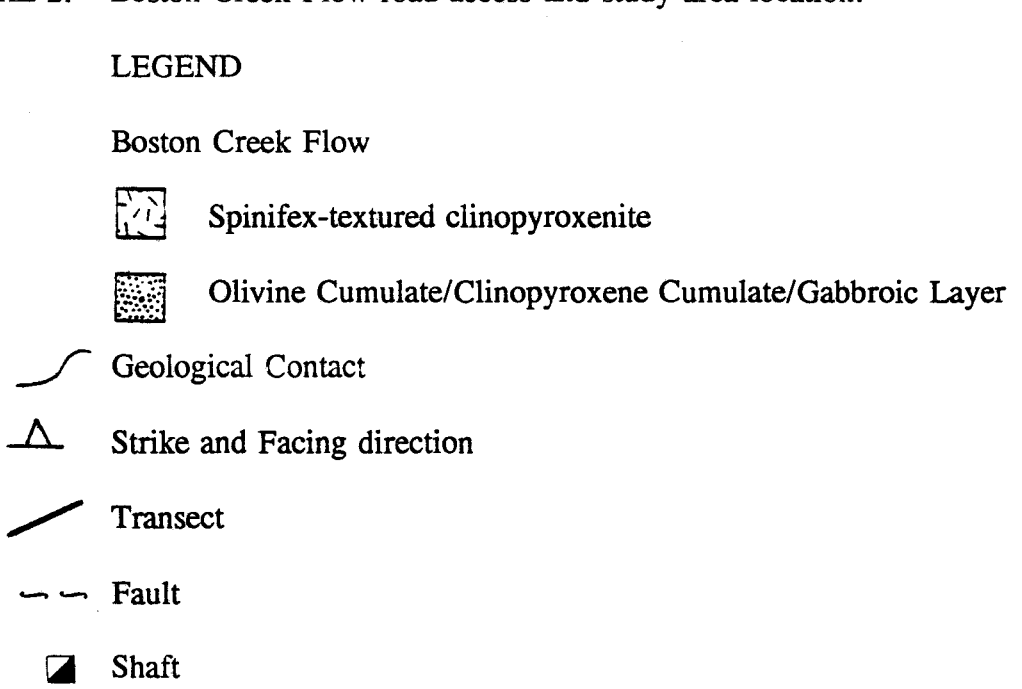

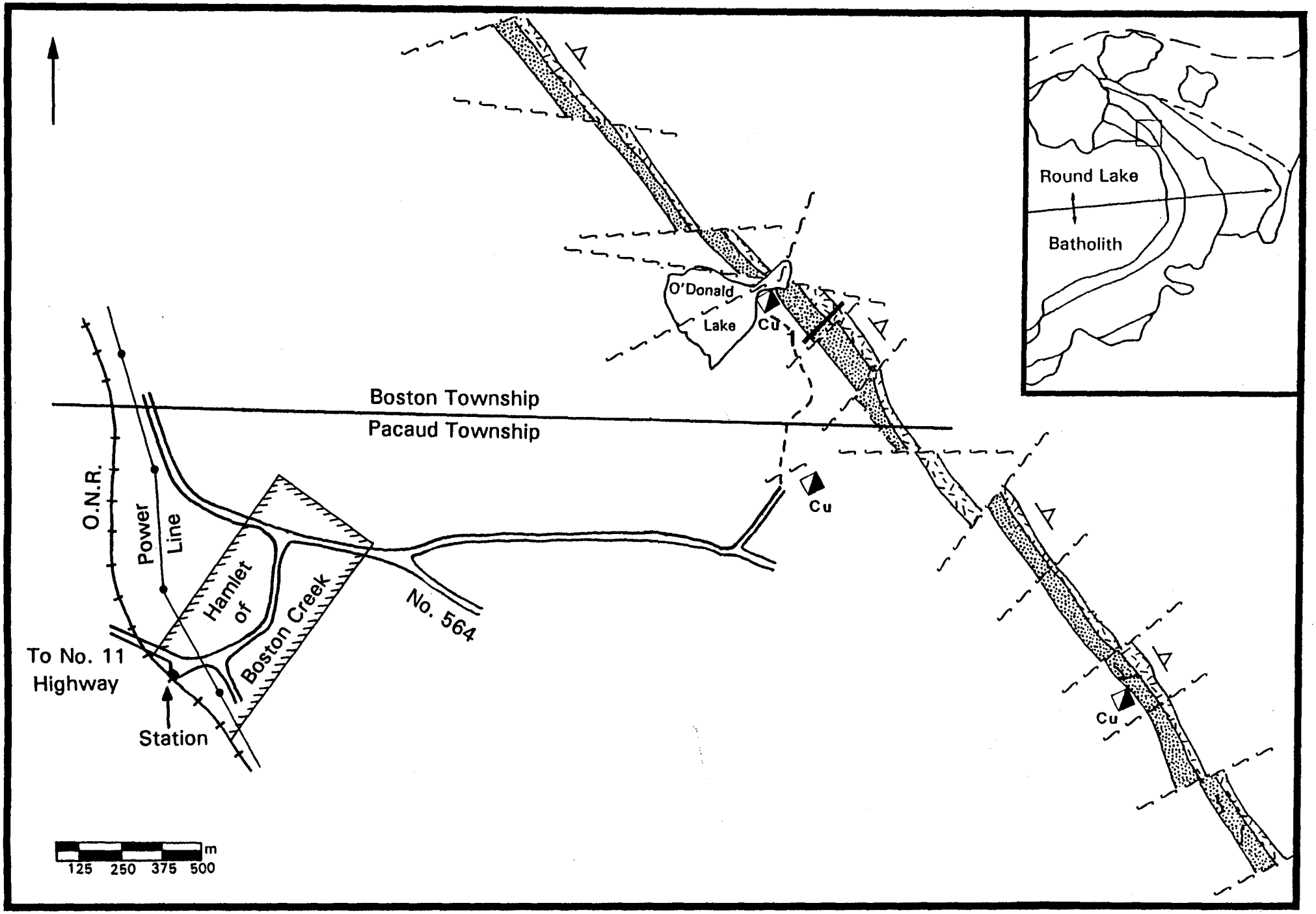
Round Lake
Batholith
O'Donald
Lake
Cu
1
Boston Township
Pacaud Township
Cu
O.N.R.
Power
Line
Hamlet
of
Boston Creek
No. 564
To No. 11
Highway
Station
Cu
m
125 250 375 500

strongly magnetic, sulfide-poor, non-serpentinized body. A second objective was to investigate the use of paleomagnetic methods in determining the history of a strongly magnetic Archean body. The usefulness of these Archean rocks in the reconstruction of the 2.7 billion year apparent polar wander path was also considered.

A differentiated ferropicrite, near Kirkland Lake, Ontario is used here as an example of a sulfide-poor, PGM bearing body, which has undergone serpentinization. Stone et al. (1992, 1993) reported the discovery of sulfide-poor, PGE mineralization hosted in the clinopyroxenite cumulate and gabbro layers of the Boston Creek Flow (BCF). The mineralization occurs as podiform zones of rare Pt, Pd and Rh minerals and a suite of gold and silver minerals in spatial association with sparsely disseminated chalcopyrite and titaniferous magnetite. The mineralization appears to be uneconomic, but is of interest because of its volcanic setting and similarity in character to reef-type mineralization (eg. Vermaak and Hendriks, 1976; Volborth et al., 1985).

Samples from the major lithologic layers of the BCF, were collected for the purpose of characterizing the natural remanent magnetization and volume susceptibility of the flow rocks. Ground magnetics and very low frequency electromagnetic (VLF) surveys were also performed along one transect across the BCF. The geophysical characterization of the platinum-group occurrences in the BCF will serve to establish and refine exploration criteria for use in geologically similar environments within the Abitibi greenstone belt and elsewhere.

*1.2 Location and Access*

The BCF crosses the boundary between Boston and Pacaud townships, 20 km south of the town of Kirkland Lake, in northeastern Ontario (Fig. 1). The study area of the BCF is between 79°50'-80°10' longitude and 47°50'-48°15' latitude, located approximately 1.5 km northeast of the hamlet of Boston Creek, in the O'Donald Lake area, (Fig. 2). This area was chosen for study because the flow is thickest here, well exposed, hosts PGM and is easily accessible by four-wheel drive vehicle from Highways 11 and 564 and several bush roads.

*1.3 Previous Work*

The Boston Creek area was first mapped and surveyed by McOuat (1872). Following the discovery of the Boston iron range, the area was remapped by Miller (1905). The Larder Lake gold rush of 1906 to 1907 led to intense gold, copper and iron prospecting in the Boston Township area. Barry Hollinger Gold Mines Ltd. held property in the BCF area (Patricia property in Pacaud Township). Work on the Hollinger prospect ended in 1936. The Bargnesi family of Boston Creek sank two shafts and established a small copper mining and milling operation along the road to O'Donald Lake (Fig. 2) in the mid 1950's. Bargnesi Mines Ltd. ceased operation in 1967.

To assist the exploration and mining activities, the Boston Creek area was remapped by Burrows and Hopkins (1916, 1921), Bell (1929), and later by Lawton (1959). These workers considered Boston Township to be underlain mainly by Keewatin (Archean) pillow basalts, and mafic sills and dykes. Lawton (1957) mapped the BCF as a Proterozoic layered

sill, specifically as a Haileyburyian Sill. Goodwin (1965), Goodwin and Ridler (1970), and Ridler (1969, 1970, 1975) mapped the area as a stratigraphic succession of low-K tholeiitic pillow basalts with associated gabbroic sills. Ridler (1970) included these within a stratigraphic unit called the Catharine Basalts. The distribution of regional and contact metamorphic mineral assemblages in the area has been documented by Jolly (1974, 1975, 1977a, 1977b, 1978, 1980).

Jensen (1978, 1985a) was the first to recognize some of these rocks, including the BCF, as komatiites rather than basalts. He distinguished them from the Catharine Basalts and included them in the Wabewawa Group. On the basis of a preliminary study, Jensen was also the first to recognize the iron-rich geochemical composition of the BCF. Stone (1985) and Stone et al. (1987) interpreted the BCF as a thick, differentiated mafic-ultramafic lava with some petrographic similarities to layered komatiitic and tholeiitic flows in the Abitibi greenstone belt at Munro Township. They also showed that the flow is characterized by unusually high iron and low alumina compared to other mafic and ultramafic rocks of similar magnesium content in the belt. Jackson and Harrap (1989) and Jackson and Fyon (1991) reinterpreted the geologic section of the BCF area to be structurally disrupted and questioned previous interpretations for the area.

Stone et al. (1992, 1993) reported the discovery of Pt and Pd minerals within the BCF. Xie et al. (1993) characterized HFSE/REE fractionation patterns for a komatiite-tholeiite sequence that may be in the BCF area and, on this basis, proposed regional

petrogenetic processes, including magma generation in conjunction with rising plume sources. More recently, Stone et al. (1994 submitted), have re-interpreted the unusual geochemical composition of the BCF to indicate that it is ferropicritic in composition and tholeiitic rather than komatiitic in affinity.

### *1.4 Methodology*

The field work for this project was done from May 18 to 22, 1993. A grid was established by pace and compass along a transect perpendicular to the flow, approximately 110 m south of O'Donald Lake (Fig. 2). The grid consisted of five lines, 115 m in length. Ground magnetic and VLF surveys were performed along each of the lines. Sixty-one, 2.4 cm diameter, oriented drill core samples were taken along line 0E for magnetic susceptibility and paleomagnetic studies. Polished sections were prepared from selected thin sections and the oxide minerals in them were analyzed by electron microprobe techniques at the University of Alabama.

# Chapter 2

## Geology of the Area

### *2.1 Regional Geology*

The geology of the BCF area has been described in detail by Jensen (1985b) and Stone et al. (1987). The BCF is part of a steeply dipping and outward facing ultramafic to felsic volcanic rock succession exposed in the Round Lake dome, to the east of the Round Lake Batholith ($\approx$2690 Ma; Corfu et al., 1989) (Fig. 3). Traditionally, the volcanic succession, from bottom to top, has been considered to be the komatiitic Wabewawa Group, tholeiitic Catharine Group, and calc-alkalic Skead Group (Jensen, 1985; Stone et al., 1987). In that stratigraphic scheme, the BCF (2720 $\pm$2 Ma; Corfu and Noble, 1992; Corfu, 1993) was considered to be komatiitic in affinity and to occur at the top of the Wabewawa Group. Recently (eg. Jackson and Harrap, 1989; Jackson and Fyon, 1991), it was argued that komatiitic rocks comprise only a small proportion of the volcanic succession. In this framework, the BCF and Wabewawa basalts were each given an informal, "formation" status within the Catharine Group. The recent recognition of the BCF as ferropicritic favours the stratigraphic scheme of Jackson and Harrap (1989), with a few modifications.

The volcanic rock succession which mantles the Round Lake dome was regionally metamorphosed to prehnite-pumpellyite facies (Jolly, 1980). The subsequent intrusion of the Round Lake Batholith resulted in the folding, faulting and contact metamorphism to greenschist facies of the volcanic succession, including the BCF. Transverse faults offset the flow left-laterally and are spatially associated with quartz vein-hosted copper mineralization.

FIGURE 3. Location and geology of the Boston Creek Flow (modified after Goodwin, 1965; Jensen, 1985; Stone et al., 1987).

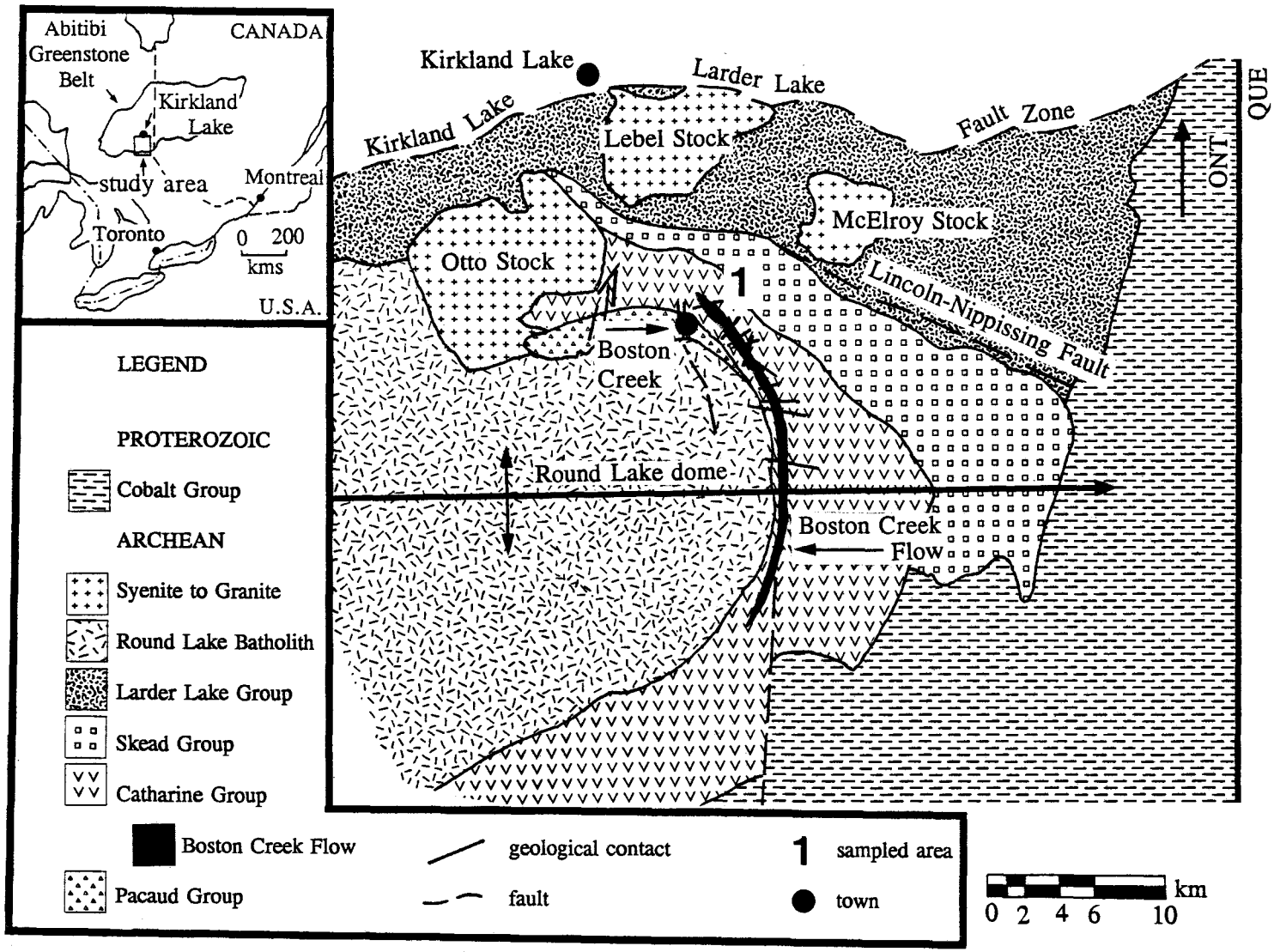
Abitibi Greenstone Belt
CANADA
Kirkland Lake
study area
Montreal
Toronto
0 200
kms
U.S.A.
Kirkland Lake
Larder Lake
Kirkland Lake
Lebel Stock
Fault Zone
ONT
QUE
McElroy Stock
Otto Stock
1
Lincoln-Nippissing Fault
Boston Creek
Round Lake dome
Boston Creek Flow
LEGEND
PROTEROZOIC
Cobalt Group
ARCHEAN
Syenite to Granite
Round Lake Batholith
Larder Lake Group
Skead Group
Catharine Group
Boston Creek Flow
Pacaud Group
geological contact
fault
1 sampled area
town
km
0 2 4 6 10

*2.2 Flow Geology and Rock Types*

The BCF strikes 315°NW, with subvertical to vertical dip, is traceable by outcrop for approximately 5 km and on government aeromagnetic maps for at least 15 km (OGS 1979). It varies in thickness from 45 to 90 m (Jackson and Harrap, 1985; Stone et al., 1987). Geochemically, the flow is characterized by higher iron (15 to 25 wt% FeO*) and lower alumina ($Al_2O_3/TiO_2$ = 6) contents compared to other mafic and ultramafic rocks of similar magnesium content in the Abitibi greenstone belt (Stone et al., 1987). This unusual geochemical composition of the BCF is primary and appears to be somewhat similar to that of Proterozoic-aged ferropicrite flows at Pechenga, Russia (cf. Hanski and Smolken, 1989; Hanski, 1992), suggesting that the BCF is ferropicritic in composition and tholeiitic, rather than komatiitic in nature (Stone et al., 1994 submitted). Previously described as an Al-depleted komatiitic basalt, the BCF is now believed to have evolved from a picritic liquid based on $TiO_2$, FeO, and MgO content. The Ti and Fe values for a fixed MgO content are much too high to suggest a komatiitic origin for the BCF. The distinction of being a ferropicrite rather than a picrite (eg. Theo's Flow, Munro Township, Ontario) is based on the extreme iron enrichment.

The geologic section (Fig. 4) along the surveyed transect across the BCF consists of altered aphanitic pyroxenite at the chilled margins and four internal layers including spinifex-textured clinopyroxenite, gabbroic rocks, clinopyroxene cumulate and olivine cumulate from stratigraphic top to bottom. The rock types have been described in detail (Stone et al., 1987, 1994 submitted) and their characteristics are noted in Table 1. In summary: 1) olivine

FIGURE 4. Idealized geologic column along the transect through the Boston Creek Flow. FM = footwall mineralization, MM = main mineralization. Section location indicated by "1" in Figure 3.

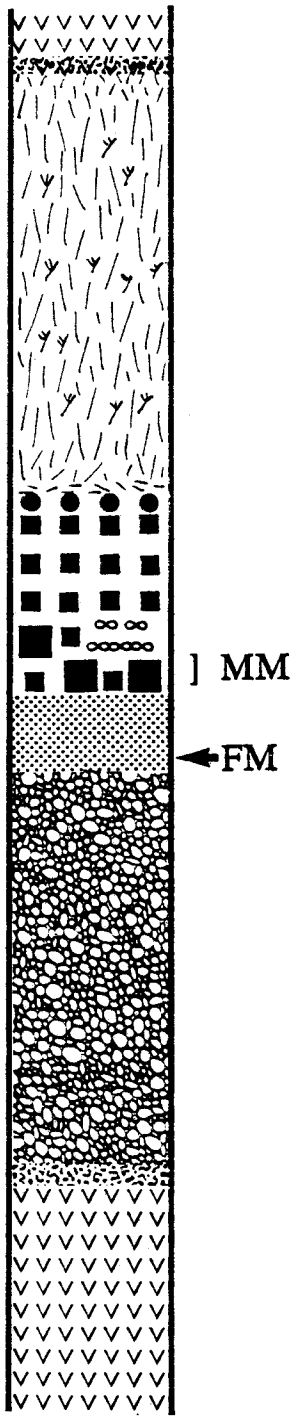


LEGEND

Tholeiitic Basalt

Marginal Pyroxenite

Spinifex-textured Clinopyroxenite

Gabbroic Layer

Amygdaloidal Clinopyroxenite

Diorite

Titaniferous-magnetite Clinopyroxenite

Gabbro

Clinopyroxene Cumulate

Olivine Cumulate

0 m

10 m

Table 1. Mineralogy of drill core samples.

Notes:

[a] Layer: h bslt = hangingwall basalt; spnfx = spinifex; gbr = gabbroic; cp cum = clinopyroxene cumulate; ol cum = olivine cumulate; f bslt = footwall basalt.

[b] Depth from flow top.

[c] Grain size: f = fine; m = medium, c = coarse; p = pegmatitic.

[d] Rock Type: t bslt = tholeiitic basalt; tmp = top marginal pyroxenite; s cpy = spinifex clinopyroxenite; a cpy = amygdaloidal clinopyroxenite; gbb = gabbro; tmc = titaniferous magnetite clinopyroxenite; cpy = clinopyroxenite; am prd = amphibole peridotite; prd = peridotite; bmp = basal marginal pyroxenite.

[e] Mineralogy: g = glass; amp = amphibole; cpx = clinopyroxene; slf = sulfide; cr-sp = chrome-spinel; chl = chlorite; cal = calcite; chr = chromite; plag = plagioclase; Fe-Ti ox = Fe-Ti oxide; ttn = titanite; ab = albite; mag = low titanium magnetite; ap = apatite; czo = clinozoisite; PGM = platinum-group mineral; $mag^2$ = secondary magnetite.

Table 1. Mineralogy of drill core samples

| Rock Layer[a] | Depth[b] (m) | Sample | Rock Type[c] | Grain Size[d] | Primary Mineralogy[e] | Modal% Chromite | Modal% Fe-Ti oxide | Modal% Magnetite | Present Mineralogy[e] |
|---|---|---|---|---|---|---|---|---|---|
| h bslt | -0.5 | MSL-61 | t bslt | f | | | | | |
| spnfx | 0.0 | MSL-60 | tmp | f | g, amp/cpx?, slf, cr-sp | <0.10 | | | amp, chl, slf, cal, chr |
| | 1.0 | MSL-59 | s cpy | f | cpx, plag, Fe-Ti ox, amp, g, slf, cr-sp | 0.00-0.05 | 5.0 | <1.0 | amp, cpx, Fe-Ti ox, ttn, ab, chl, cal, chr, mag, slf |
| | 2.5 | MSL-58 | | | | | | | |
| | 4.9 | MSL-57 | | | | | | | |
| | 6.0 | MSL-56 | | c | | | | | |
| | 7.0 | MSL-55 | | | | | | | |
| | 8.5 | MSL-54 | | | | | | | |
| | 10.0 | MSL-53 | | | | | | | |
| | 11.0 | MSL-52 | | | | | | | |
| | 12.5 | MSL-51 | | | | | | | |
| | 14.0 | MSL-50 | | | | | | | |
| | 15.0 | MSL-49 | | | | | | | |
| | 26.7 | MSL-48 | | | | | | | |
| | 28.2 | MSL-47 | | | | | | | |
| | 30.7 | MSL-46 | | | | | | | |
| | 31.2 | MSL-45 | | | | | | | |
| | 31.8 | MSL-44 | | | | | | | |
| gbr | 32.6 | MSL-43 | a cpy | c | cpx, plag, Fe-Ti ox, mag, amp, ap, slf | | <10.0 | <1.0 | amp, cpx, Fe-Ti ox, ab, chl, ttn, mag, cal, czo, ap, slf |
| | 33.3 | MSL-42 | gbb | m-c | cpx, plag, Fe-Ti ox, g, amp, mag, ap, slf, PGM | | 5.0-10.0 | 2.0 | cpx, amp, ab, Fe-Ti ox, ttn, PGM chl, mag, czo, cal, ap, slf |

Table 1. Mineralogy continued

| Rock Layer[a] | Depth[b] (m) | Sample | Rock Type[c] | Grain Size[d] | Primary Mineralogy[e] | Modal% Chromite | Modal% Fe-Ti oxide | Modal% Magnetite | Present Mineralogy[e] |
|---|---|---|---|---|---|---|---|---|---|
| gbr | 35.7 | MSL-41 | tmc | c | cpx, Fe-Ti ox, plag, g, amp, mag, ap, slf, PGM | | 10.0-15.0 | 1.0 | cpx, amp, Fe-Ti ox, ab, ttn, chl, mag, czo, cal, ap, slf, PGM |
| | 37.2 | MSL-40 | gbb | m-c | see above | | | | |
| | 38.7 | MSL-39 | | | | | | | |
| | 39.4 | MSL-38 | | | | | | | |
| | 39.9 | MSL-37 | | | | | | | |
| | 41.7 | MSL-36 | | | | | | | |
| | 41.9 | MSL-35 | | | | | | | |
| | 42.0 | MSL-34 | tmc | c-p | see above | | | | |
| | 43.3 | MSL-33 | | | | | | | |
| | 44.0 | MSL-32 | | | | | | | |
| | 45.1 | MSL-31 | | | | | | | |
| | 45.6 | MSL-30 | | | | | | | |
| | 46.1 | MSL-29 | | | | | | | |
| | 46.6 | MSL-28 | | | | | | | |
| | 46.8 | MSL-27 | gbb | m-c | see above | | | | |
| | 47.3 | MSL-26 | | | | | | | |
| | 47.5 | MSL-25 | | | | | | | |
| | 47.7 | MSL-24 | | | | | | | |
| | 48.0 | MSL-23 | gbb | m-c | | | | | |
| cp cum | 48.1 | MSL-22 | cpy | m | cpx, plag, Fe-Ti ox, mag, amp, ap, slf, PGM | | 5.0 | <1.0 | amp, cpx, Fe-Ti ox, ab, chl, ttn, mag, cal, czo, ap, slf, PGM |
| | 48.4 | MSL-21 | | | | | | | |
| | 48.9 | MSL-20 | | | | | | | |
| | 51.4 | MSL-19 | | | | | | | |
| | 52.5 | MSL-18 | | | | | | | |

Table 1. Mineralogy continued

| Rock Layer[a] | Depth[b] (m) | Sample | Rock Type[c] | Grain Size[d] | Primary Mineralogy[e] | Modal% Chromite | Modal% Fe-Ti oxide | Modal% Magnetite | Present Mineralogy[e] |
|---|---|---|---|---|---|---|---|---|---|
| cp cum | 53.0 | MSL-17 | | | | | | | |
| | 53.2 | MSL-16 | | | | | | | |
| ol cum | 56.1 | MSL-15 | am prd | m | ol, cr-sp, cpx, amp, g, slf | | | 10.0 | serp, mag[2], amp, chl, cal, chr, ttn, slf |
| | 58.7 | MSL-14 | | | | | | | |
| | 59.3 | MSL-13 | | | | | | | |
| | 61.3 | MSL-12 | | | | | | | |
| | 62.1 | MSL-11 | prd | m | ol, cr-sp, cpx, g, slf | 0.25-0.50 | | 10.0 | serp, mag[2], amp, chl, chr, ttn, cal, cpx, slf |
| | 62.2 | MSL-10 | | | | | | | |
| | 63.2 | MSL-9 | | | | | | | |
| | 67.0 | MSL-8 | | | | | | | |
| | 73.7 | MSL-7 | | | | | | | |
| | 77.7 | MSL-6 | | | | | | | |
| | 79.7 | MSL-5 | | | | | | | |
| | 83.6 | MSL-4 | | | | | | | |
| f bslt | 88.7 | MSL-3 | t bslt | f | | | | | |
| | 95.7 | MSL-2 | | | | | | | |
| | 96.2 | MSL-1 | | | | | | | |

cumulate is an orthocumulate and consisted of olivine + chrome-spinel and intercumulus clinopyroxene or amphibole; 2) clinopyroxene cumulate is a meso- to orthocumulate which contained primary cumulus clinopyroxene and intercumulus Fe-Ti oxide, plagioclase and primary amphibole; 3) gabbro consisted of clinopyroxene and interstitial plagioclase, Fe-Ti oxide (up to 10 modal%), primary amphibole and glass; 4) titaniferous magnetite clinopyroxenite (TMC) occurs as minor, metre-scale patches of pegmatite that appear to have been richer in clinopyroxene and magnetite-ilmenite (up to 15 modal%) compared to the gabbro; 5) diorite consisted of plagioclase and primary amphibole with glass occurring as minor, metre-scale patches, dikelets and discontinuous bands within gabbro and TMC; 6) clinopyroxenite occurring at the top of the gabbroic layer has vesicular cavities which are now filled with pyrite or calcite and is referred to as amygdaloidal clinopyroxenite; 7) spinifex-textured clinopyroxenite consisted of clinopyroxene and interstitial plagioclase, Fe-Ti oxide, primary amphibole and chromite or glass; and 8) marginal pyroxenite, now amphibolite, appears to have been composed of glass, primary amphibole or clinopyroxene, chromite and sulfides.

A subaqueous effusive origin has been suggested for the BCF based on (i) the thickness of the spinifex-textured layer (30 m) and the chilled flow top margin (50 cm), (ii) high proportion of altered 'glass' and presence of vesicles and cooling fractures in the flow top; (iii) the lateral persistence of a cherty horizon immediately above the flow top; and (iv) the presence of pillowed basalt in the section. The flow is considered to have formed by submarine eruption of parental melt, quenching of the flow margins, fractionation of olivine

+ chromite followed by some clinopyroxene and crystallization of the trapped residual liquid (ie. gabbro) and late stage segregations (ie. diorite; Stone et al., 1987, 1994 submitted).

Although primary igneous textures and minerals are preserved, metamorphic recrystallization effects are ubiquitous and the rocks are locally deformed (Stone et al., 1993). The olivine is completely altered to serpentine (antigorite) + magnetite, chrome-spinel is altered to ferrichromite + chromium magnetite ± chlorite, and plagioclase is completely altered to albite + hornblende-actinolite + chlorite + clinozoisite. Clinopyroxene, Fe-Ti oxide and primary amphibole are generally preserved despite pseudomorphous alteration to tremolite + titanite + calcite + secondary diopside in the olivine cumulate, and hornblende-actinolite + titanite + chlorite + clinozoisite in the other rock types. Deformation is manifest as narrow shear zones at the flow margins, the olivine cumulate-clinopyroxenite cumulate contact, and within the clinopyroxenite layer. This deformation is likely related to the volume expansion of the rock during serpentinization (eg. Hostetler et al., 1966), and not the transverse faulting associated with the development of the Round Lake dome.

### *2.3 PGE mineralization*

The PGE mineralization within the BCF has been previously described in detail (Stone et al., 1992, 1993, in review) and its characteristics are summarized in Table 2. The mineralization occurs in three horizons i) main mineralization (MM), ii) footwall mineralization (FM) and iii) hanging-wall mineralization (Fig. 4). Only the MM and FM

Table 2. Summary of PGE Mineralization in the Boston Creek Flow

| | Footwall Mineralization | Main Mineralization |
|---|---|---|
| Depth (m) from flow top | 43.25 | 46.75-45.25 |
| Host Rock | clinopyroxenite | titaniferous magnetite clinopyroxenite |
| Strike Length | very localized | at least 100 m |
| Primary Mineralogy | clinopyroxene - cumulus<br>- 70 modal %<br>- 3 to 5 mm<br>Fe-Ti oxide - intercumulus<br>- minor<br>plagioclase - interstitial<br>- major | clinopyroxene - 60 modal %<br>- 5 to 20 mm<br>Fe-Ti oxide - interstitial<br>- 5 to 10 modal %<br>plagioclase - interstitial<br>- major |
| ΣPGE+Au | 100 ppb | 300 ppb |
| PGM | stibiopalladinite<br>or mertieite - $Pd_5Sb_2$<br>Pd-Ag sulfide - $Pd_2AgS_2$?<br>sperrylite - $PtAs_2$ | bismuthian merenskyite - $Pd(Te,Bi)_2$<br>merenskyite - $PdTe_2$<br>bismuthian kotulskite - Pd(Te,Bi)<br>sperrylite - $PtAs_2$<br>hollingworthite - (Rh,Pt,Pd)AsS<br>moncheite - $PtTe_2$ |
| Other Precious Metal Phases | native gold<br>electrum<br>native silver<br>naumannite - $Ag_2Se$<br>Ag-Bi selenide<br>hessite - $Ag_2Se$ | native gold<br>hessite |
| Sulfides | 0.2 modal %<br><br>chalcopyrite<br>bornite<br>pyrite - minor<br>cobaltite - very minor | <br><br>chalcopyrite<br>pyrite<br>bornite - trace<br>sphalerite - rare<br>linneite - very rare<br>mackinawite - very rare |

Modified after Stone et al., 1993.

occur along the surveyed transect of this project. The highest PGE concentrations are within the base of the gabbroic layer, in association with titaniferous magnetite and zones of disseminated chalcopyrite and pyrite. The PGE are concentrated as rare micrometre-sized grains of Pt, Pd and Rh arsenides and bismuthotellurides in spatial association with chalcopyrite, pyrite and titaniferous magnetite.

The stratigraphic level of PGE mineralization is characterized by anomalous diversity of textures and rock types. The MM occurs in the base of the gabbroic unit (37.2 to 38.5 m above flow base) as discontinuous, stratabound zones of disseminated chalcopyrite and pyrite within TMC that carry PGM. The MM is the richest in precious metal values [$\Sigma$(PGE+Au) = up to 1000 ppb in hand specimen], thickest (up to 5 m), and most continuous of the three mineralized horizons. Although stratabound, the sulfides are concentrated ($\leq$0.5 modal %) as isolated, metre-sized podiform zones. PGE are concentrated in some of the sulfide enriched zones and occur with native gold, a suite of silver minerals, chalcopyrite, pyrite and titaniferous magnetite.

The FM [$\Sigma$(PGE+Au) = 115 ppb] occurs within the clinopyroxenite cumulate layer, 30.5 m above the flow base and is very sporadically distributed. Table 3 shows the compositions of some of the PGM and associated sulfides common to the BCF.

Table 3. Composition (wt %) of PGM and Associated Sulfides in the Boston Creek Flow

| Rock Type<br>Mineral | cpy$^{x}$<br>Hll | cpy$^{x}$<br>Mrn | cpy$^{+}$<br>Ccp | cpy$^{+}$<br>Cbl | gbb$^{x}$<br>Py | gbb$^{x}$<br>Mck | gbb$^{x}$<br>Lnn |
|---|---|---|---|---|---|---|---|
| Fe | 2.48 | 2.42 | 30.55 | 2.87 | 45.29 | 59.08 | 2.04 |
| Ni | ------ | ------ | 0.00 | 1.65 | 0.01 | 4.11 | 24.57 |
| Cu | 1.71 | 1.62 | 34.33 | 0.00 | 0.02 | ------ | 0.00 |
| Co | ------ | ------ | 0.00 | 30.40 | 1.13 | ------ | 30.53 |
| Pt | 23.03 | 11.76 | 0.00 | 0.00 | 0.03 | ------ | 0.00 |
| Pd | 1.90 | 18.72 | 0.00 | 0.00 | 0.01 | ------ | 0.00 |
| Rh | 12.23 | 0.37 | ------ | ------ | ------ | ------ | ------ |
| Te | 13.16 | 57.33 | ------ | ------ | ------ | ------ | ------ |
| Bi | 1.22 | 5.92 | ------ | ------ | ------ | ------ | ------ |
| As | 30.79 | 0.64 | 0.00 | 45.52 | 0.06 | ------ | 0.00 |
| Sb | 0.13 | 0.00 | ------ | ------ | ------ | ------ | ------ |
| S | 7.76 | 1.29 | 34.47 | 20.50 | 53.48 | 36.81 | 42.86 |
| Total | 94.39 | 100.07 | 99.36 | 100.95 | 100.02 | 100.00 | 100.00 |

cpy = clinopyroxene cumulate; gbr = gabbroic layer

$^{x}$ MM host rock.

$^{+}$ FM host rock.

Mineral: Hll = hollingworthite; Mrn = merenskyite; Ccp = chalcopyrite; Cbl = cobaltite; Mck, mackinawite; Lnn = linnaeite.

Hollingworthite and merenskyite analyses reflect beam overlap onto adjacent material during analysis.

----, not determined.

After Stone et al., 1993.

# Chapter 3

## Oxide Petrology and Composition

The primary oxide mineral phases in the BCF appear to have been chromite, magnetite-ilmenite and magnetite. Detailed knowledge of the petrography and chemical composition of all the oxide minerals is required for any understanding of the geophysical response of the BCF rock types.

### *3.1 Analytical Techniques*

The petrography and mineralogy of the oxides were determined by transmitted and reflected light microscopy, and by back-scattered electron imagery using a electron microprobe at the University of Alabama. Analysis of the oxides was made with a JEOL JXA-8600/3 electron microprobe which is equipped with five wavelength-dispersion X-ray spectrometers and a TN-5400 energy-dispersion X-ray analysis spectrometer. The analyses were made using wavelength dispersion (WDS) techniques, an accelerating voltage of 15 kV, a nominal beam size of 1 $\mu$m, a Faraday cup current of 20 nA, and maximum count time of 40 s. Bulk analyses of lamellar intergrown magnetite-ilmenite were made with a defocused beam between 5 and 20 $\mu$m in diameter. Natural silicates and oxides were used as standards and are listed in Table A-1 (Appendix A). Corrections were made on-line using a Bence-Albee program provided by Tracor-Northern. Each analysis was checked by qualitative energy-dispersion (EDS) scan with a count time of 30 s. Samples from each major rock type were chosen for analysis and representative results are shown in Tables 4 through 6 for chromite and secondary magnetite, primary iron- and iron-titanium oxides and bulk

composition. Complete results are list in Appendix A, Tables A-2 through A-5.

*3.2 Chromite*

Chromite is altered to ferrichromite and chromium magnetite as a result of serpentinization in the olivine cumulate and metamorphic recrystallization in the flow top spinifex. Chromite in the olivine cumulate occurs as both, isolated and aggregate grains, within interstitial serpentine pseudomorphs of olivine. The chromite grains are up to 100 $\mu$m in size and contain a zoned, euhedral core surrounded by an irregular rim (Fig. 5a). The grain core is zoned from ferrochromite (high $Fe^{2+}$ and Cr, low Al and Mg) in the centre to secondary ferrichromite (high $Fe^{3+}$ $\pm$ chromium magnetite) around the margin (Fig. 5b). The grain rim is of secondary chromium magnetite with $Cr_2O_3$ contents ranging between 0.25 and 0.42 wt% (Table 4). Up section, the abundance of chromite decreases from about 0.50 to 0.25 modal percent. This is simply a result of the early crystallization and density of the Cr-spinel, that is, greater accumulation occurred towards the base of the flow as a result of gravity settling.

Ferrichromite is believed to have formed from the alteration of Cr-spinel by iron-rich fluids during serpentinization. Through this process, the olivine structure is destroyed and Fe is released. Fe forms magnetite in the groundmass and also reacts with Cr-spinel to form the secondary Fe-rich rims. Iron substitutes for Mg and Al in the spinel structure. These elements, after release from the spinel structure likely contribute to formation of serpentine and chlorite respectively. In summary, the alteration of primary Cr-spinel resulted in the

FIGURE 5. Photomicrographs of BCF chromite grains.

5a) MSL-11, olivine cumulate. Zoned, euhedral chromite core surrounded by secondary irregular magnetite rim. Scale bar is 100 microns.

5b) MSL-11. Zonation from ferrochromite (centre) to ferrichromite and then chromium magnetite in the rim. Scale bar is 100 microns.

5c) MSL-58, spinifex-textured clinopyroxenite. Large ferrichromite core with thin ferrochromite zone around it. Scale bar is 100 microns.

5d) MSL-58. Chlorite lamellae in magnetite rim. Scale bar is 10 microns.

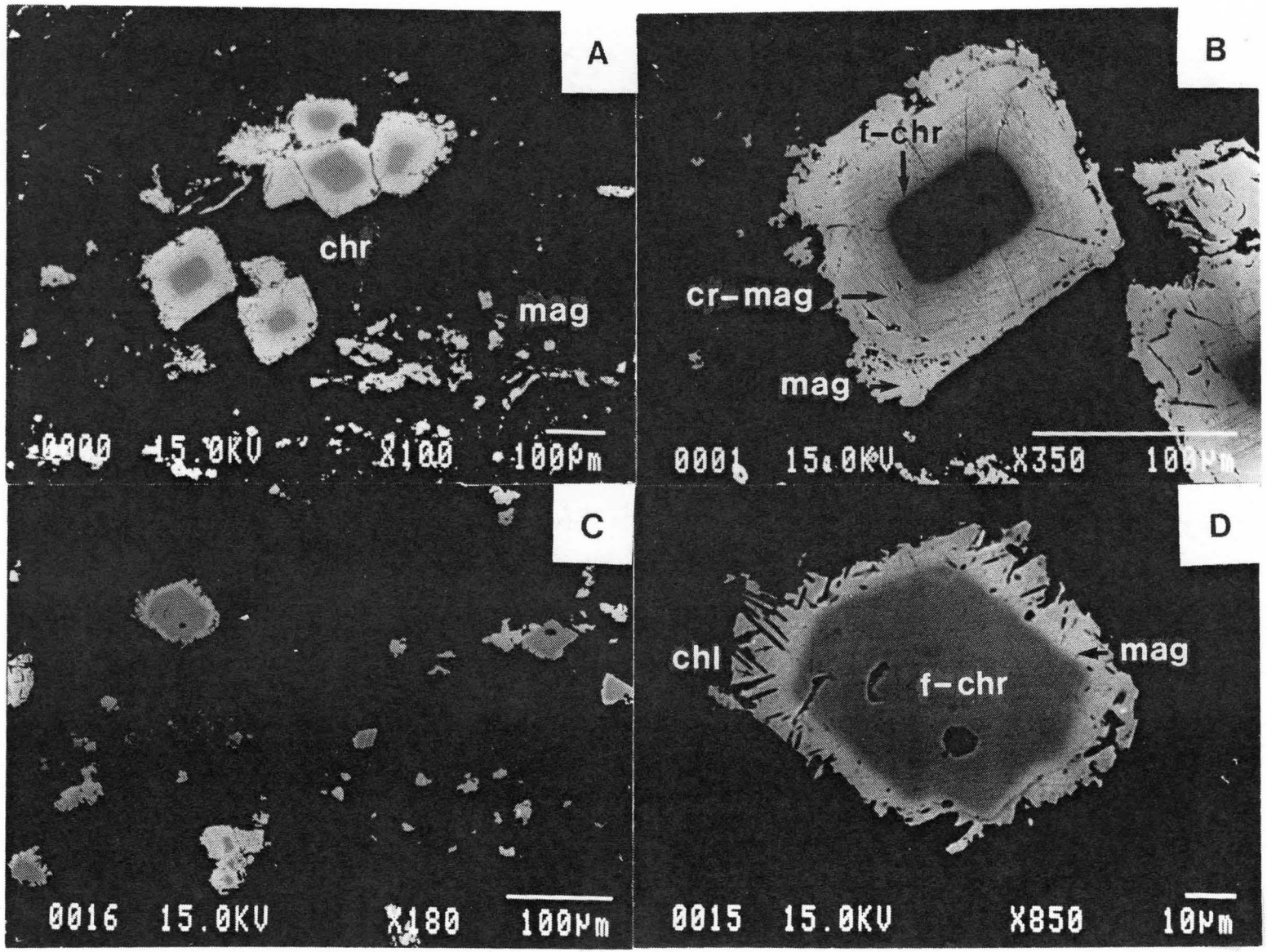
A
chr
mag
0000 15.0KV X100 100µm
B
f-chr
cr-mag
mag
0001 15.0KV X350 100µm
C
0016 15.0KV X180 100µm
D
chl
mag
f-chr
0015 15.0KV X850 10µm

Table 4. Chromite analyses

| Sample | MSL-11[a] | MSL-11[b] | MSL-11[c] | MSL-58[a] | MSL-58[c] |
|---|---|---|---|---|---|
| $SiO_2$ | 0.00 | 0.00 | 0.02 | 0.05 | 0.57 |
| $TiO_2$ | 1.75 | 0.43 | 0.02 | 1.27 | 0.01 |
| $Al_2O_3$ | 5.64 | 0.27 | 0.01 | 6.06 | 0.01 |
| $Cr_2O_3$ | 36.09 | 10.21 | 0.25 | 43.68 | 0.29 |
| $Fe_2O_3$ | 21.20 | 56.12 | 67.99 | 13.45 | 65.80 |
| FeO | 27.48 | 29.54 | 30.51 | 29.59 | 30.56 |
| MnO | 3.90 | 1.14 | 0.07 | 1.45 | 0.03 |
| MgO | 0.35 | 0.00 | 0.03 | 0.18 | 0.19 |
| ZnO | 1.21 | 0.18 | 0.02 | 1.48 | 0.02 |
| CaO | 0.01 | 0.00 | 0.01 | 0.03 | 0.12 |
| NiO | 0.13 | 0.22 | 0.19 | 0.08 | 0.08 |
| Total | 97.76 | 98.20 | 99.13 | 97.31 | 97.68 |
| | | | | | |
| $Fe^{+3}$ | 1.951 | 1.987 | 1.988 | 1.963 | 1.977 |
| $Fe^{+2}$ | 1.046 | 1.007 | 0.997 | 1.035 | 1.022 |

Notes: MSL-11 = olivine cumulate; MSL-58 = spinifex-textured clinopyroxenite; a = ferrochromite core; b = chromium magnetite rim; c = secondary magnetite rim.

Ferric iron determined by stoichiometric calculations.

formation of zoned ferrichromites which often became enveloped in a ring of secondary magnetite by the solid state replacement of $MgAl_2O_4$ for $FeFe_2O_4$ (Beeson and Jackson, 1964; Ulmer, 1974; Fleet et al., 1993).

In the spinifex-textured layer, chromite is restricted in distribution to the top 5 to 10 m of the layer, and, from the whole-rock Cr contents, is estimated to comprise only up to 0.10 modal percent of the rock (Stone et al., 1993). Chromite occurs as small euhedral cores of ferrichromite that are rimmed by secondary chromium magnetite and/or magnetite (Fig. 5c and 5d). A curious feature of the chromite in this layer is what appears to be coarse "exsolution lamellae" of chlorite along partings or cleavage planes in the secondary magnetite rims. This is not observed in the olivine cumulate. The chlorite lamellae are unlikely to be primary features when the extreme alteration of the flow top is considered. This suggests that the lamellae may be a secondary phase, which developed during chromite alteration. As a result, the chlorite nucleated along partings or cleavage planes in the chromium magnetite rims. Chlorite development is indicative of low temperature metasomatic events, and therefore likely developed in response to the invasion of low temperature hydrothermal fluids. These fluids may have been associated with the magma that formed the Round Lake Batholith.

### *3.3 Magnetite-ilmenite*

Magnetite-ilmenite makes up to 5 modal percent of the clinopyroxene cumulate and spinifex-textured layer and up to 15 modal percent in TMC within the gabbroic layer.

Although normally preserved in the flow, the Fe-Ti oxides are completely altered to amphibole and titanite in the lower half of the clinopyroxene cumulate, probably as a result of serpentinization of the underlying olivine cumulate. This is also one of the features that makes this layer geophysically distinctive. The base of this layer is not very well exposed but is easily identified by the lack of magnetic response.

The preserved magnetite-ilmenite grains in the flow are generally restricted to the interstices between clinopyroxenes, up to 2 cm in maximum dimension, and are cruciform to feathery in shape (Fig. 6, 7 and 8). According to the classification of Buddington and Lindsley (1964) trellis, internal and external granular textures are observed in the Fe-Ti oxides; Haggerty (1976) terms these trellis and composite exsolution textures. The grains contain a relatively large core of lamellar intergrown titanium bearing magnetite (up to 3.0 wt% $TiO_2$) and manganiferous ilmenite (up to 4.0 wt% MnO) and a thin margin of end-member magnetite (Table 5). The lamellar intergrowth of magnetite and ilmenite is much more intricate in grains from the clinopyroxene cumulate than those in the gabbroic layer, suggesting slower cooling rates in the latter (Buddington and Lindsley, 1964; Haggerty et al., 1976; Fig. 9). The exsolved ilmenite phase is often found along fractures in the Fe-Ti oxide grains and is commonly altered to chlorite and titanite (Fig. 9c). From broad beam analysis of the magnetite-ilmenite grain cores, the Fe-Ti oxides have 20 wt% $TiO_2$ on average (Table 6). The compositions and textures of the grains are similar to those reported by Stone et al. (1987, 1993). These are consistent with an origin for magnetite-ilmenite by unmixing of a higher-temperature Fe-Ti oxide phase at intermediate temperatures during cooling of the flow

FIGURE 6. Drill core photo of cruciform Fe-Ti oxides. The drill core is 2.4 cm in diameter. MSL-20; clinopyroxene cumulate. CPX grains are the rounded grey grains; the oxides are black.

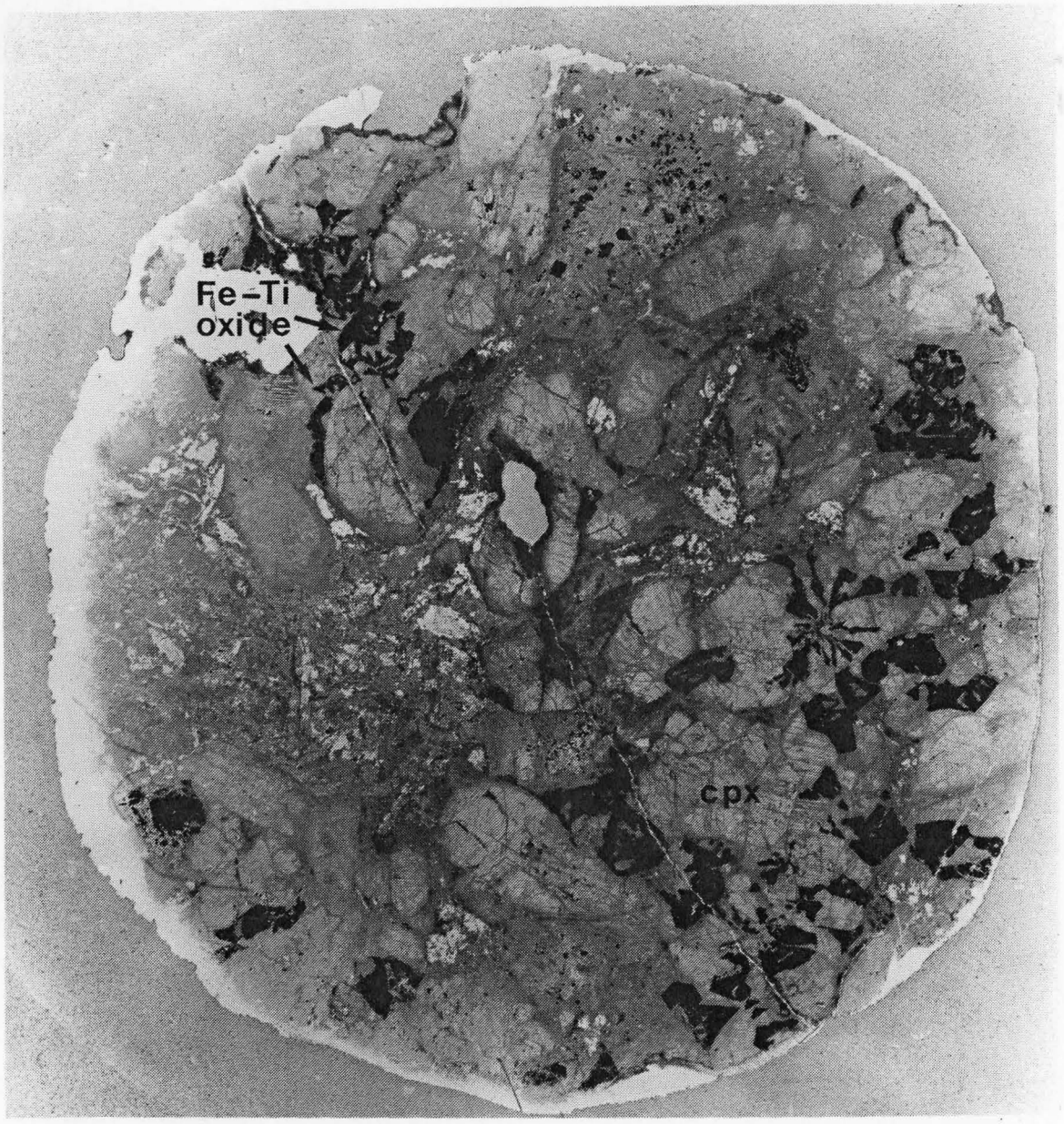
Fe–Ti
oxide
cpx

FIGURE 7. Drill core photo of feathery Fe-Ti oxide in lower half of the core. The drill core is 2.4 cm in diameter. MSL-34; TMC. Note the Fe-Ti oxides occurring interstitially to the CPX grains.

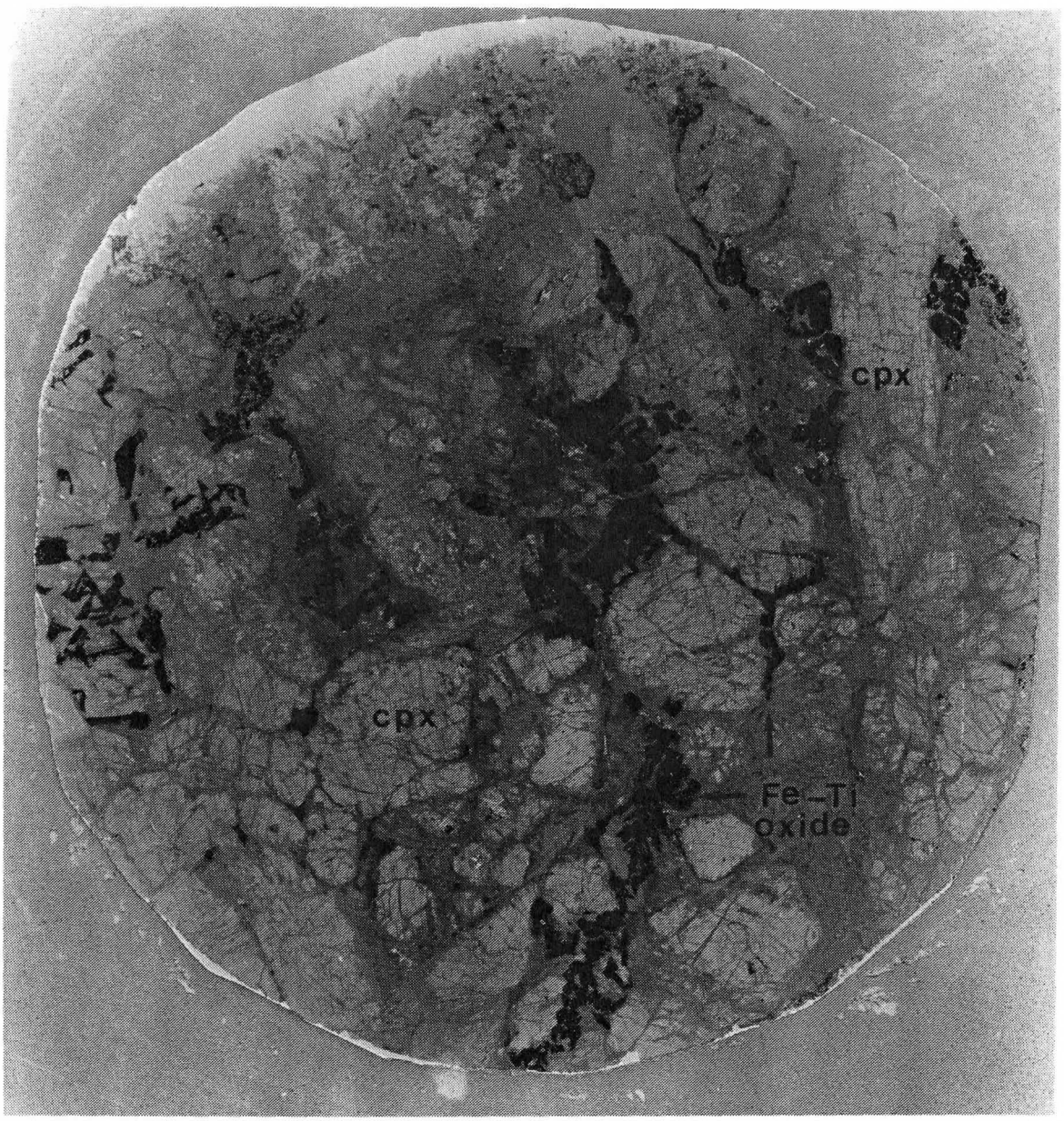
cpx
cpx
Fe–Ti
oxide

FIGURE 8. Drill core photo of spinifex-textured clinopyroxenite (MSL-49). The drill core is 2.4 cm in diameter. Fe-Ti oxides are finer grained than in Figures 6 and 7. Clinopyroxene spinifex grains oriented subperpendicular to the flow top. Note CPX grain at the top of the photo showing the hollow core.

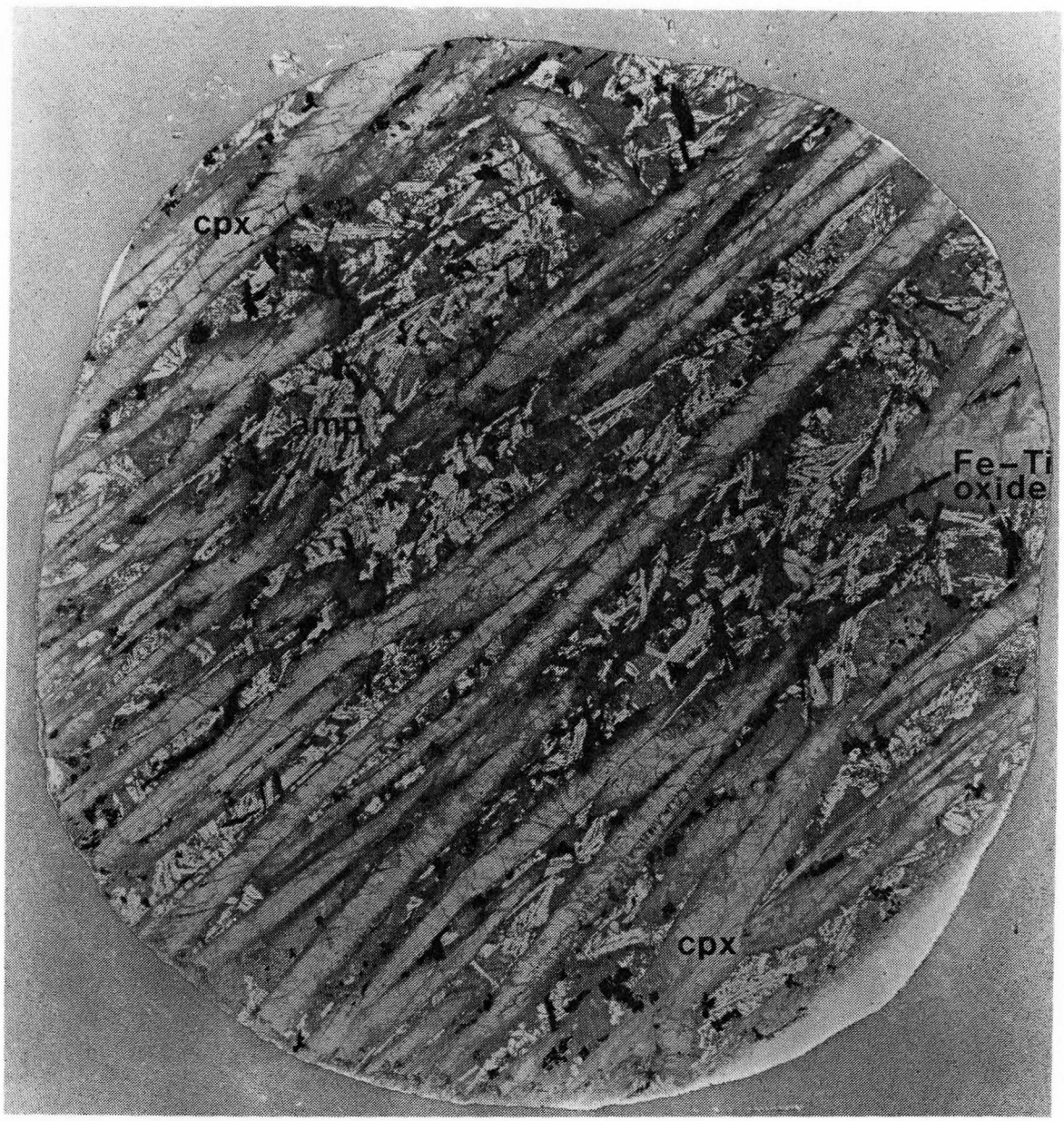
cpx
amp
Fe–Ti
oxide
cpx

Table 5. Titanifeous magnetite, ilmenite and primary magnetite analyses

| Sample | MSL-20[a] | MSL-20[b] | MSL-34[c] | MSL-34[d] | MSL-20[e] | MSL-34[f] |
|---|---|---|---|---|---|---|
| $SiO_2$ | 0.02 | 0.01 | 0.13 | 0.00 | 0.10 | 0.10 |
| $TiO_2$ | 2.73 | 51.07 | 0.82 | 50.84 | 0.57 | 0.02 |
| $Al_2O_3$ | 0.05 | 0.02 | 0.07 | 0.00 | 0.07 | 0.02 |
| $Cr_2O_3$ | 0.07 | 0.03 | 0.07 | 0.00 | 0.02 | 0.02 |
| $Fe_2O_3$ | 63.02 | 2.11 | 65.77 | 1.40 | 66.28 | 67.67 |
| FeO | 33.16 | 41.76 | 31.42 | 42.34 | 30.99 | 30.75 |
| MnO | 0.17 | 0.04 | 0.03 | 0.04 | 0.05 | 0.00 |
| MgO | 0.03 | 4.02 | 0.00 | 3.22 | 0.06 | 0.01 |
| CaO | 0.03 | 0.06 | 0.04 | 0.04 | 0.03 | 0.02 |
| Total | 99.28 | 99.12 | 98.35 | 97.89 | 98.18 | 98.61 |
| | | | | | | |
| $Fe^{+3}$ | 1.919 | 2.034 | 1.970 | 2.050 | 1.979 | 1.995 |
| $Fe^{+2}$ | 1.081 | 1.973 | 1.030 | 1.960 | 1.022 | 1.006 |

Notes: (a) titaniferous magnetite from clinopyroxene cumulate with ilmenite exsolution, represented by analysis (b); (c) titaniferous magnetite from TMC (lower gabbro) with ilmenite exsolution, represented by analysis (d); (e) primary euhedral magnetite in groundmass of clinopyroxene cumulate; (f) primary euhedral magnetite in groundmass of TMC.

Nickel and zinc sought but not determined.

Ferric iron determined by stoichiometric calculations.

FIGURE 9. Photomicrographs of BCF Fe-Ti oxides. Scale bar is 10 microns.

9a) MSL-20; clinopyroxene cumulate. Very fine intergrowth of magnetite (light) and ilmenite (dark). Black = silicate minerals.

9b) MSL-34; TMC. Coarse intergrowth of magnetite and ilmenite. Bright white minerals are chalcopyrite and pyrite.

9c) MSL-58; spinifex-textured clinopyroxenite. Note large intergrown core surrounded by secondary magnetite rim with chlorite lamellae development.

9d) MSL-58. Fe-Ti oxide with finely intergrown magnetite and ilmenite core and secondary altered rim (magnetite + chlorite).

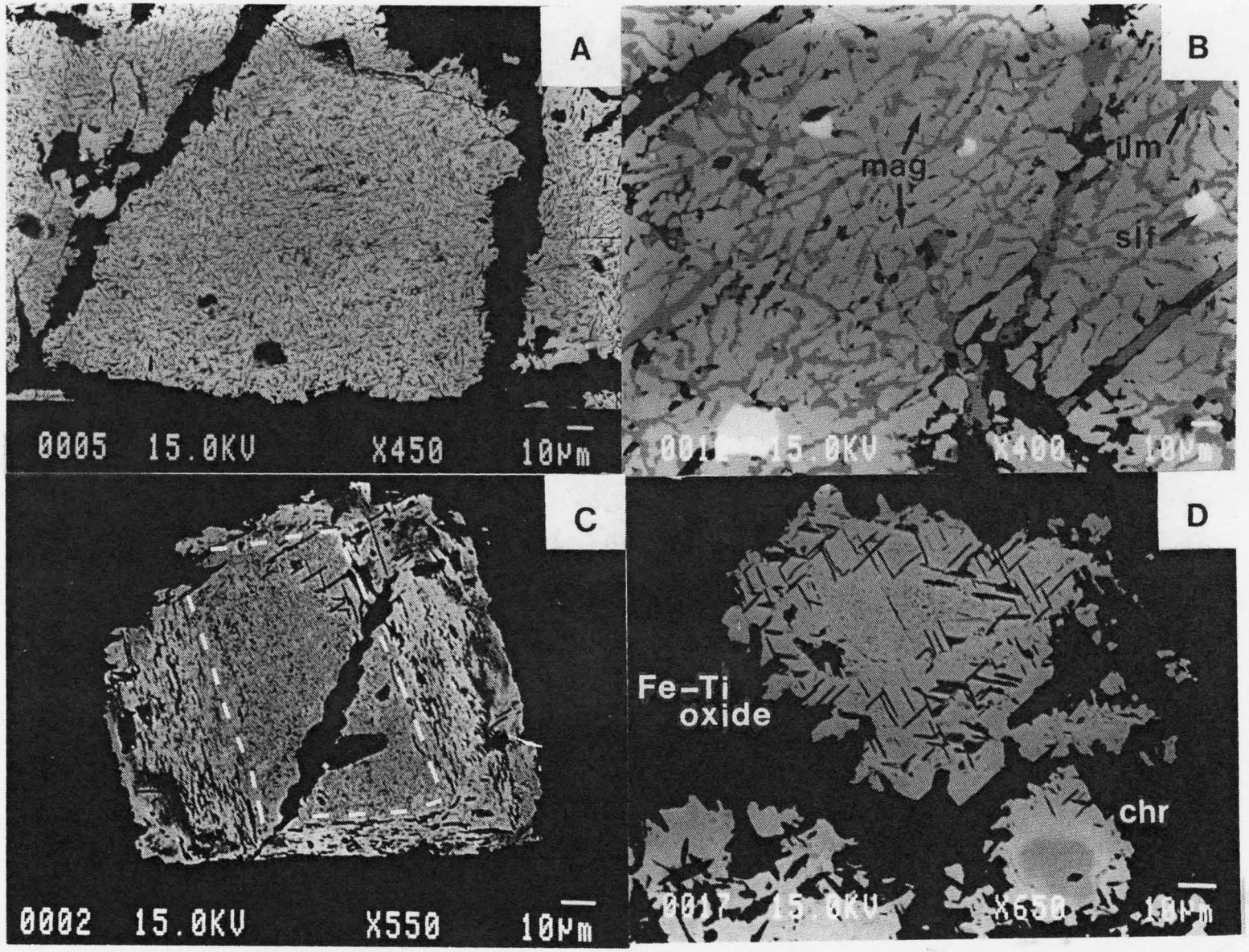
A
0005 15.0KV X450 10µm
B
mag
ilm
slf
C
0002 15.0KV X550 10µm
D
Fe-Ti
oxide
chr

Table 6. Broadbeam analyses of Fe-Ti oxide

| Sample | MSL-20 | MSL-34 | MSL-58 |
|---|---|---|---|
| $SiO_2$ | 0.14 | 0.11 | 0.15 |
| $TiO_2$ | 15.48 | 18.91 | 11.21 |
| $Al_2O_3$ | 0.23 | 0.00 | 0.05 |
| $Cr_2O_3$ | 0.05 | 0.06 | 0.03 |
| $Fe_2O_3$ | 37.85 | 32.45 | 45.70 |
| FeO | 44.00 | 47.85 | 39.87 |
| MnO | 1.24 | 0.86 | 1.07 |
| MgO | 0.07 | 0.05 | 0.07 |
| CaO | 0.03 | 0.09 | 0.06 |
| Total | 99.09 | 100.38 | 98.21 |
| | | | |
| $Fe^{+3}$ | 1.000 | 1.000 | 1.000 |
| $Fe^{+2}$ | 2.000 | 2.000 | 2.000 |

Notes: 20 $\mu$m beam diameter used for analyses of MSL-20 (clinopyroxene cumulate) and MSL-34 (TMC); 10 $\mu$m beam diameter used for analyses of MSL-58 (spinifex-textured clinopyroxenite).

Nickel and zinc sought but not determined.

Ferric iron determined by stoichiometric calculations.

(eg. Buddington and Lindsley, 1964; Haggerty, 1976; Stormer, 1983).

The composition of the exsolved ilmenite in the Fe-Ti oxides of the gabbroic layer is approximately the same as that found in the clinopyroxenite cumulate. The magnetite composition however, appears to be somewhat variable with respect to its titanium and manganese content, which is higher in the clinopyroxenite samples. The iron-titanium ratio therefore varies slightly from the clinopyroxenite cumulate to the gabbroic layer. This may simply be a result of beam overlap and would be expected and more pronounced in the clinopyroxenite cumulate since the exsolution lamellae are much finer and more intricately intergrown than those in the gabbroic layer. This makes it more difficult to analyze the separate phases of magnetite and ilmenite. Overlap onto titanite (an alteration product of ilmenite) may have influenced the titanium content. If this is the case, then the calcium contents should be higher and proportional to the titanium content if overlap with titanite is the problem. Silica should also be somewhat higher than what the analyses show.

Buddington and Lindsley (1964) devised a means of determining temperature based on the MnO content of coexisting titaniferous magnetite and ilmenite phases. Based on their work, the BCF should plot in the area of the metamorphic or gabbroic rock trends. Typically, 0.1 wt% MnO is found in the magnetite, but the amount of MnO in the ilmenite ranges between 3 to 4 wt%. This suggests that some process (metasomatic event) has preferentially concentrated manganese in the ilmenite. The experimentally determined relationships however, are not well defined. For example, the granitic trend is constrained

by only two points. Further detailed study is therefore, necessary to clarify the relationship between MnO content in coexisting magnetite-ilmenite phases. In light of this, an accurate determination of the temperature and oxygen fugacity at the time of formation is not possible.

Magnetite-ilmenite grains in the gabbroic layer, specifically the TMC are spatially associated with the PGE mineralization. The PGE are found in sulfide-rich patches often in chalcopyrite and occasionally pyrite. Isolated PGM do occur but all are spatially associated with the titaniferous magnetite. Figure 9b, a polished probe section of drill core MSL-34 is a potentially mineralized TMC sample. Note the occurrence of chalcopyrite (bright white), and pyrite set in the magnetite grain. The darker grey phases are magnetite and ilmenite (darkest grey). The main objective of the probe analyses was to analyze the oxide phases, however, a silver sulfide mineral was found in one section. No PGM were observed during a quick inspection of the TMC sections.

The titaniferous magnetite grains in the spinifex-textured layer are different from those found in the layers below. Coarse, chlorite intergrowths, similar to those that occur in the rims of chromite within the spinifex-textured clinopyroxenite, are observed. The intergrowth of chlorite during chromite alteration is also suggested for their origin. Fine grained exsolution of ilmenite has occurred and is preserved however, in the cores of these Fe-Ti oxides (Fig. 9c and 9d). As is the case of the chromite, it appears that the lamellae are simply an intergrowth of chlorite with the secondary magnetite rims of these grains

resulting from a low temperature alteration process.

### *3.4 Primary Magnetite*

Primary magnetite occurs as a minor phase ($\leq$ 2 modal%) in the groundmass of the clinopyroxene cumulate and gabbroic layers and as a minor phase (5 modal%) in the diorite segregations within the gabbroic layer. The magnetite grains are euhedral, up to 50 $\mu$m in size, and nearly end-member magnetite in composition (Table 5), like the marginal magnetite on the large magnetite-ilmenite grains. The low Ti content of this magnetite suggests that it was the final oxide phase to crystallize during the cooling of the flow. Figure 10a shows the distribution of these small, euhedral grains set in a groundmass consisting mainly of amphibole.

The primary magnetite in the clinopyroxene cumulate which is not typically preserved may have been destroyed by reaction with calcium which was mobilized during amphibolitization of the BCF during metamorphism. This is suggested by the abundance of amphibole and titanite in this layer.

### *3.5 Secondary Magnetite*

The magnetite in the olivine cumulate (up to 10 modal%) is secondary in origin. The amount of magnetite in this layer decreases up toward the clinopyroxene cumulate because of greater accumulation of olivine at the base of the peridotite during fractionation. The magnetite grains are irregular in shape and occur in a net- or mesh-like distribution about the

FIGURE 10. Primary low-Ti magnetite photomicrograph and peridotite drill core photo

10a) Primary, euhedral, low-Ti magnetite masses in a groundmass consisting mainly of amphibole. The large bright white grains are pyrite. Scale bar is 100 microns.

10b) MSL-11; olivine cumulate. Drill core photo of olivine cumulate. Dark phase is magnetite; the lighter phase is mostly serpentine pseudomorphs of olivine. Note the even dissemination of magnetite in a mesh- or net-like texture around the serpentine grains. The drill core is 2.4 cm in diameter.

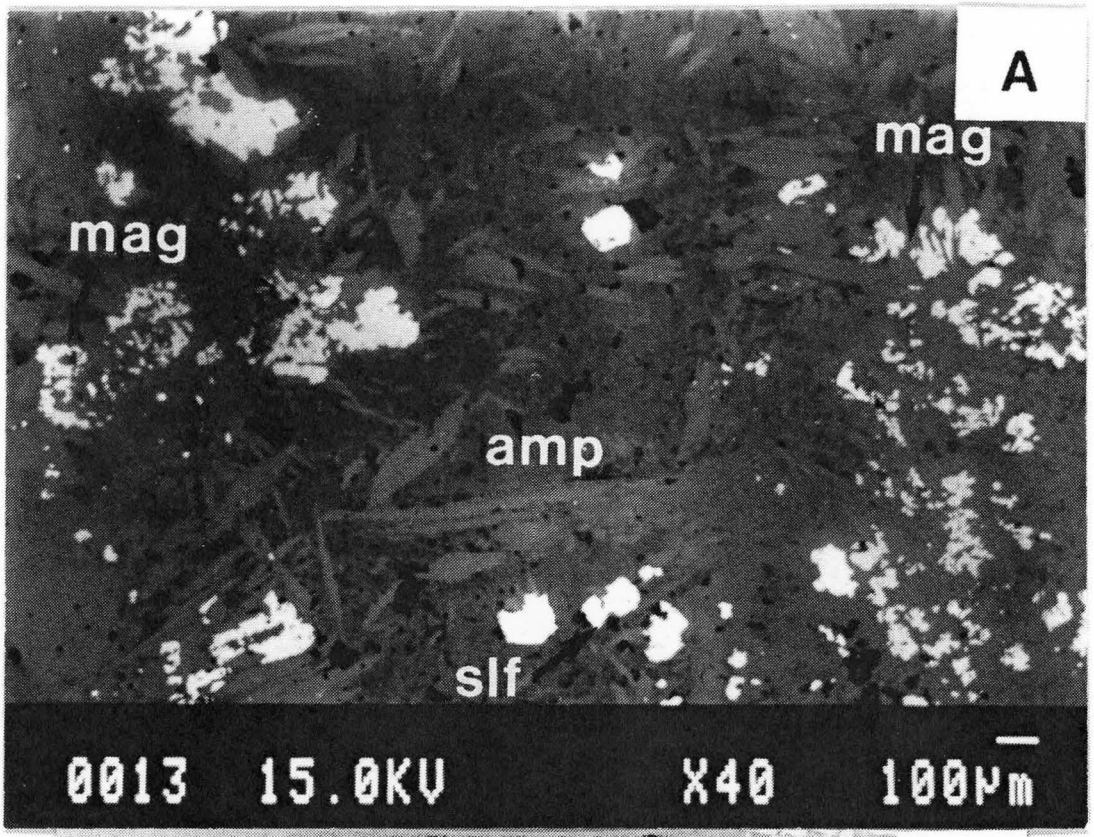
A
mag
mag
amp
slf
0013 15.0KV X40 100µm

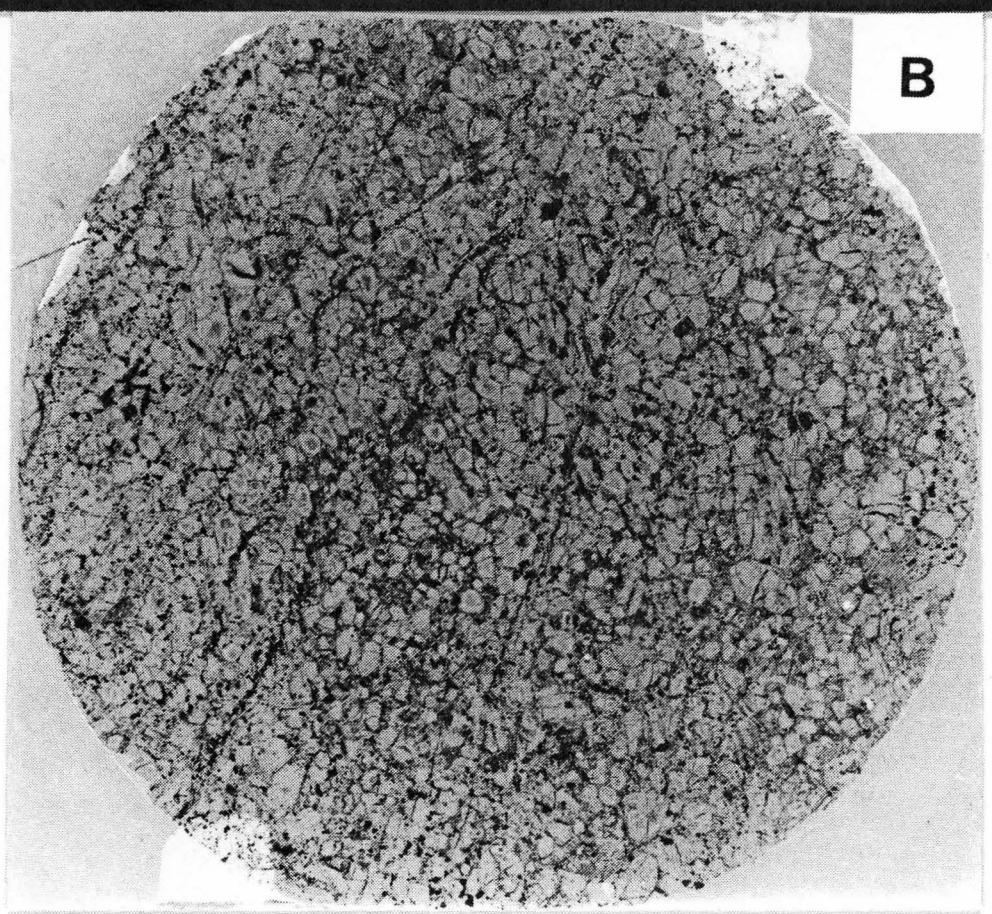
B

serpentine pseudomorphs of olivine (Fig. 10b). Compositionally, the magnetite is virtually identical to that which rims the chromite and occurs in the groundmass of the upper flow layers (Table 5). The secondary magnetite probably formed as a byproduct of the serpentinization of the olivine (Toft et al., 1990).

# Chapter 4

## Physical Methods and Results

### *4.1 Magnetics*

A grid was established such that the base of the BCF is at approximately 8N on the grid, and the flow top is at approximately 92N. Two GSM-18 proton precession magnetometers were used to conduct the magnetic survey; one for mobile station readings and the second for base station readings. Down and cross line readings were taken at 2.5 m intervals (station spacing = 5 m). Base station readings were recorded every 3 seconds and were later used in a data reduction routine to correct for diurnal drift. A grid was established with 5, 115 m lines at 5 m station and line spacings. The following parameters were used for the survey:

| | |
|---|---|
| PARAMETER MEASURED | Earth's total magnetic field |
| INSTRUMENT | GSM-18 Proton Precession Magnetometer |
| RESOLUTION | 0.1 nT |
| ACCURACY | 0.2 nT (over operating range) |
| RANGE | 20000 - 100000 nT |
| GRADIENT TOLERANCE | up to 5000 nT/meter |
| READING INTERVAL | 2.5 m down and across lines |

The GMS-18 units are easily portable with built in processors and memory, enabling complete field data storage and retrieval. Drift corrections were made by the instrument automatically and no further data reduction was necessary. Proton procession magnetometers do not require sensor levelling and the survey was performed quickly with a minimum time between consecutive readings of only 3 seconds.

FIGURE 11. Residual magnetic field anomaly map. Note the podiform shaped anomaly centred at approximately 53N on the grid. Stratigraphically this anomaly correlates with the main PGE mineralization in the Boston Creek Flow.

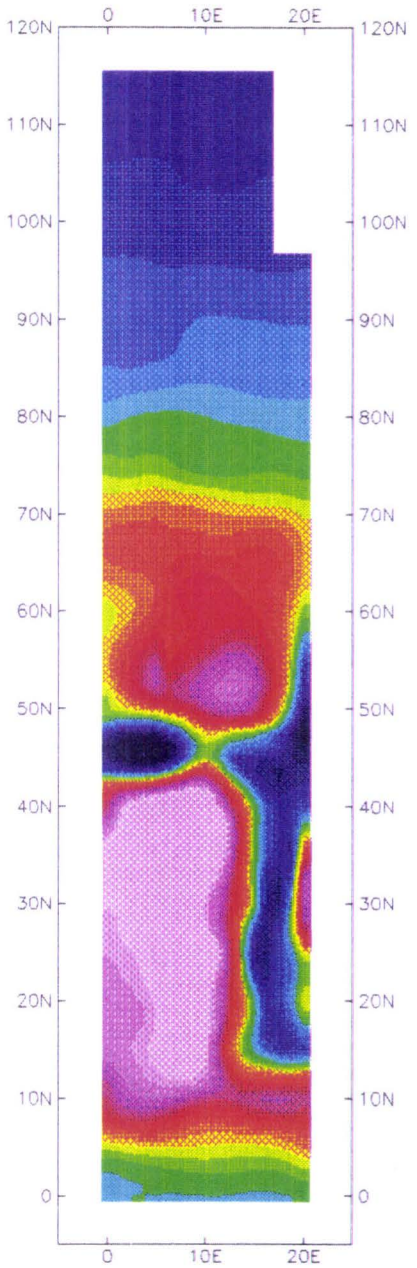


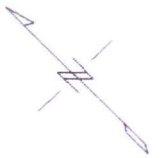

Scale 1:500

5 0 5 10

(meters)

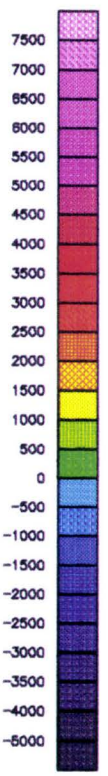


Residual Total Magnetic Field (nT)

| Residual Total Magnetic Field (nT) |
| --- |
| **Boston Creek Flow** |
| Michelle Larson<br>McMaster University |

Cross and down line data are presented separately in Tables B-1 and B-2 (Appendix B) because: (i) separate data sets ensures that single point anomalies are not represented in subsequent plots and (ii) the griding algorithm used for analysis and magnetic map production is incapable of handling a data file with both sets of data. Single point anomalies were eliminated by adding the two grids together and taking an average of the measured values at every point. The down and cross line grids were merged using Boolean algorithms to produce Figure 11. Profiles are normalized to the regional field of 59500 nT.

*4.2 VLF*

This survey was conducted along the same grid as the magnetic survey with readings taken along lines at 2.5 m intervals. The VLF-EM survey was carried out using the following parameters:

| | |
|---|---|
| INSTRUMENT | GEONICS EM-16 |
| TRANSMITTER STATIONS | Seattle and Annapolis (stations 1 and 2) |
| PARAMETERS MEASURED | in phase-dip angles, quadrature |
| FREQUENCY | 24.8 kHz (1) and 21.4 kHz (2) |

VLF (very low frequency) works on the principal that a very low frequency wave will "shift" in phase when it encounters a change in conductivity of the medium through which it is travelling (Telford et al., 1976). The receiver for detecting VLF signals measures a tilt angle and a quadrature component. A clinometer on the instrument allows tilt angle measurement while the quadrature or "out of phase" component is read from a dial on the instrument as a percent plus or minus. The VLF signals (5 to 25 kHz) are transmitted from permanent ground stations such as those at Seattle and Annapolis and are usually used for air

FIGURE 12. VLF profile. Station 1, Seattle Washington. Noisy profile.

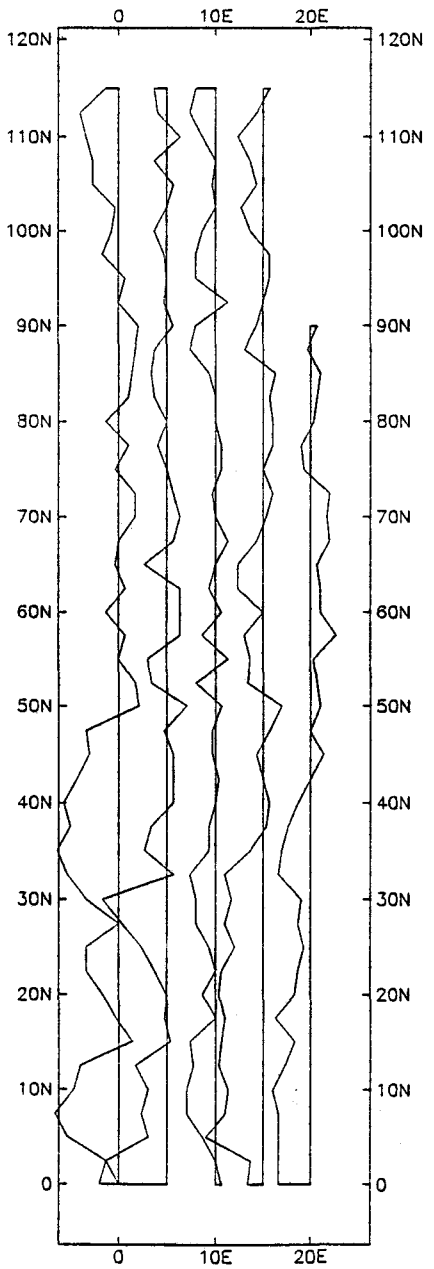


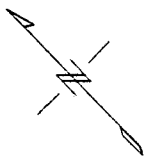

Scale 1:500

5 0 5 10

(meters)

| VLF Profiles |
| --- |
| Boston Creek Flow<br>Station 1 - Seattle, Washington |
| Michelle Larson<br>McMaster University |

FIGURE 13. VLF profile. Station 2, Annapolis Maine. Note that the signal flattens out between 40 and 50N along the grid. The olivine cumulate below this area appears to be conductive while the overlying rocks are not.

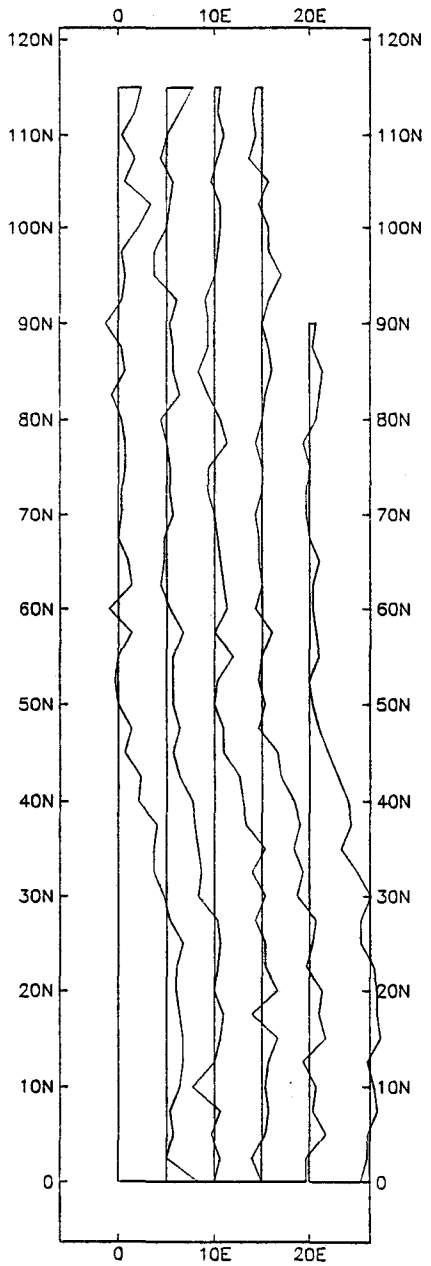


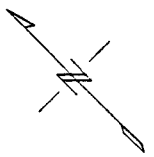

Scale 1:500

5 0 5 10

(meters)

# VLF Profiles

Boston Creek Flow
Station 2 - Annapolis, Maine

Michelle Larson
McMaster University

and marine navigation. Geologically, VLF is a very useful prospecting tool especially for locating massive sulfide deposits.

The survey results are listed in Table B-3 (Appendix B), and the profiles are presented in Figures 12 and 13. The VLF profiles obtained using Station 1 are quite noisy, suggesting that the direction of the survey was not in the direction of the transmitting station. To maximize the EM response or to minimize noise, the survey should be conducted such that the traverse lines are parallel to the direction to the station; this maximizes coupling between the transmitter and the receiver. This was not possible to do if a complete stratigraphic section was to be traversed across the flow, and hence a clear signal was sacrificed for stratigraphic continuity.

### *4.3 Susceptibility*

Volume magnetic susceptibility measurements were made using a Bartington MS.2B. susceptibility meter on 61, 2.4 cm diameter drill core samples taken from outcrop along line 0E of the surveyed transect. The volume susceptibility (K) of the drill core samples was measured with instrument accuracy of 1% and precision of $2 \times 10^{-7}$ cgs. Low frequency measurements were made for each of the samples. Null readings were taken after every five readings and variations were negligible.

In the BCF magnetite, titaniferous-magnetite and chromite are the possible major contributors to the susceptibility of the rock. Magnetite, however, is the main phase that

controls the susceptibility because of its abundance relative to chromite. Grain size, dissemination, modal percent and mineral composition are all variable parameters which need to be considered when examining the susceptibility data. If the composition of the magnetic phase is the same, then the grain size is the most important factor. Susceptibility varies from low to high for a fine grained mineral and coarse grained mineral respectively (Parry, 1965; Dunlop et al., 1973). This reflects the size of the individual magnetic domains which make up the mineral. When placed in an alternating field, large magnetic domains are easily shifted and are in this way, more susceptible to a magnetic field. Hence, the Fe-Ti oxide grains with very coarse exsolution, like those in the TMC, are more susceptible than those at other stratigraphic levels.

The results of the susceptibility measurements are listed in Table B-4 (Appendix B) and a profile of the measured volume susceptibility is plotted in Figure 14 along with the different lithologies. The gap between 10 and 35 m below the flow top is a reflection of a more sparse sampling density. Sixteen samples were collected from the spinifex-textured clinopyroxenite, but they were not collected at evenly spaced intervals. When the data was smoothed as discussed above, the sampling density problem became evident, and therefore, some samples were omitted from the plot. For the purpose of this thesis, the spinifex-textured clinopyroxenite is of little significance as it does not host any PGM or contain a large volume of magnetite.

FIGURE 14. Susceptibility versus lithology. The TMC is characterized by a very high susceptibility. Three patches in the gabbroic layer are evident in the profile.

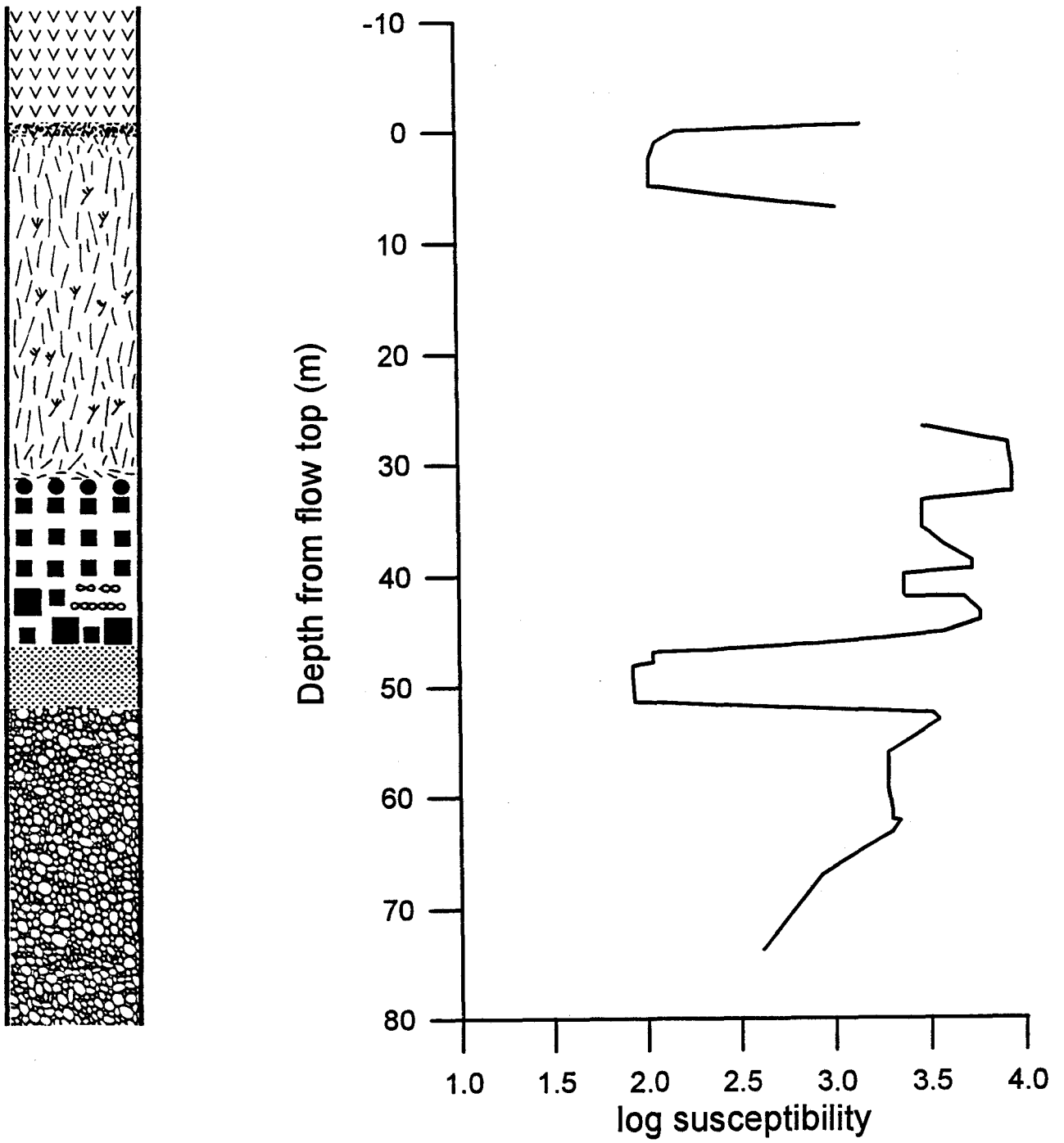
-10
0
10
20
30
40
50
60
70
80
Depth from flow top (m)
1.0
1.5
2.0
2.5
3.0
3.5
4.0
log susceptibility

*4.4 Interpretation*

The magnetics map shows a very large magnetic high (> 7500 nT) between 10 and 40 N which is bound on the northeast and southeast margins by two very low intensity zones (shown in dark blue on Figure 10). The magnetic high corresponds with the olivine cumulate layer at the base of the BCF and the magnitude of the anomaly is directly related to the high proportion of fine grained, end-member magnetite (up to 10% modal%) within the layer. A fault which cuts up through the olivine and clinopyroxene cumulates, terminates in the gabbroic layer and correlates with the position of the SE trending magnetic low. The fault may have acted as a fluid pathway or channel and as a result the magnetic in this area may have been altered or destroyed. Maghemite or hematite may be developed but no samples have been collected from this area to confirm this.

The magnetic intensity decreases gradually from 50 N to the northernmost margin of the grid except where two podiform (up to 7 m in diameter) magnetic highs occur within the middle of the study area, centred about 53 N. The background magnetism is generated by titaniferous magnetite which decreases in abundance toward the flow top. It should be noted that ilmenite does not impart any geophysical response in the magnetic methods employed in this study, and the concentrations of chromite and primary low-titanium magnetite are of so low that their contribution to the geophysics is negligible. It is therefore only the magnetite portion of the Fe-Ti oxide grains, and the secondary magnetite that play an important role in this study.

The isolated magnetic highs are located within the lower gabbroic layer and correlate with a stratigraphic position of 42.0 to 46.6 m below the flow top. This is the area that is known to host the main PGE mineralization (45.2 to 46.7 m, Table 2). The location and extent of the PGE mineralized horizons has been previously determined through extensive geochemical, petrological and lithological studies by Stone et al. (1987, 1993, in review). The podiform shaped anomalies are a result of high concentrations of titaniferous magnetite with which the PGM are known to be spatially associated. The areal extent of the podiform shapes is much larger than the area previously defined by geochemical sampling, which is known to host high concentrations of PGM. This may simply be a result of sampling density; the magnetic mapping was performed over a much larger area than outcrop sampling. Further geochemical sampling and microprobe work is necessary to confirm the extent of mineralization. It is clear however, that detailed magnetic mapping can locate titaniferous magnetite-rich pods with which PGM may be associated. Whether PGM occur in these pods is dependent on various factors including partition coefficients, initial sulfide/PGE ratios, etc. The association with titaniferous magnetite is only a key in identifying potentially mineralized sites.

The VLF profiles from both stations show a relatively large deviation from zero until around 40 and 50N on the grid where the signal begins to flatten out and hover about zero (indicating that there is no or little conductivity). Where the signal flattens out, this correlates stratigraphically with clinopyroxene cumulate layer indicating that the rocks above this point are virtually nonconductive.

The BCF consists of rocks that are sulfide-poor (<0.5 modal% sulfide). Silicate and oxide minerals are much more abundant but less conductive than sulfides. Therefore, the VLF method did not prove to be very useful in determining the different lithologies within the flow.

Although there appears to be a shift in the signal, it can not be determined whether the shift is a result of variations in oxide grain sizes, dissemination, modal percent or mineral composition. In general, oxides are conductive but because of their high concentration and distribution throughout the BCF, it seems unlikely that any significant variation should be evident across strike. It is possible however, that the conductivity may have been increased in this area below 40 and 50N by a higher porosity and water content. This cannot be accurately determined at this stage; however, considering that the olivine cumulate below this area was completely serpentinized, porosity had to be relatively high for this type of fluid migration. Alteration of magnetite (both Fe- and Ti-rich phases) in the clinopyroxenite cumulate, to titanite and amphibole was a direct result of the motion of the serpentinizing fluid. Alteration at higher stratigraphic levels, especially in the spinifex-textured clinopyroxenite is also quite pronounced as a result of fluid channelling between the oriented clinopyroxene grains. It would seem that all of the lithologic layers show a relatively high degree of porosity and it would seem unlikely that this would cause the conductive deviation in the southern part of the grid. A possible implication of the oxide textures is that the net-like texture of the magnetite grains in the olivine cumulate should be significantly more conductive than the unevenly disseminated magnetite which occurs at higher stratigraphic

levels in the flow, even considering the grain size variation. This appears to be the best explanation for the VLF profiles. The VLF method was not helpful in defining the mineralized horizons, but was capable of separating the olivine cumulate from the other lithostratigraphic layers.

No correlation between volume magnetic susceptibility and the electromagnetic conductance of the flow can be established. However, changes in volume susceptibility mimic changes in lithology (Fig. 14). Variation in magnetic susceptibility, as previously discussed, is a function of the grain size of magnetite (both primary exsolved and secondary phases), and hence, the variation in volume susceptibility reflects grain size variation of magnetite within the different lithologies of the BCF.

The olivine cumulate contains very fine grained magnetite, and should therefore have a comparatively low volume susceptibility. The high magnetite content in this layer appears to counteract the grain size effect, as well, the magnetite content decreases slightly up through the layer because of the greater accumulation of olivine toward the base during fractionation and crystallization. The overlying rocks have a maximum of 15 modal% Fe-Ti oxide (in TMC) but only about half of this is magnetite (the remainder is ilmenite), whereas the olivine cumulate contains up to 10 modal% magnetite. Volume susceptibility of the olivine cumulate layer increases from its base up to the contact with the overlying clinopyroxene cumulate layer. This may simply reflect a slight increase in the magnetite grain size toward the top of this layer.

The clinopyroxenite and approximately the lower 2 m of the gabbroic layer are characterized by a very low susceptibility. In this area, there is typically less than 1 modal% magnetite in the groundmass and up to 5 modal% titaniferous magnetite, of which approximately 3 modal% is magnetite. The magnetite component is very fine grained in the Fe-Ti oxides. This coupled with the low proportion of magnetite reflects the very low susceptibility of these rocks.

Significant variation in susceptibility is observed in the gabbroic layer, but a high susceptibility is maintained throughout. The high volume susceptibility is caused by: (i) a higher proportion of magnetite (up to 15% in TMC) and (ii) the more coarsely developed magnetite of the Fe-Ti oxide. The TMC with the most coarsely developed magnetite, shows a much higher susceptibility than the other rock types within the layer. Note that three occurrences of TMC are evident in the diagram. TMC does not only occur in the lower part of the gabbroic layer but also as irregular patches at higher stratigraphic positions. Clearly, susceptibility mapping in exploration for PGE in sulfide-poor environments associated with high concentrations of titaniferous magnetite is quite important. The very high susceptibility of these titaniferous magnetite-rich horizons could be quickly and easily established in the field with a hand held susceptibility meter. The identification of high susceptibility areas is no guarantee that Pt-metal mineralization is hosted in these rocks; it simply an indicator of high concentrations of titaniferous magnetite, in this case, with which PGM may be associated. Susceptibility mapping should be used as a guide in the exploration for PGE mineralization in similar rock types.

# Chapter 5

## Paleomagnetic Methods and Results

### *5.1 Rock Magnetism*

Paleomagnetic methods make use of the phenomenon that certain minerals are capable of retaining a record of the past direction of the Earth's magnetic field. Certain of these paramagnetic minerals with many unpaired electrons, called ferromagnetics, have a number of magnetic domains which are coupled by the interaction of the magnetic field with the unpaired electrons. These interactions are only possible at temperatures below the *Curie Temperature*. At temperatures exceeding the *Curie Point*, magnetic bonding is prohibited and the substance behaves as an ordinary paramagnetic.

Within each domain there is an alignment of the magnetic dipoles and this causes the domain to have a net magnetic direction. When placed in a magnetic field, domains with their net magnetic direction oriented parallel to the direction of the external field, grow larger at the expense of domains aligned in the opposite direction. When the external field is removed, the overall magnetic direction that remains is referred to as the permanent or remanent magnetization (Keary and Vine, 1990).

### *5.2 Primary and Secondary Magnetization*

The concept of natural remanent magnetization (NRM) as it relates to igneous bodies has been previously described in detail (eg. Telford et al., 1976; Collinson, 1983; Piper, 1987). In most rocks, NRM is carried by members of the iron-titanium oxide series of

minerals. Primary NRM for igneous rocks is generally obtained by thermal remanent magnetization (TRM), during which a lava or intrusion crystallizes and the constituent magnetic minerals cool through their Curie or blocking temperatures in the ambient magnetic field. The orientation of the TRM acquired through crystallization was parallel to the ambient magnetic field at the time of formation. The ambient field is relatively weak, but is stable and therefore TRM has a strong resistance to demagnetizing influences, and is commonly preserved even after millions of years. In the BCF, titaniferous magnetite is the main oxide phase which would contribute to the TRM.

PTRM or partial thermal remanent magnetization is acquired by rocks which are subjected to burial or are adjacent to an intrusion and undergo a rise in temperature. If this temperature exceeds the blocking temperature of any magnetic grains present they will acquire a partial thermoremanence when they cool (effectively, a second TRM). Considering the proximity of the Round Lake Batholith and the metamorphism to lower greenschist facies, it is likely that PTRM is a major factor in the history of magnetization of the BCF.

CRM or chemical remanent magnetization is a second type of primary magnetization that can be acquired by igneous body by either the precipitation of a magnetic mineral out of solution or by alteration of one mineral to another. An example of CRM specific to the BCF would be the remanent magnetization acquired by the Fe-rich magnetite which formed by the alteration of olivine to magnetite + serpentine by hydrous fluids, or the CRM of the chromite by the alteration of its parent Cr-spinel.

Secondary components of magnetization may also be acquired over time by physical processes. Viscous remanent magnetization (VRM) is acquired when a rock is subjected to an external field which is at an angle to the previous orientation of the magnetic field. This effect would be expected for example, in a rotated terrain. On a small scale, the suite of specimens collected from the BCF should all have the same VRM component.

The rocks involved in this study have been subjected to prehnite-pumpellyite or lowermost greenschist facies of regional metamorphism (Jolly, 1980). Pullaiah et al. (1975), showed that magnetization of single-domain pure magnetite should survive this type of metamorphism provided there has been no chemical change of the iron minerals. In this case, the expected NRM contained in this study may be TRM. Alternatively, secondary magnetization events may also have occurred. The vector sum of primary and secondary magnetization as they exist at present in the rock is called the *natural remanence magnetization.* Even though the NRM of rocks consists of a combination of these components, only the primary NRM is of interest in paleomagnetic interpretation. It is therefore necessary to remove the secondary components to isolate the primary NRM. This is done by partial demagnetization.

### *5.3 Field and Analytical Procedures*

For this study, 61 drill cores with a 2.4 cm diameter representing each of the lithologies were taken with a water cooled, gasoline powered drill along line 0E of the survey grid. The cores were oriented with both magnetic and sun compasses. The magnetic

compass readings were however, generally unreliable because of the overwhelming magnetic intensity of the rocks.

The samples were thermally demagnetized in a stepwise manner up to 600°C in field-free space using a Molspin ring fluxgate spinner magnetometer. Rock specimens were spun at 6 Hz for 6 seconds in six mutually orthogonal orientations (each of the three axes in two directions) with an instrument accuracy of $0.5 \times 10^{-7}$ A/m$^2$. The six orientations provided four determinations of the X, Y and Z components; two, of each sign. The intensity, declination and inclination of the magnetization was then obtained from the average values of the X, Y and Z components.

The changes in NRM that occurred during thermal demagnetization are illustrated with demagnetization curves (normalized NRM intensity versus treatment or temperature; Fig. 15), stereographic projections and Zijderveld diagrams (Zijderveld, 1967). The NRM intensity of many of the study specimens is quite high, reflecting the generally fine grain size and high concentration of magnetic phases. This is discussed in further detail below. In each of the examples shown in Figure 15, there appears to be two temperatures at which the intensity noticeably decreases; 350°C and 550°C. The 350°C drop in NRM intensity can be explained in terms of different mineralogy and therefore different Curie Temperatures. In the olivine cumulate (samples MSL-5, MSL-8 and MSL-13), chromite is a ubiquitous phase and has a known Curie point 350°C. Once the Curie Point of a mineral is reached, it no longer carries a magnetic orientation, unless subjected to an external field and

FIGURE 15. NRM versus treatment. Decreases in intensity occur at 350°C and approximately 575°C. These are the Curie points of chromite + titaniferous magnetite, and end-member magnetite respectively.

MSL-5

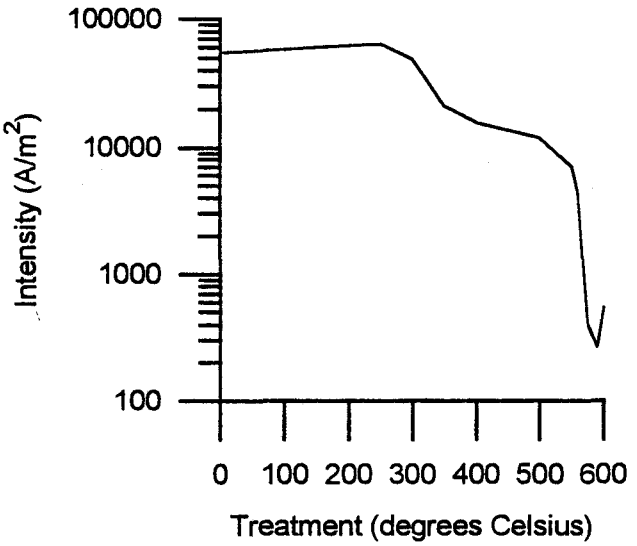


MSL-8

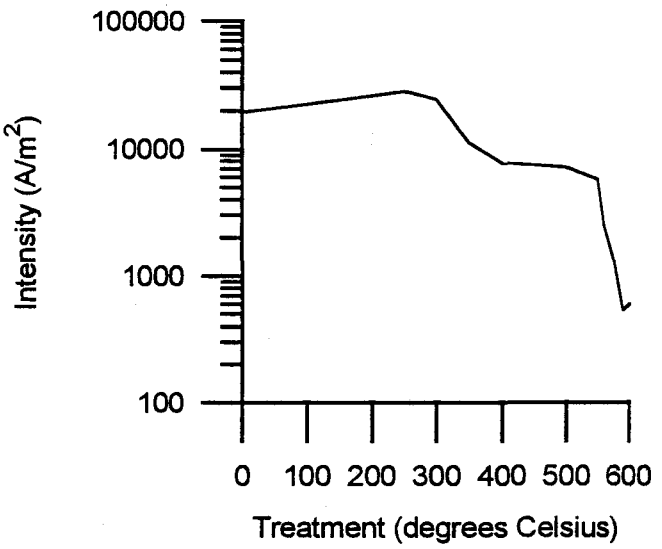


MSL-13

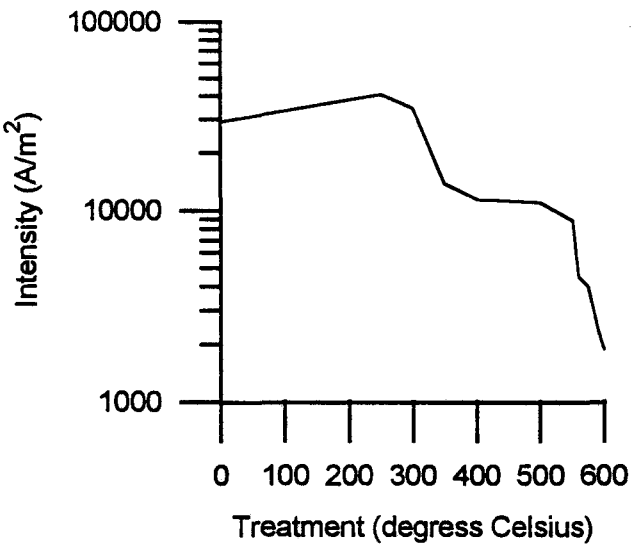


MSL-34

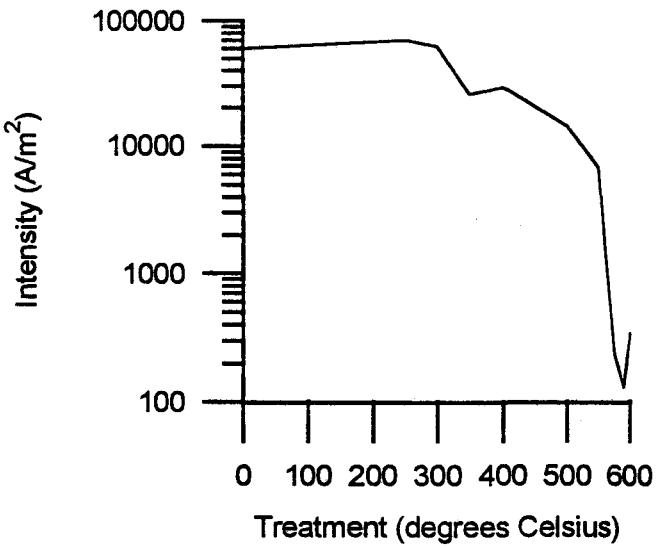


MSL-47

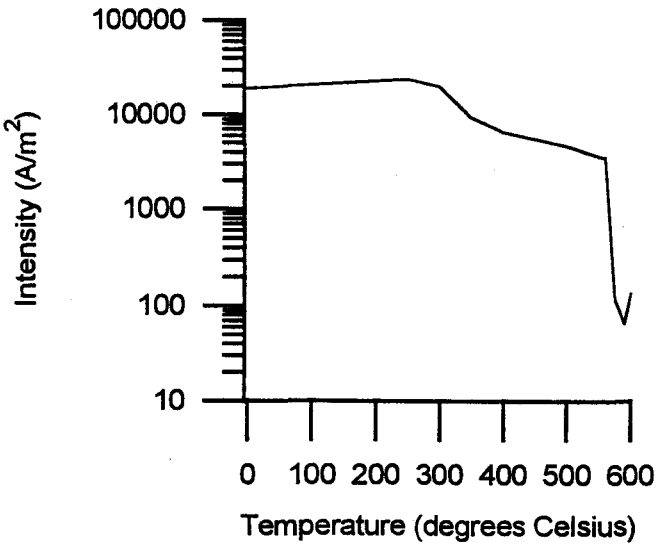


MSL-54

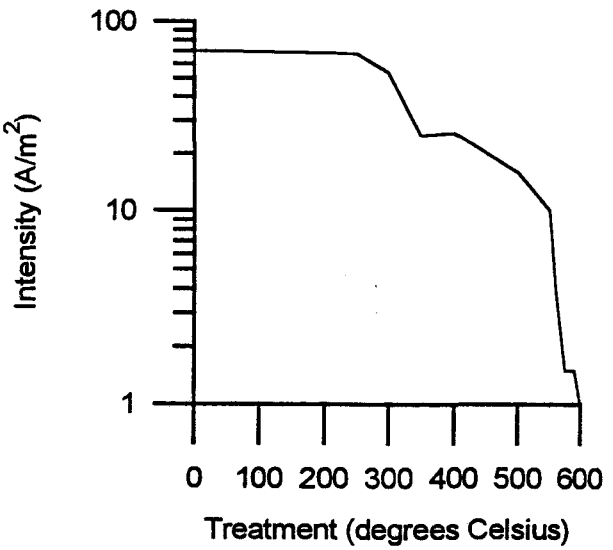

this is why the NRM intensity decreases at this point. No chromite is found in the clinopyroxene cumulate nor the gabbroic layer (sample MSL-34). Titaniferous magnetite is likely responsible for the intensity change at 350°C in these rocks. The predicted Curie Point of high Ti magnetite is between 200°C and 250°C (Piper, 1987) but is entirely dependent on the titanium content. The titanium content of the BCF magnetite in these layers is lower than the amount associated with the 200°C temperature. Pyrrhotite is another mineral which has a Curie Point at 350°C, but in the BCF is only present in trace amounts in the spinifex-textured clinopyroxenite and therefore is not responsible for the change in intensity. Both titaniferous magnetite and chromite occur in the spinifex-textured clinopyroxenite (samples MSL-47 and MSL-54) and are believed to be responsible for the decrease in intensity at this treatment level.

Pure end-member magnetite has a Curie Temperature of 578°, whereas the temperature determined in this experiment for magnetite was only 550°C. This discrepancy is explained in part by impurities in the magnetite, but the main source of error is associated with the furnace. At approximately the 550° demagnetization step, the thermocouple inside the furnace became dislodged from its standard position and was not registering the temperature properly. As well, the thermocouple was broken at some point in the demagnetization sequence and a replacement found. Some of the samples were therefore subjected to temperatures higher and/or lower than the set treatment temperature. The calibration of the new thermocouple was also done rather hastily and may also have been in err. Regardless of the problems at the high treatment temperatures, the temperature at which

the NRM intensity decreases the most, is representative of the Curie Point of magnetite.

The Zijderveld diagrams were constructed using the demagnetized results in order to determine the paleomagnetic directions by principal component analysis (Kirchsvink, 1981). A computer program called LSQ1 was used for this purpose. These diagrams are a combination of intensity and directional change plotted on a common axis for a given specimen. The intensity of each projected NRM component (after each demagnetization step) is proportional to the distance from the origin to the corresponding point. As demagnetization proceeds, the points on each plane will trace out paths according to the changes in declination, inclination and intensity. One and occasionally two lines of were fit to the NRM decay curve. The lines were generally anchored to the origin but in the case when two lines were fit to the data set, only one line was anchored. The declination and inclination for a line were calculated and considered to be the characteristic or NRM of the specimen. Variable directions were obtained and the results were subdivided by stereonet analysis. Approximately one-third of the specimens had to be rejected from the analyses. These samples had paleodirections which were due north and east, and were not specific to any one rock type. This may be a natural phenomenon, but seems unlikely. The large concentration of magnetite in these samples may have had the effect of saturating the measurement coil in the spinner magnetometer with respect to these two components and the resulting paleodirection (due NE) is therefore incorrect.

A summary of the experimental results are listed in Table 7, and the derived intensities and directions of the primary NRM of all 61 specimens are shown in Table C-1 (Appendix C). The samples were subdivided into four groups based on direction and the mean pole for each group was calculated using the Stereo subroutine, a Rockworks application. Group 1 contains both normal and reversed polarity samples with equivalent orientations. Eigenvectors were used in determination of the pole orientation and not Fisher statistics. The distribution of poles was not spherical as dictated by Fisherian statistics, but was more elongate or elliptical and therefore, best defined by Eigenvalues. The mean pole and Eigenvalues for each group are listed in Table 8 and shown in Figure 16.

Initial volume susceptibilities were used in the calculation of the Köenigsberger Q ratio (intensity ratio of NRM / induced magnetization). A constant of 0.55 was used in the calculations. NRM and Q are plotted in Figures 17 and 18 versus stratigraphic position. Data was smoothed using a three point running median routine. A running median filter was used rather than a running average routine because it does not introduce new (and possibly false) values into the data set. The gap in the plots between 10 and 35 m below the flow top is again, a reflection of the sampling density as discussed in the susceptibility section.

Table 7. Direction and pole of selected demagnetized samples

| Sample | Depth[a] (m) | Group | Direction | | Pole | |
|---|---|---|---|---|---|---|
| MSL-57 | 4.97 | 3 | 301.0 | 0.1 | 166.1 | 20.2 |
| MSL-56 | 6.00 | 1 | 128.2 | -25.0 | 169.0 | 34.9 |
| MSL-54 | 8.50 | 1 | 148.0 | -33.7 | 152.6 | 50.7 |
| MSL-53 | 10.00 | 3 | 314.3 | 11.3 | 157.8 | 32.6 |
| MSL-52 | 11.00 | 3 | 339.5 | -9.1 | 125.1 | 34.4 |
| MSL-51 | 12.50 | 3 | 325.2 | -3.8 | 142.2 | 31.6 |
| MSL-47 | 28.25 | 4 | 239.0 | -5.2 | 212.4 | -22.2 |
| MSL-45 | 31.25 | 4 | 228.2 | -33.2 | 210.4 | -40.9 |
| MSL-43 | 32.60 | 3 | 285.5 | -10.9 | 174.8 | 6.1 |
| MSL-42 | 33.35 | 4 | 225.1 | -21.5 | 219.1 | -37.4 |
| MSL-40 | 37.25 | 4 | 237.6 | -29.8 | 203.8 | -33.3 |
| MSL-39 | 38.75 | 3 | 305.1 | -6.7 | 160.4 | 19.9 |
| MSL-37 | 39.95 | 1R | 343.8 | 27.8 | 154.0 | 45.2 |
| MSL-35 | 41.95 | 3 | 317.1 | -3.9 | 150.3 | 27.7 |
| MSL-34 | 42.00 | 3 | 315.1 | -13.4 | 149.4 | 22.5 |
| MSL-33 | 43.30 | 3 | 322.3 | 3.0 | 147.1 | 33.3 |
| MSL-32 | 44.05 | 1 | 125.5 | -36.4 | 177.3 | 38.4 |
| MSL-29 | 46.15 | 3 | 342.2 | -12.5 | 121.5 | 33.5 |
| MSL-28 | 46.65 | 3 | 321.9 | -15.4 | 142.4 | 24.8 |
| MSL-26 | 47.30 | 1 | 144.2 | -33.0 | 156.7 | 48.2 |
| MSL-25 | 47.55 | 3 | 280.1 | 5.2 | 184.3 | 8.7 |
| MSL-24 | 47.75 | 3 | 309.7 | -9.1 | 155.6 | 21.5 |
| MSL-23 | 48.00 | 3 | 282.3 | -9.5 | 177.7 | 4.6 |
| MSL-22 | 48.15 | 3 | 300.6 | -11.6 | 162.7 | 15.2 |
| MSL-21 | 48.40 | 2 | 229.8 | 36.0 | 235.5 | -8.8 |
| MSL-20 | 48.90 | 2 | 225.3 | 45.0 | 240.4 | -5.1 |
| MSL-14 | 58.75 | 2 | 254.3 | 50.2 | 222.1 | 13.1 |
| MSL-13 | 59.35 | 2 | 217.7 | 50.4 | 248.5 | -3.9 |
| MSL-12 | 61.35 | 2 | 257.1 | 28.6 | 209.8 | 2.9 |
| MSL-11 | 62.10 | 2 | 245.3 | 51.4 | 228.9 | 9.1 |
| MSL-9 | 63.25 | 1R | 286.8 | 35.5 | 191.5 | 25.6 |
| MSL-8 | 67.00 | 1R | 313.6 | 30.3 | 166.5 | 40.6 |
| MSL-7 | 73.75 | 1R | 292.9 | 31.7 | 185.0 | 27.9 |
| MSL-5 | 79.75 | 1 | 144.0 | -27.3 | 154.0 | 45.2 |
| MSL-3 | 88.75 | 1 | 157.2 | -33.2 | 139.8 | 54.8 |
| MSL-1 | 96.25 | 1 | 169.8 | -39.2 | 121.2 | 62.9 |

[a]Depth from flow top.

R = reversed polarity.

Table 8. Mean pole and Eigenvalues

| Group | Pole | | Eigenvalues | | |
|---|---|---|---|---|---|
| | | | 1st | 2nd | 3rd |
| 1+1R | 162.1 | 45.8 | 0.903 | 0.094 | 0.003 |
| 2 | 235.0 | 0.8 | 0.952 | 0.043 | 0.005 |
| 3 | 153.6 | 25.1 | 0.974 | 0.021 | 0.005 |
| 4 | 31.4 | 33.6 | 0.979 | 0.015 | 0.006 |

R = reversed polarity.

FIGURE 16. Paleopole distribution. Group 1 contains both reversed and normal poles. Note the elongate distribution of poles in Groups 1 and 3.

Group 1 Poles

Mean Pole: 162.1 N, 45.8 E

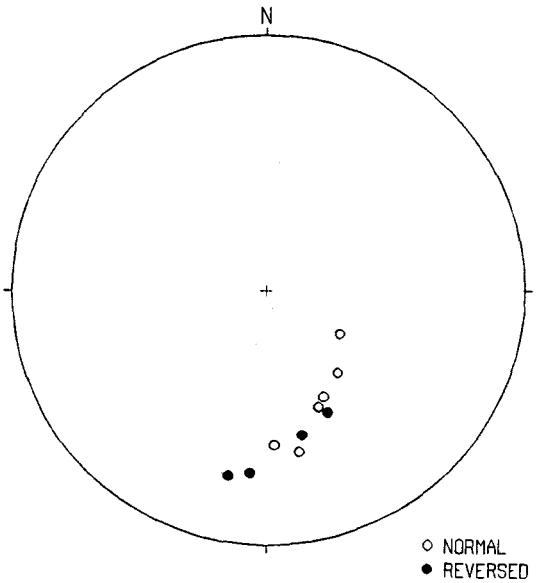


Group 2 Poles

Mean Pole: 235.0 N, 0.8 E

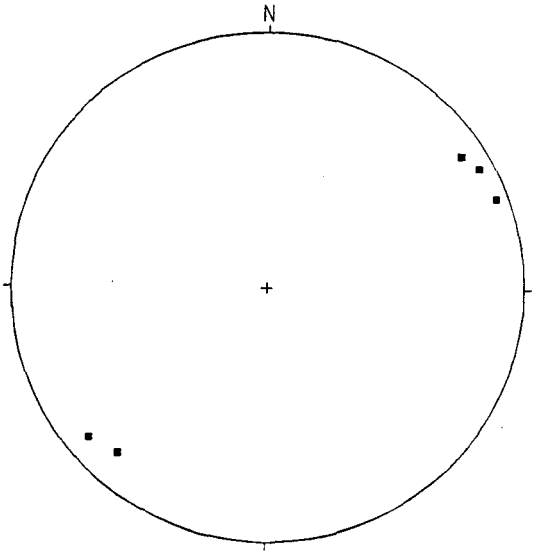


Group 3 Poles

Mean Pole: 153.6 N, 25.1 E

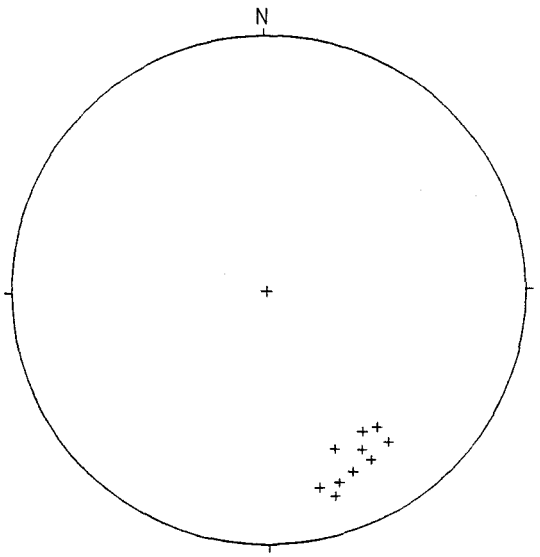


Group 4 Poles

Mean Pole: 31.4 N, 33.6 E

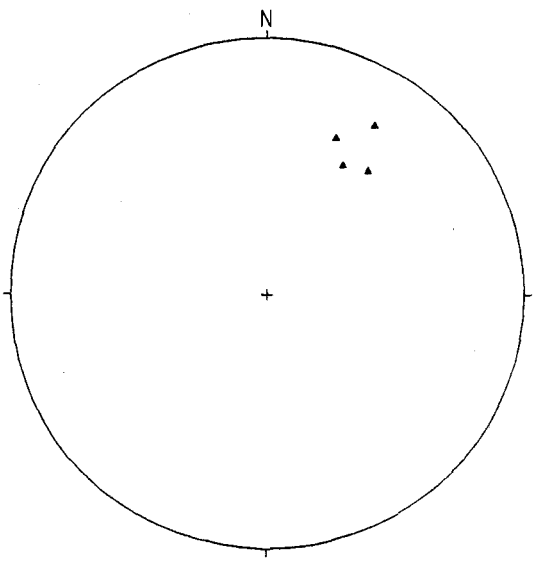

FIGURE 17. NRM versus stratigraphic position. TMC patches evident in the profile, similar to the susceptibility plot. The TMC is characterized by a high NRM intensity.

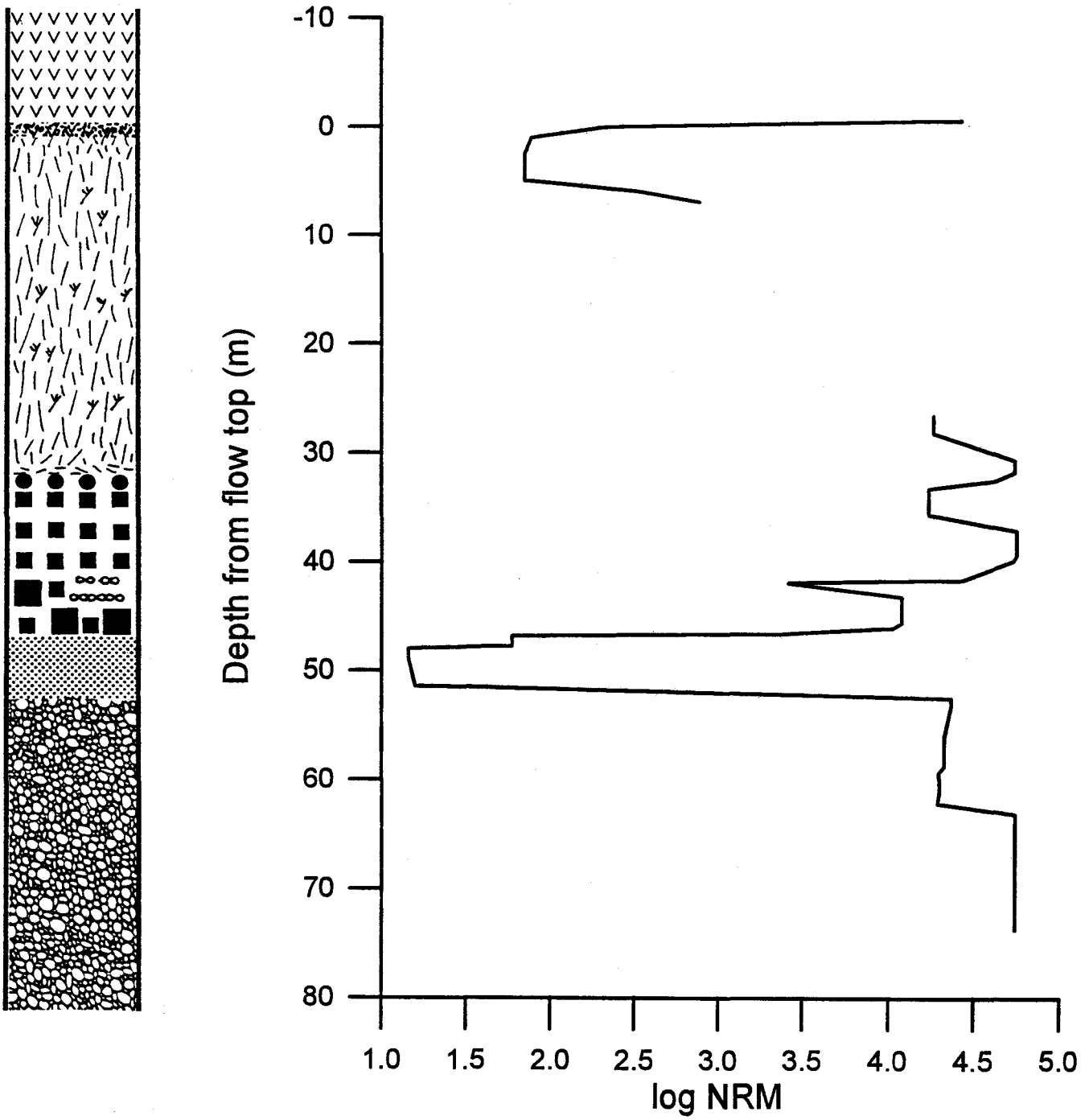
-10
0
10
20
30
40
50
60
70
80
Depth from flow top (m)
1.0
1.5
2.0
2.5
3.0
3.5
4.0
4.5
5.0
log NRM

FIGURE 18. Q versus stratigraphic position. The main PGE mineralization is evident in the profile along the gabbroic layer. The other TMC horizons are not readily apparent.

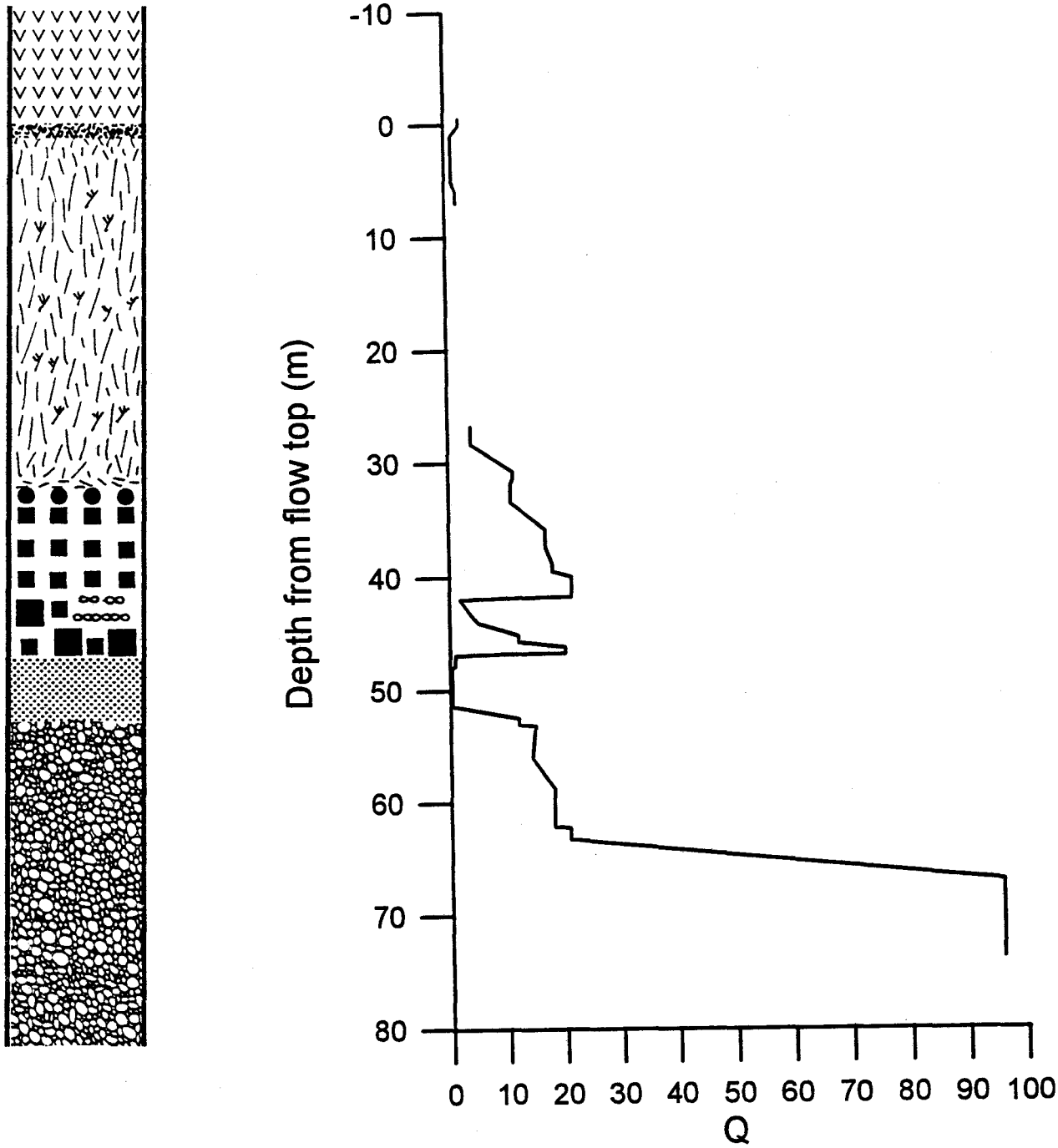
-10
0
10
20
30
40
50
60
70
80
Depth from flow top (m)
0
10
20
30
40
50
60
70
80
90
100
Q

## *5.4 Paleomagnetic Interpretation*

### *Paleopole groups and Archean Pole Wander*

The four different paleopole orientations roughly correspond to different lithologies as shown in Table 9 and Figure 19. The coloured blocks represent areas inferred to possess the same pole orientation. The olivine cumulate is characterized by Group 1 and 2 poles. Group 1 corresponds with the peridotite, and Group 2 roughly corresponds with the upper, amphibole peridotite. The clinopyroxene cumulate is characterized by Group 1, Group 2 and Group 3 poles. The lower part of the gabbroic layer is mainly characterized by Group 3, but the Group 1 orientation is also present. The spinifex-textured clinopyroxenite is characterized by Group 4 and Group 3 toward the base and top of the layer, respectively. The significant variation in the paleopoles suggests that the BCF has had a complex magnetization history. It is debatable whether the primary NRM is actually preserved; these poles may all be a result of CRM or PTRM. Nonetheless, the paleopole orientations allows for a clear distinction between the lithologies.

The reversal apparent in the Group 1 remanence directions is likely related to the serpentinization of the olivine cumulate. During serpentinization, fluids were pulsing through the olivine cumulate oxidizing the olivine and producing magnetite. The magnetite formed during this time likely recorded the reversal, that is, when the magnetite was formed the earth's magnetic field was in a reversed state. Further alteration or deformation effects on the magnetite in the olivine cumulate would probably have very little effect on the NRM, as this magnetite has a "hard" remanence. It has a hard or stable remanence because of the

Table 9. Lithology and remanence group

| Sample | Depth[a] (m) | Rock Type | Rock Layer | NRM Group |
|---|---|---|---|---|
| MSL-57 | 4.9 | spnfx | s cpy | 3 |
| MSL-56 | 6.0 | spnfx | s cpy | 1 |
| MSL-54 | 8.5 | spnfx | s cpy | 1 |
| MSL-53 | 10.0 | spnfx | s cpy | 3 |
| MSL-52 | 11.0 | spnfx | s cpy | 3 |
| MSL-51 | 12.5 | spnfx | s cpy | 3 |
| MSL-47 | 28.2 | spnfx | s cpy | 4 |
| MSL-45 | 31.2 | spnfx | s cpy | 4 |
| MSL-43 | 32.6 | gbr | a cpy | 3 |
| MSL-42 | 33.3 | gbr | gbb | 4 |
| MSL-40 | 37.2 | gbr | gbb | 4 |
| MSL-39 | 38.7 | gbr | gbb | 3 |
| MSL-37 | 39.9 | gbr | gbb | 1R |
| MSL-35 | 41.9 | gbr | gbb | 3 |
| MSL-34 | 42.0 | gbr | tmc | 3 |
| MSL-33 | 43.3 | gbr | tmc | 3 |
| MSL-32 | 44.0 | gbr | tmc | 1 |
| MSL-29 | 46.1 | gbr | tmc | 3 |
| MSL-28 | 46.6 | gbr | tmc | 3 |
| MSL-26 | 47.3 | gbr | gbb | 1 |
| MSL-25 | 47.5 | gbr | gbb | 3 |
| MSL-24 | 47.7 | gbr | gbb | 3 |
| MSL-23 | 48.0 | gbr | gbb | 3 |
| MSL-22 | 48.1 | cp cum | cpy | 3 |
| MSL-21 | 48.4 | cp cum | cpy | 2 |
| MSL-20 | 48.9 | cp cum | cpy | 2 |
| MSL-14 | 58.7 | ol cum | am prd | 2 |
| MSL-13 | 59.3 | ol cum | am prd | 2 |
| MSL-12 | 61.3 | ol cum | am prd | 2 |
| MSL-11 | 62.1 | ol cum | prd | 2 |
| MSL-9 | 63.2 | ol cum | prd | 1R |
| MSL-8 | 67.0 | ol cum | prd | 1R |
| MSL-7 | 73.7 | ol cum | prd | 1R |
| MSL-5 | 79.7 | ol cum | prd | 1 |
| MSL-3 | 88.7 | f bslt | t bslt | 1 |
| MSL-1 | 96.2 | f bslt | t bslt | 1 |

[a] Depth from flow top.

Rock type and rock layer are the same as in Table 1.

FIGURE 19. NRM characteristic remanence. The different lithologies are characterized by difference remanence directions. The shaded blocks are inferred to have the same paleopole orientation. The main PGE mineralized horizon exhibits two remanence directions suggesting a complex magnetization history of these rocks.

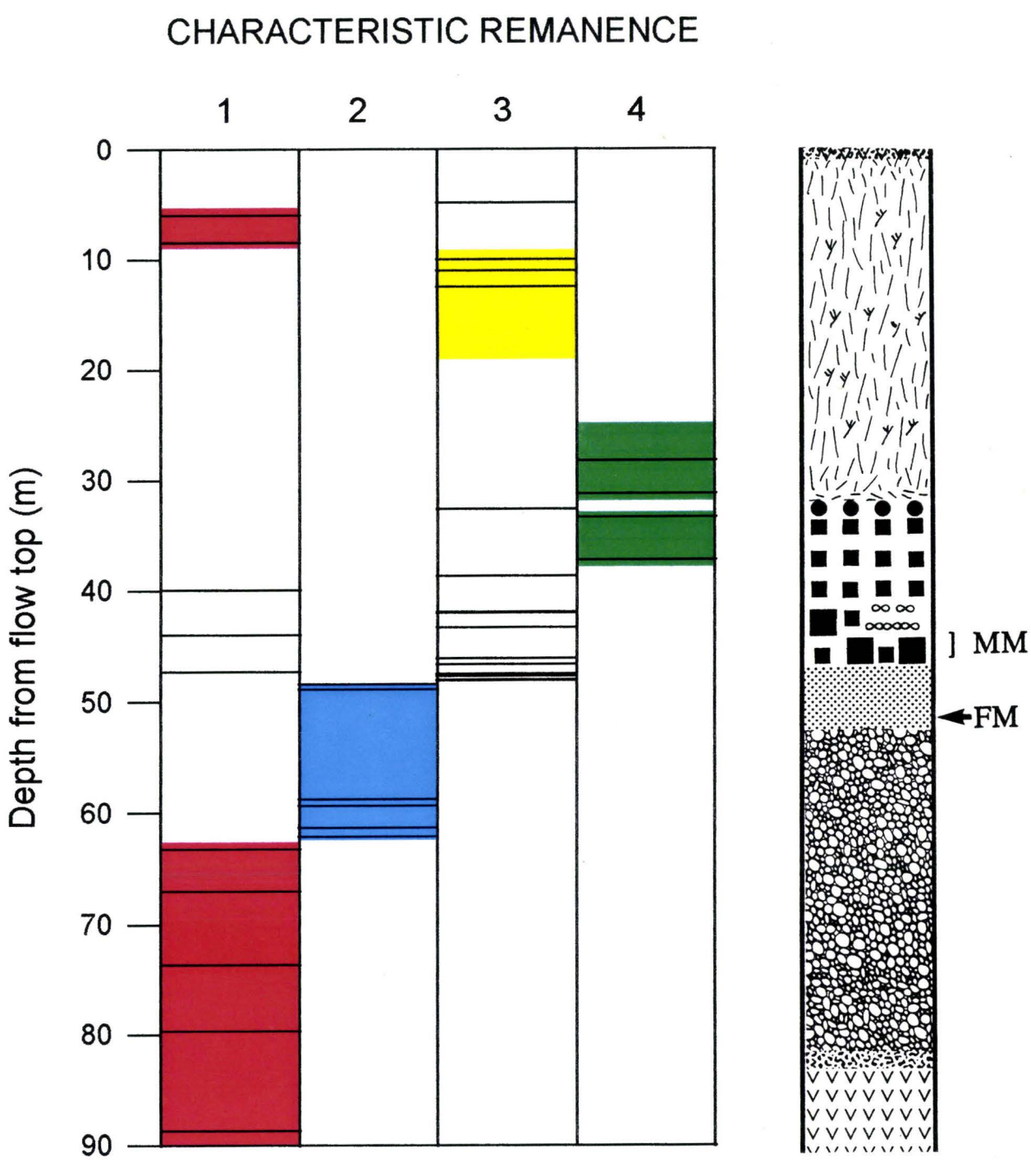
CHARACTERISTIC REMANENCE
1
2
3
4
0
10
20
30
40
50
60
70
80
90
Depth from flow top (m)
] MM
FM

grain size. There appears to have been either two episodes of serpentinization, or one that lasted a considerable amount of time. The latter possibility seems unlikely since serpentinization would have had to persist through a reversal and a period of normal polarity, this suggests that more than one episode of serpentinization likely resulted in the variable remanence directions found in the olivine cumulate. One event is characterized by the reversed and normal polarity of Group 1, and the second is that of Group 2. The order in which magnetization proceeded cannot be determined exclusively from the paleomagnetic data. It seems likely that the Group 1 event occurred first with the onset of serpentinization, and the second event pushed the serpentinizing front up further into the BCF, and resulted in Group 2 magnetization at higher stratigraphic levels within the olivine cumulate.

The Group 4 directions occur about the contact between the upper gabbroic layer and the spinifex-textured clinopyroxenite. This area is believed to have been a pathway for fluids as the BCF cooled. The flat-lying spinifex at the base of the spinifex-textured clinopyroxenite is believed to represent clinopyroxene grains which were originally perpendicular to layering, and were essentially broken off by the migration of fluids (Stone et al., in review). The remanence of this group may actually be the primary NRM. It is difficult to confirm this hypothesis because of the widespread alteration throughout the BCF. The top ten metres of the flow for example, display two remanence directions (both of normal polarity), which are likely related to different episodes of alteration. The clinopyroxene spinifex would have easily channelled fluids because of the subparallel orientation of the grains to the flow top.

Along with the significant pole variation, the four groups do not appear to follow the apparent polar wander path as described by Irving and Naldrett et al. (1976), or Geissmen et al. (1982). Specific to the work of Geissmen et al., the pole orientation defined for the Ghost Range intrusive complex (2710-2703 Ma) is 280°N, 2°E. This is similar to that of Group 2 as defined in this study (235°N, 0.8°E), which as previously discussed, may have been the result of serpentinization of the olivine cumulate at the base of the BCF (2720±2 Ma; Corfu and Noble, 1992; Corfu, 1993). The serpentinization was probably associated with fluids which were expelled from the Round Lake dome area during batholith emplacement (≈2690, Corfu et al., 1980). If this premise is correct, the pole orientation of the Ghost Range complex does not represent the primary NRM.

*NRM and Q Ratio*

The log plot of NRM versus stratigraphic position (Fig. 17) is virtually identical to that of susceptibility. The NRM intensity is a function of magnetite grain size and abundance, as magnetite is the main NRM carrier and has virtually the same composition at any stratigraphic level. It is also important to note the very high NRM intensity associated with the magnetite regardless of its origin; that is, whether magnetite is primary or secondary. NRM and susceptibility are opposite in relation to grain size. A fine grained mineral will have a higher NRM than a coarse grained mineral but the susceptibility is lower. Hence, the olivine cumulate is represented by a higher NRM intensity than the most of the gabbroic layer, where the magnetite is coarser grained. The gabbroic layer is characterized by a slightly lower NRM, because of its characteristic coarse grained

magnetite, but shows similar variability with regards to the distribution of the TMC as does the susceptibility. These are areas of the highest magnetite volume and therefore have a higher NRM. The magnetite volume compensates for the grain size effect in these rocks. The BCF contains trace amounts of pyrrhotite, but may be a major sulfide phase in other environments. The occurrence of pyrrhotite in sulfide-enriched zones can be distinguished from TMC patches based on a much lower susceptibility and NRM intensity.

From the Köenigsberger Q ratio plot (Fig. 18), the rocks types are generally characterized by a high Q value. A high Q value is characteristic of a rock which is magnetically stable and therefore acts as a stable recorder of the ancient geomagnetic field. Rocks with low Q values are unstable. The Q values for the olivine cumulate are extremely high in comparison to those of the other lithologies. This is likely a reflection of the very fine grained magnetite found in this layer. The Q values are considerably less for the other rock types but are nonetheless quite high. The one exception is the clinopyroxene cumulate layer, where the magnetite concentration is so small that it exhibits extremely weak magnetic properties.

# Chapter 6

## Discussion

The magnetic highs associated with the base of the gabbroic layer of the BCF define a prominent positive anomaly that appears to be podiform in outline and up to ten metres in lateral extent. This suggests that the titaniferous magnetite-rich rock is itself podiform, like the enclosed PGE mineralization. This magnetic anomaly is not extensive enough to be visible on a regional scale aeromagnetic map as a separate anomaly within the BCF, but is evident on a property scale ground magnetic survey. By upward continuing the BCF property scale magnetics data 2 m above the sensor height (approximately 4 m above the ground), the anomalies associated with the mineralization are lost and the olivine cumulate signal predominates. Susceptibility mapping has proven to be very useful in defining areas of titaniferous magnetite enrichment, in which PGM may be concentrated.

Difficulties arise if exploration criteria developed for PGE deposits associated with massive sulfide, are applied to a sulfide-poor environment. In the BCF, VLF is not an effective tool in delineating sulfide-rich horizons with which PGE are commonly associated. The mineralization is also not visible in outcrop in the traditional sense, that is, the presence of altered sulfides. Exploration methods therefore need to be developed which are useful in identifying sulfide-poor PGE deposits.

The important association in a sulfide-poor environment between primary titaniferous magnetite and concentrations of platinum-group minerals (PGM) is useful in defining exploration criteria. Specifically, the identification of a positive magnetic anomaly over a PGE mineralized horizon becomes possible. This presents an additional problem however of being able to distinguish between a strongly magnetic, sulfide-poor, PGM-bearing rock and an unmineralized serpentinized peridotite? These peridotite bodies are known to form very extensive, positive anomalies on aeromagnetic maps.

The characteristics of the PGM-chalcopyrite-titaniferous magnetite association of the mineralization within the BCF, may be analogous to larger scale PGE mineralization within similar rock types of mafic-ultramafic flows or intrusions. The geochemical relationship between the PGE mineralization and titaniferous magnetite needs to be further studied and described but ultimately provides a key to exploration in sulfide-poor environments.

Exploration criteria that may be useful in the search for economic concentrations of PGE in similar environments as defined by this study, are summarized in Table 10. Property scale magnetic and susceptibility surveys are key in distinguishing the rock types associated with PGE mineralization.

Table 10. Exploration criteria

I. Selection of mafic/ultramafic rock bodies for exploration

(1) Location of a regional scale, positive aeromagnetic anomaly
(2) Identification of main rock types focusing mainly on pyroxenitic and gabbroic rocks
(3) Ignore serpentinites, unless there are large concentrations of primary titaniferous magnetite, associated with them

II. Recognition of ore environments within selected rock bodies

(1) Property scale magnetic and susceptibility mapping concentrating on pyroxenitic and gabbroic rocks
(2) Positive magnetic anomaly or areas of high magnetic susceptibility
(3) Diversity in rock type, for example, felsic segregations
(4) Variations in textures, especially pegmatite development
(5) Abundant chalcopyrite $\pm$ pyrite; weakly disseminated but in strong association with titaniferous magnetite

# Chapter 7

## Conclusions

Geophysical studies of rocks hosting platinum-group occurrences and microprobe analyses of the oxide phases present in the BCF have provided insight into the characteristics of sulfide-poor PGE mineralization in differentiated, ultramafic rock terrains. Different lithologies within the BCF are easily identified through detailed magnetic and susceptibility mapping. More importantly, a positive magnetic anomaly is associated with the PGE mineralization. This anomaly is podiform in outline and further constrains the geometric shape of the 'ore'. This provides a basis for further interpretive study of the mineralization process and is important in defining exploration strategies in the search of economic concentrations of PGE in sulfide-poor environments. VLF methods were not useful in defining the mineralized horizons because of the lack of sulfide. The identification of isolated positive magnetic anomalies with high susceptibilities within a strongly magnetic body is only possible by detailed ground-based magnetic and susceptibility surveys. This is the most important contribution to the development of exploration criteria for economic concentrations of sulfide-poor PGE mineralization in geologically similar environments within the Abitibi greenstone belt and elsewhere. Refinements in exploration strategies should be made to incorporate detailed magnetic and susceptibility mapping in primary exploration stages.

As evident from the paleomagnetic study, the BCF has had a long and complex magnetization history. The primary NRM or TRM has been overprinted by various episodes

of fluid migration including serpentinization and amphibolitization. The paleopole representing the primary NRM could not be established. The results of the BCF study have shown that the pole used for the Ghost Range intrusive complex is not that of primary NRM and therefore should not be used in the construction of the Archean apparent polar wander path.

## References

Beeson, M. H., and Jackson, E. D. 1964. Chemical composition of altered chromites from the Stillwater Complex, Montana. American Mineralogist, 1969.

Buddington, A. F., and Lindsley, D. H. 1964. Iron-titanium oxide minerals and synthetic equivalents. Journal of Petrology, **5:** 310-356.

Carmichael, R. S. 1989. CRC Practical handbook of physical properties of rocks and minerals. CRC Press, Inc., pp. 299-356.

Chandler, V. W. 1990. Geologic interpretation of gravity and magnetic data over the central part of the Duluth Complex, Northeastern Minnesota. Economic Geology, **85:** 816-829.

Corfu, F. 1993. The evolution of the Southern Abitibi greenstone belt in light of precise U-Pb geochronology. Economic Geology, **88:** 1323-1340.

Corfu, F., Krogh, T. E., Kwok, Y. Y., and Jensen, L. S. 1989. U-Pb zircon geochronology in the southwestern Abitibi greenstone belt, Superior Province. Canadian Journal of Earth Sciences, **26:** 1747-1763.

Corfu, F., and Noble, S. R. 1992. Genesis of the southern Abitibi greenstone belt, Superior Province. Canadian Journal of Earth Sciences, **26:** 1747-1763.

Dunlop, D. J. 1973. Thermoremanent magnetization in submicroscopic magnetite. Journal of Geophysical Research, **78:** 7602-7613.

Dunlop, D. J., Hanes, J. A., and Buchan, K. L. 1973. Indices of multidomain magnetic behaviour in basic igneous rocks: Alternating-field demagnetization, Hysteresis, and Oxide Petrology. Journal of Geophysical Research, **78**: 1387-1393.

Fleet, M. E., Angeli, N., and Pan, Y. 1993. Oriented chlorite lamellae from the Pedra Bancha Mafic-Ultramafic Complex, Ceará Brazil. American Mineralogist **78:** 68-74.

Goodwin, A. M. 1965. Mineralized volcanic complexes in Porcupine-Kirkland Lake-Noranda region, Canada. Economic Geology, **60:** 955-971.

Goodwin, A. M., and Ridler, R. H. 1970. The Abitibi orogenic belt. *In* Symposium on basins and geosynclines of the Canadian Shield. *Edited by* A. J. Baer. Geological Survey of Canada, Paper 70-40, pp. 1-30.

Haggerty, S. E. 1976. Opaque oxide minerals in terrestrial rocks. Mineralogical Society of America Short Course Notes, **3:** 101-300.

Hanski, E. J. 1992. Petrology of the Pechenga ferropicrites and cogenetic, Ni-bearing gabbro-wherlite intrusions, Kola Penninsula, Russia. Geologic Survey of Finland Bulletin 367: pp. 193.

Hanski, E. J., and Smolkin, V. F. 1989. Pechenga ferropicrites and other early Proterozoic picrites in the eastern part of the Baltic Shield. Precambrian Research, **45:** 63-82.

Hostetler, P. B., Coleman,, R. G., and Mumpton, F. A. 1966. Brucite in alpine serpentinites. American Mineralogist, **51:** 75-98.

Jackson, S., and Fyon, A. The western Abitibi subprovince in Ontario. *In* Geology of Ontario. *Edited by* P. C. Thurston, H. R. Williams, R. H. Sutcliffe and G. M. Stott. Ontario Geological Survey, Special Volume 4, Part 1: pp. 441-444.

Jackson, S., and Harrap, R. 1989. Geology of parts of the Pacaud, Catharine, and southernmost Boston and McElroy Townships. *In* Summary of field work and other activities 1989. Ontario Geological Survey, Miscellaneous Paper 146: pp. 125-131.

Jensen, L. S. 1981. A petrogenetic model for the Archean Abitibi belt in the Kirkland Lake area, Ontario. Ph.D. Thesis, University of Saskatchewan, Saskatoon, Sask.

Jensen, L. S. 1985a. Stratigraphy and petrogenesis of Archean metavolcanic sequences, southwestern Abitibi subprovince, Ontario. *In* Evolution of Archean supracrustal sequences. *Edited by* Ayers, L. D., Thurston, P. C., Card K. D., and Weber, W., Geological Association of Canada, Special Paper 28, pp. 65-87.

Jensen, L. S., and Langford, F. F. 1985b. Geology and Petrogenesis of the Archean Abitibi Belt in the Kirkland Lake Area, Ontario. Ontario Geological Survey, Miscellaneous Paper 123, pp. 10-66.

Jolly, W. T. 1974. Regional metamorphic zonation as an aid in study of Archean terrains. Canadian Mineralogist, **12:** 499-508.

Jolly, W. T. 1975. Subdivision of Archean lavas of the Abitibi area, Canada, from Fe-Mg-Ni-Cr relations. Earth and Planetary Science Letters **27:** 200-210.

Jolly, W. T. 1977a. Metamorphic history of the Archean Abitibi belt: Sample distribution and partial metamorphism and zonation. Geological Survey of Canada, Paper 77-1A, pp. 191-196.

Jolly, W. T. 1977b. Relations between Archean lavas and intrusive rocks of the Abitibi area, Canada. Spec. Geological Association of Canada, Special Paper 16, pp. 311-330.

Jolly, W. T. 1978. Metamorphic history of the Archean Abitibi belt. Geological Survey of Canada, Special Paper 78-10, pp. 63-77.

Jolly, W. T. 1980. Development and degradation of Archean lavas, Abitibi area, Canada, in light major element geochemistry. Journal of Petrology, Vol. 21, Part 2: pp. 323-363.

Keary, P., and Vine, F. J. 1990. Global tectonics. Blackwell Scientific Publications, pp. 53-58.

Kirschvink, J. L. 1980. The least-squares line and plane and the analysis of paleomagnetic data. Geophysical Journal of the Royal Astronomical Society, **62:** 699-718.

Klemm, D. D., Henckel, J., and Dehm, R. M. 1985. Exsolution features in titanomagnetites from massive magnetite layers and their host rocks of the Upper Zone, Eastern Bushveld Complex. Economic Geology, **80:** 1049-1061.

Lawton, K. D. 1957. Geology of Boston Township and part of Pacaud Township. Ontario Department of Mines, Vol. 67, Part 5: pp. 1-55.

MERQ-OGS. 1983. Lithostratigraphic map of the Abitibi Subprovince. Ministere de l'Énergie et des Ressources du Québec - Ontario Geologic Survey, DV 83-16 and Map 2484, scale 1:500000.

Lienert, B. R., and Wasilewski, P. J. 1976. A magnetic study of the serpentinization process at Burro Mountain, California. Earth and Planetary Science Letters, **43:** 406-416.

Mohide, T. P. 1979. Platinum group metals - Ontario and the world. Ministry of Natural Resources, Ontario Mineral Policy Background Paper No. 7.

Ontario Geological Survey. 1979. Airborne electromagnetic and total intensity magnetic survey, Kirkland Lake area, District of Timiskaming; Ontario Geological Survey, Preliminary Maps P.2270, P.2271, P.2273 and P.2274, scale 1:20000.

Parry, L. G. 1965. Magnetic properties of dispersed magnetite powders. Philosophical Magazine, **11**: 303-312.

Piper, J. D. A. 1987. Paleomagnetism and the continental crust. Halsted Press, pp. 5-189.

Postle, J. T., Roscoe, W. E., Watanabe, R. Y., and Martin, P. S. 1986. Review of platinum group element deposits in Ontario. Ministry of Northern Development and Mines, Mineral Policy Background Paper No. 24.

Pullaiah, G., Irving, E., Buchan, K. and Dunlop, J. 1975. Magnetization changes caused by burial and uplift. Earth and Planetary Science Letters, **28:** 133-143.

Reynolds, I. M. 1985. Contrasted mineralogy and textural relationships in the uppermost titaniferous magnetite layers of the Bushveld Complex in the Bierkraal area north of Rustenberg. Economic Geology, **80:** 1027-1048.

Ridler, R. H. 1969. The relation of mineralization to volcanic stratigraphy in the Kirkland Lake area, Ontario. Ph.D. thesis, University of Wisconsin, Madison, WI.

Ridler, R. H. 1970. Relationship of mineralization to volcanic stratigraphy in the Kirkland Lake-Larder Lake area, Ontario. Geological Association of Canada, Proceedings **21:** 33-42.

Ridler, R. H. 1975. Regional metallogeny and volcanic stratigraphy of the Superior Province. *In* Report of Activities, part A. Geological Survey of Canada, Paper 75-1A, pp. 353-355.

Saad, A. H. 1969. Magnetic properties of ultramafic rocks from Red Mountain, California. Geophysics, **34:** 974-987.

Schutts, L. D., and Dunlop, D. J. 1981. Proterozoic overprinting of Archean rocks in the Canadian Superior Province. Nature, **291:** 642-645.

Shive, P. N., Frost, B. R., and Peretti, A. 1988. The magnetic properties of metaperidotitic rocks as a function of metamorphic grade: Implications for crustal magnetic anomalies. Journal of Geophysical Research, Vol. 93, No. B10: pp. 12187-12959.

Spencer, K. J., and Lindsley, D. H. 1981. A solution model for co-existing iron-titanium oxides. American Mineralogist, **66:** 1189-1201.

Stacey, F. D. and Banerjee, S. K. 1974. Developments in solid earth geophysics. Elsevier Scientific Publishing Company, pp. 25-63, 105-118.

Stone, W. E., Crocket, J. H., and Fleet, M. E. Differentiation processes in a peculiar iron-rich alumina-poor Archean ultramafic/mafic flow, Ontario. In review.

Stone, W. E., Crocket, J. H., Dickin, A. P., and Fleet, M. E. 1994. Geochemical constraints on the origin of Archean ferropicrite: Example of the Boston Creek Flow, Abitibi greenstone belt, Ontario. Submitted.

Stone, W. E., Crocket, J. H., and Fleet, M. E. 1993. Sulfide poor platinum-group systems: example of the Boston Creek Flow layered basaltic komatiite, Abitibi belt, Ontario. Economic Geology, **88:** 817-836.

Stone, W. E., Crocket, J. H., Fleet, M. E., and Kingston, D. M. 1992. Platinum-group minerals in pyroxenite from the Boston Creek Flow basaltic komatiite, Abitibi greenstone belt, Ontario. Canadian Mineralogist, **30:** 109-119.

Stone, W. E., Jensen, L. S., and Church, W. R. 1987. Petrography and geochemistry of an unusual Fe-rich basaltic komatiite from Boston Township, northeastern Ontario. Canadian Journal of Earth Science, **24:** 2537-2550.

Stormer, J. C. 1983. The effects of recalculation on estimates of temperature and oxygen fugacity from analyses of multicomponent iron-titanium oxides. American Mineralogist, **68:** 586-594.

Telford, W. M., Geldart, L. P., Sheriff, R. E., and Keys, D. A. 1976. Applied Geophysics. Cambridge University Press, pp. 105-200, 500-611.

Thompson, R., and Oldfield, F. 1986. Environmental magnetism. Allen & Unwin Publishers Ltd., pp. 3-38.

Toft P. B., Arkani-Hamed, J., and Haggerty, S. E. 1990. The effect of serpentinization on density and magnetic susceptibility: a petrophysical model. Physics of the Earth and Planetary Interiors, **65:** 137-157.

Ulmer, G. C. 1974. Alteration of chromite during serpentinization in the Pennsylvania-Maryland district. American Mineralogist, **59:** 1236-1241.

Vermaak, C. F., and Hendriks, L. P. 1976. A review of the mineralogy of the Merensky reef with special reference to new data on the precious metal mineralogy. Econommic Geology, **71:** 1244-1269.

Volborth, A. A., Stumpfl, E. F., Tarkin, M., and Housley, R. M. 1985. Examples of Pd-Pt mineralization along the 35 km strike of the Stillwater reef, Montana. Canadian Mineralogist, **23:** 329-346.

Xie, Q., Kerrich, R., and Fan, J. 1993. HFSE/REE fractionations recorded in three komatiite-basalt sequences, Archean Abitibi greenstone belt: Implications for multiple plume sources and depths. Geochimica et Cosmochimica Acta, **57:** 4111-4118.

# APPENDIX A

MICROPROBE DATA:

NATURAL SILICATE AND OXIDE STANDARDS (A-1)
CHROMITE ANALYSES (A-2)
MAGNETITE ANALYSES (A-3)
ILMENITE ANALYSES (A-4)
BROADBEAM ANALYSES (A-5)

Table A-1. Natural silicate and oxide standards used in microprobe analyses

| | Anorthite | Chromite | Chromite #5 | Diopside 5a | Ilmenite | Magnetite | Olivine #1 | Spessartine Garnet 4b | Rutile | Willemite |
|---|---|---|---|---|---|---|---|---|---|---|
| | USNM-137041 | USNM-117075 | | | USNM-96189 | USNM-114887 | | | | |
| | $CaAl_2Si_2O_6$ | $Fe(Cr,Fe)_2O_4$ | $(Mg,Fe)(Cr,Al)_2O_4$ | $(Ca,Mg)SiO_3$ | $FeTi_3O_4$ | $Fe_3O_4$ | $(Mg,Fe)_2SiO_4$ | $Mn_3Al_2(SiO_4)_3$ | $TiO_2$ | $Zn_2SiO_4$ |
| $SiO_2$ | 44.00 | | 0.03 | 55.19 | | | 41.15 | 36.39 | | 27.2 |
| $TiO_2$ | 0.03 | | 0.12 | 0.002* | 45.7 | 0.16 | | 0.03 | 100 | |
| $Al_2O_3$ | 36.03 | 9.92 | 23.91 | 0.43 | | | | 20.62 | | |
| $Cr_2O_3$ | | 60.50 | 45.65 | | | 0.25 | 0.01 | | | |
| FeO | 0.62 | 13.04 | 12.72 | 0.89 | 46.53* | 90.94* | 7.62 | 1.78 | | |
| MnO | | 0.11 | 0.13 | 0.05* | 4.77 | < 0.01 | 0.10 | 40.71 | | 6.17 |
| MgO | < 0.02 | 15.20 | 17.26 | 17.94 | 0.31 | 0.05 | 50.78 | | | 0.26 |
| ZnO | | | 0.01? (NLD) | | | | | | | 66.3 |
| CaO | 19.09 | 0.12 | | 25.18 | | | | 0.36 | | |
| NiO | | | 0.17 | | | | 0.29 | | | |
| $K_2O$ | 0.03 | | | | | | | | | |
| $Na_2O$ | 0.53 | | | 0.38 | | | | | | |
| $SnO_2$ | | | | | | | | 0.05 | | |
| $Nb_2O_5$ | | | | | 0.92 | | | | | |
| $O_2$ | | | | | 1.16 | | | | | |
| $V_2O_3$ | | | 0.17 | | | | | | | |

chromite: * total Fe as FeO
ilmenite: * total Fe as FeO; FeO = 36.1%, $Fe_2O_3$ = 11.16%
magneite: * total Fe as FeO; FeO = 30.2%, $Fe_2O_3$ = 67.5%

## Table A-2. Chromite analyses

| Sample | Analysis | SiO2 | TiO2 | Al2O3 | Cr2O3 | V2O3 | Fe2O3 | total | FeO | MnO | MgO | ZnO | CaO | NiO | Total | TOTAL | Cr/ (Al+Cr) | Cr/ (Al+Cr+Fe) | Fe/ Al+Cr+Fe | Mg/ (Fe+Mg) |
|---|---|---|---|---|---|---|---|---|---|---|---|---|---|---|---|---|---|---|---|---|
| MSL-58 | 6c2 | 0.05 | 1.27 | 5.95 | 44.17 | | | | 41.31 | 1.48 | 0.16 | 1.41 | 0.03 | 0.12 | 95.96 | | | | | |
| | | 0.001 | 0.016 | 0.058 | 0.291 | 0.000 | 0.000 | | 0.575 | 0.021 | 0.004 | 0.025 | 0.001 | 0 001 | | | | | | |
| | | 0.002 | 0.032 | 0.175 | 0.872 | 0.000 | 0.000 | | 0.575 | 0.021 | 0.004 | 0.025 | 0.001 | 0.001 | 1.707 | | | | | |
| | | 0.004 | 0.074 | 0.410 | 2.043 | 0.000 | 0.000 | | 1.347 | 0.049 | 0.009 | 0.059 | 0.001 | 0.003 | | | | | | |
| | | 0.002 | 0.037 | 0.273 | 1.362 | 0.000 | 0.000 | | 1.347 | 0.049 | 0.009 | 0.059 | 0.001 | 0.003 | | | | | | |
| | | | | | | | | | 0.082 | | | | | | | | | | | |
| | | | | | | | 13.000 | | 29.598 | | | | | | | 97.238 | | | | |
| | | 0.001 | 0.016 | 0.058 | 0.291 | 0.000 | 0.081 | | 0.412 | 0.021 | 0.004 | 0.025 | 0.001 | 0.001 | | | | | | |
| | | 0.002 | 0.032 | 0.175 | 0.872 | 0.000 | 0.244 | | 0.412 | 0.021 | 0.004 | 0.025 | 0.001 | 0.001 | 1.788 | | | | | |
| | | 0.004 | 0.071 | 0.392 | 1.950 | 0.000 | 0.546 | | 0.921 | 0.047 | 0.009 | 0.056 | 0.001 | 0.003 | | | | | | |
| | | 0.002 | 0.036 | 0.261 | 1.300 | 0.000 | 0.364 | 1.962 | 0.921 | 0.047 | 0.009 | 0.056 | 0.001 | 0.003 | 1.034 | 2.997 | 0.833 | 0.675 | 0.189 | 0.010 |
| | 6c3 | 0.04 | 1.26 | 6.47 | 43.96 | | | | 40.79 | 1.58 | 0.15 | 1.32 | 0.02 | 0.13 | 95.72 | | | | | |
| | | 0.001 | 0.016 | 0.063 | 0.289 | 0.000 | 0.000 | | 0.568 | 0.022 | 0.004 | 0.024 | 0.000 | 0.002 | | | | | | |
| | | 0.001 | 0.032 | 0.190 | 0.868 | 0.000 | 0.000 | | 0.568 | 0.022 | 0.004 | 0.024 | 0.000 | 0.002 | 1.710 | | | | | |
| | | 0.003 | 0.074 | 0.445 | 2.029 | 0.000 | 0.000 | | 1.328 | 0.052 | 0.009 | 0.055 | 0.001 | 0.004 | | | | | | |
| | | 0.002 | 0.037 | 0.297 | 1.353 | 0.000 | 0.000 | | 1.328 | 0.052 | 0.009 | 0.055 | 0.001 | 0.004 | | | | | | |
| | | | | | | | | | 0.078 | | | | | | | | | | | |
| | | | | | | | 12.422 | | 29.599 | | | | | | | 96.951 | | | | |
| | | 0.001 | 0.016 | 0.063 | 0.289 | 0.000 | 0.078 | | 0.412 | 0.022 | 0.004 | 0.024 | 0.000 | 0.002 | | | | | | |
| | | 0.001 | 0.032 | 0.190 | 0.868 | 0.000 | 0.233 | | 0.412 | 0.022 | 0.004 | 0.024 | 0.000 | 0.002 | 1.788 | | | | | |
| | | 0.003 | 0.071 | 0.426 | 1.941 | 0.000 | 0.522 | | 0.922 | 0.050 | 0.008 | 0.053 | 0.001 | 0.004 | | | | | | |
| | | 0.001 | 0.035 | 0.284 | 1.294 | 0.000 | 0.348 | 1.963 | 0.922 | 0.050 | 0.008 | 0.053 | 0.001 | 0.004 | 1.033 | 2.996 | 0.820 | 0.672 | 0.181 | 0.009 |
| | g2, s1c | 0.07 | 1.78 | 6.35 | 39.47 | | | | 44.45 | 1.49 | 0.14 | 1.36 | 0.05 | 0.16 | 95.32 | | | | | |
| | | 0.001 | 0.022 | 0.062 | 0.260 | 0.000 | 0.000 | | 0.619 | 0.021 | 0.003 | 0.024 | 0.001 | 0.002 | | | | | | |
| | | 0.002 | 0.045 | 0.187 | 0.779 | 0.000 | 0.000 | | 0.619 | 0.021 | 0.003 | 0.024 | 0.001 | 0.002 | 1.683 | | | | | |
| | | 0.006 | 0.106 | 0.444 | 1.852 | 0.000 | 0.000 | | 1.470 | 0.050 | 0.008 | 0.058 | 0.002 | 0.005 | | | | | | |
| | | 0.003 | 0.053 | 0.296 | 1.234 | 0.000 | 0.000 | | 1.470 | 0.050 | 0.008 | 0.058 | 0.002 | 0.005 | | | | | | |
| | | | | | | | | | 0.100 | | | | | | | | | | | |
| | | | | | | | 16.022 | | 30.015 | | | | | | | 96.908 | | | | |
| | | 0.001 | 0.022 | 0.062 | 0.260 | 0.000 | 0.100 | | 0.418 | 0.021 | 0.003 | 0.024 | 0.001 | 0.002 | | | | | | |
| | | 0.002 | 0.045 | 0.187 | 0.779 | 0.000 | 0.301 | | 0.418 | 0.021 | 0.003 | 0.024 | 0.001 | 0.002 | 1.783 | | | | | |
| | | 0.005 | 0.100 | 0.419 | 1.748 | 0.000 | 0.675 | | 0.937 | 0.047 | 0.008 | 0.054 | 0.002 | 0.004 | | | | | | |
| | | 0.003 | 0.050 | 0.279 | 1.165 | 0.000 | 0.450 | 1.947 | 0.937 | 0.047 | 0.008 | 0.054 | 0.002 | 0.004 | 1.048 | 2.996 | 0.807 | 0.615 | 0.238 | 0.008 |
| MSL-11 | g1, s1r | 0.02 | 0.02 | 0.01 | 0.25 | | | | 91.77 | 0.07 | 0.03 | 0.02 | 0.01 | 0.19 | 92.39 | | | | | |
| | | 0.000 | 0.000 | 0.000 | 0.002 | 0.000 | 0.000 | | 1.277 | 0.001 | 0.001 | 0.000 | 0.000 | 0.002 | | | | | | |
| | | 0.001 | 0.001 | 0.000 | 0.005 | 0.000 | 0.000 | | 1.277 | 0.001 | 0.001 | 0.000 | 0.000 | 0.002 | 1.288 | | | | | |
| | | 0.002 | 0.002 | 0.001 | 0.015 | 0.000 | 0.000 | | 3.966 | 0.003 | 0.002 | 0.001 | 0.001 | 0.007 | | | | | | |
| | | 0.001 | 0.001 | 0.001 | 0.010 | 0.000 | 0.000 | | 3.966 | 0.003 | 0.002 | 0.001 | 0.001 | 0.007 | | | | | | |
| | | | | | | | | | 0.426 | | | | | | | | | | | |
| | | | | | | | 67.992 | | 30.515 | | | | | | | 99.128 | | | | |
| | | 0.000 | 0.000 | 0.000 | 0.002 | 0.000 | 0.426 | | 0.425 | 0.001 | 0.001 | 0.000 | 0.000 | 0.002 | | | | | | |
| | | 0.001 | 0.001 | 0.000 | 0.005 | 0.000 | 1.277 | | 0.425 | 0.001 | 0.001 | 0.000 | 0.000 | 0.002 | 1.713 | | | | | |
| | | 0.002 | 0.001 | 0.001 | 0.012 | 0.000 | 2.983 | | 0.992 | 0.002 | 0.002 | 0.001 | 0.000 | 0.005 | | | | | | |
| | | 0.001 | 0.001 | 0.000 | 0.008 | 0.000 | 1.988 | 1.998 | 0.992 | 0.002 | 0.002 | 0.001 | 0.000 | 0.005 | 0.997 | 2.995 | 0.944 | 0.004 | 0.996 | 0.002 |
| | g2, s1r | 0 | 0.43 | 0.27 | 10.21 | | | | 80.18 | 1.14 | 0 | 0.18 | 0 | 0.22 | 92.64 | | | | | |
| | | 0.000 | 0.005 | 0.003 | 0.067 | 0.000 | 0.000 | | 1.116 | 0.016 | 0.000 | 0.003 | 0.000 | 0.003 | | | | | | |
| | | 0.000 | 0.011 | 0.008 | 0.202 | 0.000 | 0.000 | | 1.116 | 0.016 | 0.000 | 0.003 | 0.000 | 0.003 | 1.358 | | | | | |
| | | 0.000 | 0.032 | 0.023 | 0.593 | 0.000 | 0.000 | | 3.287 | 0.047 | 0.000 | 0.009 | 0.000 | 0.008 | | | | | | |
| | | 0.000 | 0.016 | 0.016 | 0.396 | 0.000 | 0.000 | | 3.287 | 0.047 | 0.000 | 0.009 | 0.000 | 0.008 | | | | | | |
| | | | | | | | | | 0.352 | | | | | | | | | | | |
| | | | | | | | 56.212 | | 29.538 | | | | | | | 98.201 | | | | |
| | | 0.000 | 0.005 | 0.003 | 0.067 | 0.000 | 0.352 | | 0.411 | 0.016 | 0.000 | 0.003 | 0.000 | 0.003 | | | | | | |
| | | 0.000 | 0.011 | 0.008 | 0.202 | 0.000 | 1.056 | | 0.411 | 0.016 | 0.000 | 0.003 | 0.000 | 0.003 | 1.709 | | | | | |
| | | 0.000 | 0.025 | 0.019 | 0.472 | 0.000 | 2.471 | | 0.962 | 0.038 | 0.000 | 0.008 | 0.000 | 0.006 | | | | | | |
| | | 0.000 | 0.013 | 0.012 | 0.314 | 0.000 | 1.647 | 1.987 | 0.962 | 0.038 | 0.000 | 0.008 | 0.000 | 0.006 | 1.007 | 2.994 | 0.962 | 0.159 | 0.834 | 0.000 |
| | g4, s2c | 0 | 1.75 | 5.64 | 36.09 | | | | 46.58 | 3.9 | 0.35 | 1.21 | 0.01 | 0.13 | 95.16 | | | | | |
| | | 0.000 | 0.022 | 0.055 | 0.237 | 0.000 | 0.000 | | 0.648 | 0.055 | 0.009 | 0.022 | 0.000 | 0.002 | | | | | | |
| | | 0.000 | 0.044 | 0.166 | 0.712 | 0.000 | 0.000 | | 0.648 | 0.055 | 0.009 | 0.022 | 0.000 | 0.002 | 1.657 | | | | | |
| | | 0.000 | 0.106 | 0.400 | 1.719 | 0.000 | 0.000 | | 1.565 | 0.133 | 0.021 | 0.052 | 0.000 | 0.004 | | | | | | |
| | | 0.000 | 0.053 | 0.267 | 1.146 | 0.000 | 0.000 | | 1.565 | 0.133 | 0.021 | 0.052 | 0.000 | 0.004 | | | | | | |
| | | | | | | | | | 0.133 | | | | | | | | | | | |
| | | | | | | | 21.199 | | 27.481 | | | | | | | 97.761 | | | | |
| | | 0.000 | 0.022 | 0.055 | 0.237 | 0.000 | 0.133 | | 0.382 | 0.055 | 0.009 | 0.022 | 0.000 | 0.002 | | | | | | |
| | | 0.000 | 0.044 | 0.166 | 0.712 | 0.000 | 0.398 | | 0.382 | 0.055 | 0.009 | 0.022 | 0.000 | 0.002 | 1.790 | | | | | |
| | | 0.000 | 0.098 | 0.371 | 1.592 | 0.000 | 0.890 | | 0.855 | 0.123 | 0.019 | 0.048 | 0.000 | 0.004 | | | | | | |
| | | 0.000 | 0.049 | 0.247 | 1.061 | 0.000 | 0.593 | 1.951 | 0.855 | 0.123 | 0.019 | 0.048 | 0.000 | 0.004 | 1.046 | 2.997 | 0.811 | 0.558 | 0.312 | 0.022 |

## Table A-2. Chromite analyses

| Sample | Analysis | SiO2 | TiO2 | Al2O3 | Cr2O3 | V2O3 | Fe2O3 | total | FeO | MnO | MgO | ZnO | CaO | NiO | Total | TOTAL | Cr/ (Al+Cr) | Cr/ (Al+Cr+Fc) | Fc/ Al+Cr+Fc | Mg/ (Fe+Mg) |
|---|---|---|---|---|---|---|---|---|---|---|---|---|---|---|---|---|---|---|---|---|
| MSL-58 | 1c | 0.03 | 1.51 | 4.82 | 43.79 | 0 | 0 | | 42.74 | 1.66 | 0.13 | 1.42 | 0.04 | 0.17 | 96.32 | | | | | |
| | | 0.000 | 0.019 | 0.047 | 0.288 | 0.000 | 0.000 | | 0.595 | 0.023 | 0.003 | 0.025 | 0.001 | 0.002 | | | | | | |
| | | 0.001 | 0.038 | 0.142 | 0.864 | 0.000 | 0.000 | | 0.595 | 0.023 | 0.003 | 0.025 | 0.001 | 0.002 | 1.694 | | | | | |
| | | 0.002 | 0.089 | 0.335 | 2.040 | 0.000 | 0.000 | | 1.404 | 0.055 | 0.008 | 0.060 | 0.002 | 0.005 | | | | | | |
| | | 0.001 | 0.045 | 0.223 | 1.360 | 0.000 | 0.000 | | 1.404 | 0.055 | 0.008 | 0.060 | 0.002 | 0.005 | | | | | | |
| | | | | | | | | | 0.092 | | | | | | | | | | | |
| | | | | | | | 14.643 | | 29.549 | | | | | | | 97.761 | | | | |
| | | 0.000 | 0.019 | 0.047 | 0.288 | 0.000 | 0.092 | | 0.411 | 0.023 | 0.003 | 0.025 | 0.001 | 0.002 | | | | | | |
| | | 0.001 | 0.038 | 0.142 | 0.864 | 0.000 | 0.275 | | 0.411 | 0.023 | 0.003 | 0.025 | 0.001 | 0.002 | 1.786 | | | | | |
| | | 0.002 | 0.085 | 0.318 | 1.936 | 0.000 | 0.616 | | 0.921 | 0.052 | 0.007 | 0.057 | 0.002 | 0.005 | | | | | | |
| | | 0.001 | 0.042 | 0.212 | 1.291 | 0.000 | 0.411 | 1.956 | 0.921 | 0.052 | 0.007 | 0.057 | 0.002 | 0.005 | 1.039 | 2.995 | 0.859 | 0.675 | 0.215 | 0.008 |
| | 2c | 0.09 | 2.05 | 6.36 | 38.2 | | | | 45.64 | 1.59 | 0.13 | 1.43 | 0.04 | 0.21 | 95.74 | | | | | |
| | | 0.001 | 0.026 | 0.062 | 0.251 | 0.000 | 0.000 | | 0.635 | 0.022 | 0.003 | 0.025 | 0.001 | 0.003 | | | | | | |
| | | 0.003 | 0.051 | 0.187 | 0.754 | 0.000 | 0.000 | | 0.635 | 0.022 | 0.003 | 0.025 | 0.001 | 0.003 | 1.685 | | | | | |
| | | 0.007 | 0.122 | 0.444 | 1.790 | 0.000 | 0.000 | | 1.508 | 0.053 | 0.008 | 0.061 | 0.002 | 0.006 | | | | | | |
| | | 0.004 | 0.061 | 0.296 | 1.193 | 0.000 | 0.000 | | 1.508 | 0.053 | 0.008 | 0.061 | 0.002 | 0.006 | | | | | | |
| | | | | | | | | | 0.107 | | | | | | | | | | | |
| | | | | | | | 17.099 | | 30.236 | | | | | | | 97.434 | | | | |
| | | 0.001 | 0.026 | 0.062 | 0.251 | 0.000 | 0.107 | | 0.421 | 0.022 | 0.003 | 0.025 | 0.001 | 0.003 | | | | | | |
| | | 0.003 | 0.051 | 0.187 | 0.754 | 0.000 | 0.321 | | 0.421 | 0.022 | 0.003 | 0.025 | 0.001 | 0.003 | 1.792 | | | | | |
| | | 0.007 | 0.115 | 0.418 | 1.683 | 0.000 | 0.717 | | 0.939 | 0.050 | 0.007 | 0.057 | 0.002 | 0.006 | | | | | | |
| | | 0.003 | 0.057 | 0.279 | 1.122 | 0.000 | 0.478 | 1.939 | 0.939 | 0.050 | 0.007 | 0.057 | 0.002 | 0.006 | 1.055 | 2.994 | 0.801 | 0.597 | 0.254 | 0.008 |
| | 3c | 0.07 | 1.98 | 6.51 | 40.46 | 0 | 0 | | 45.6 | 1.25 | 0.21 | 1.3 | 0.05 | 0.22 | 97.64 | | | | | |
| | | 0.001 | 0.025 | 0.064 | 0.266 | 0.000 | 0.000 | | 0.635 | 0.018 | 0.005 | 0.023 | 0.001 | 0.003 | | | | | | |
| | | 0.002 | 0.050 | 0.192 | 0.799 | 0.000 | 0.000 | | 0.635 | 0.018 | 0.005 | 0.023 | 0.001 | 0.003 | 1.726 | | | | | |
| | | 0.005 | 0.115 | 0.444 | 1.850 | 0.000 | 0.000 | | 1.471 | 0.041 | 0.012 | 0.054 | 0.002 | 0.006 | | | | | | |
| | | 0.003 | 0.057 | 0.296 | 1.234 | 0.000 | 0.000 | | 1.471 | 0.041 | 0.012 | 0.054 | 0.002 | 0.006 | | | | | | |
| | | | | | | | | | 0.101 | | | | | | | | | | | |
| | | | | | | | 16.072 | | 31.121 | | | | | | | 99.243 | | | | |
| | | 0.001 | 0.025 | 0.064 | 0.266 | 0.000 | 0.101 | | 0.433 | 0.018 | 0.005 | 0.023 | 0.001 | 0.003 | | | | | | |
| | | 0.002 | 0.050 | 0.192 | 0.799 | 0.000 | 0.302 | | 0.433 | 0.018 | 0.005 | 0.023 | 0.001 | 0.003 | 1.827 | | | | | |
| | | 0.005 | 0.109 | 0.419 | 1.749 | 0.000 | 0.661 | | 0.949 | 0.039 | 0.011 | 0.051 | 0.002 | 0.006 | | | | | | |
| | | 0.003 | 0.054 | 0.280 | 1.166 | 0.000 | 0.441 | 1.943 | 0.949 | 0.039 | 0.011 | 0.051 | 0.002 | 0.006 | 1.051 | 2.994 | 0.807 | 0.618 | 0.234 | 0.012 |
| | 5r1 | 0.57 | 0.01 | 0.01 | 0.29 | | | | 89.84 | 0.03 | 0.19 | 0.02 | 0.12 | 0.08 | 91.17 | | | | | |
| | | 0.009 | 0.000 | 0.000 | 0.002 | 0.000 | 0.000 | | 1.250 | 0.000 | 0.005 | 0.000 | 0.002 | 0.001 | | | | | | |
| | | 0.019 | 0.000 | 0.000 | 0.006 | 0.000 | 0.000 | | 1.250 | 0.000 | 0.005 | 0.000 | 0.002 | 0.001 | 1.284 | | | | | |
| | | 0.059 | 0.001 | 0.001 | 0.018 | 0.000 | 0.000 | | 3.895 | 0.001 | 0.015 | 0.001 | 0.006 | 0.003 | | | | | | |
| | | 0.030 | 0.000 | 0.001 | 0.012 | 0.000 | 0.000 | | 3.895 | 0.001 | 0.015 | 0.001 | 0.006 | 0.003 | | | | | | |
| | | | | | | | | | 0.413 | | | | | | | | | | | |
| | | | | | | | 65.799 | | 30.561 | | | | | | | 97.681 | | | | |
| | | 0.009 | 0.000 | 0.000 | 0.002 | 0.000 | 0.412 | | 0.425 | 0.000 | 0.005 | 0.000 | 0.002 | 0.001 | | | | | | |
| | | 0.019 | 0.000 | 0.000 | 0.006 | 0.000 | 1.236 | | 0.425 | 0.000 | 0.005 | 0.000 | 0.002 | 0.001 | 1.695 | | | | | |
| | | 0.045 | 0.001 | 0.001 | 0.014 | 0.000 | 2.917 | | 1.004 | 0.001 | 0.011 | 0.001 | 0.005 | 0.002 | | | | | | |
| | | 0.022 | 0.000 | 0.000 | 0.009 | 0.000 | 1.944 | 1.977 | 1.004 | 0.001 | 0.011 | 0.001 | 0.005 | 0.002 | 1.022 | 2.998 | 0.951 | 0.005 | 0.995 | 0.011 |
| | 6r1 | 0.84 | 0 | 0.09 | 0.42 | | | | 89.52 | 0.02 | 0.32 | 0 | 0.19 | 0.14 | 91.55 | | | | | |
| | | 0.014 | 0.000 | 0.001 | 0.003 | 0.000 | 0.000 | | 1.246 | 0.000 | 0.008 | 0.000 | 0.003 | 0.002 | | | | | | |
| | | 0.028 | 0.000 | 0.003 | 0.008 | 0.000 | 0.000 | | 1.246 | 0.000 | 0.008 | 0.000 | 0.003 | 0.002 | 1.298 | | | | | |
| | | 0.086 | 0.000 | 0.008 | 0.026 | 0.000 | 0.000 | | 3.840 | 0.001 | 0.024 | 0.000 | 0.010 | 0.005 | | | | | | |
| | | 0.043 | 0.000 | 0.005 | 0.017 | 0.000 | 0.000 | | 3.840 | 0.001 | 0.024 | 0.000 | 0.010 | 0.005 | | | | | | |
| | | | | | | | | | 0.409 | | | | | | | | | | | |
| | | | | | | | 65.259 | | 30.728 | | | | | | | 98.007 | | | | |
| | | 0.014 | 0.000 | 0.001 | 0.003 | 0.000 | 0.409 | | 0.428 | 0.000 | 0.008 | 0.000 | 0.003 | 0.002 | | | | | | |
| | | 0.028 | 0.000 | 0.003 | 0.008 | 0.000 | 1.226 | | 0.428 | 0.000 | 0.008 | 0.000 | 0.003 | 0.002 | 1.706 | | | | | |
| | | 0.066 | 0.000 | 0.006 | 0.019 | 0.000 | 2.875 | | 1.003 | 0.001 | 0.019 | 0.000 | 0.008 | 0.004 | | | | | | |
| | | 0.033 | 0.000 | 0.004 | 0.013 | 0.000 | 1.917 | 1.966 | 1.003 | 0.001 | 0.019 | 0.000 | 0.008 | 0.004 | 1.030 | 2.996 | 0.758 | 0.007 | 0.991 | 0.018 |
| | 6c1 | 0.05 | 1.27 | 6.06 | 43.68 | | | | 41.7 | 1.45 | 0.18 | 1.48 | 0.03 | 0.08 | 95.98 | | | | | |
| | | 0.001 | 0.016 | 0.059 | 0.287 | 0.000 | 0.000 | | 0.580 | 0.020 | 0.004 | 0.026 | 0.001 | 0.001 | | | | | | |
| | | 0.002 | 0.032 | 0.178 | 0.862 | 0.000 | 0.000 | | 0.580 | 0.020 | 0.004 | 0.026 | 0.001 | 0.001 | 1.707 | | | | | |
| | | 0.004 | 0.074 | 0.418 | 2.020 | 0.000 | 0.000 | | 1.360 | 0.048 | 0.010 | 0.062 | 0.001 | 0.002 | | | | | | |
| | | 0.002 | 0.037 | 0.279 | 1.347 | 0.000 | 0.000 | | 1.360 | 0.048 | 0.010 | 0.062 | 0.001 | 0.002 | | | | | | |
| | | | | | | | | | 0.084 | | | | | | | | | | | |
| | | | | | | | 13.447 | | 29.586 | | | | | | | 97.313 | | | | |
| | | 0.001 | 0.016 | 0.059 | 0.287 | 0.000 | 0.084 | | 0.412 | 0.020 | 0.004 | 0.026 | 0.001 | 0.001 | | | | | | |
| | | 0.002 | 0.032 | 0.178 | 0.862 | 0.000 | 0.253 | | 0.412 | 0.020 | 0.004 | 0.026 | 0.001 | 0.001 | 1.791 | | | | | |
| | | 0.004 | 0.071 | 0.398 | 1.925 | 0.000 | 0.564 | | 0.920 | 0.046 | 0.010 | 0.059 | 0.001 | 0.002 | | | | | | |
| | | 0.002 | 0.035 | 0.265 | 1.284 | 0.000 | 0.376 | 1.963 | 0.920 | 0.046 | 0.010 | 0.059 | 0.001 | 0.002 | 1.035 | 2.998 | 0.829 | 0.667 | 0.195 | 0.011 |

# Table A-3. Magnetite analyses

| Sample | Analysis | SiO2 | TiO2 | Al2O3 | Cr2O3 | V2O3 | Fe2O3 | total | FeO | MnO | MgO | CaO | NiO | ZnO | Total | TOTAL |
|---|---|---|---|---|---|---|---|---|---|---|---|---|---|---|---|---|
| MSL-20 | g1,1 | 0.06 | 1.83 | 0.07 | 0.07 | | | | 89.35 | 0.12 | 0.01 | 0 | | | 91.52 | |
| Fe-Ti oxide | | 0.001 | 0.023 | 0.001 | 0.000 | 0.000 | 0.000 | | 1.244 | 0.002 | 0.000 | 0.000 | 0.000 | 0.000 | | |
| | | 0.002 | 0.046 | 0.002 | 0.001 | 0.000 | 0.000 | | 1.244 | 0.002 | 0.000 | 0.000 | 0.000 | 0.000 | 1.297 | |
| | | 0.006 | 0.141 | 0.006 | 0.004 | 0.000 | 0.000 | | 3.836 | 0.005 | 0.001 | 0.000 | 0.000 | 0.000 | | |
| | | 0.003 | 0.071 | 0.004 | 0.003 | 0.000 | 0.000 | | 3.836 | 0.005 | 0.001 | 0.000 | 0.000 | 0.000 | | |
| | | | | | | | | | 0.399 | | | | | | | |
| | | | | | | | 63.613 | | 32.041 | | | | | | | 97.814 |
| | | 0.001 | 0.023 | 0.001 | 0.000 | 0.000 | 0.398 | | 0.446 | 0.002 | 0.000 | 0.000 | 0.000 | 0.000 | | |
| | | 0.002 | 0.046 | 0.002 | 0.001 | 0.000 | 1.195 | | 0.446 | 0.002 | 0.000 | 0.000 | 0.000 | 0.000 | 1.694 | |
| | | 0.005 | 0.108 | 0.005 | 0.003 | 0.000 | 2.821 | | 1.053 | 0.004 | 0.001 | 0.000 | 0.000 | 0.000 | | |
| | | 0.002 | 0.054 | 0.003 | 0.002 | 0.000 | 1.881 | 1.943 | 1.053 | 0.004 | 0.001 | 0.000 | 0.000 | 0.000 | 1.058 | 3.000 |
| | 3 | 0.1 | 2.58 | 0.1 | 0.05 | | | | 90.86 | 0.14 | 0.03 | 0 | | | 93.87 | |
| | | 0.002 | 0.032 | 0.001 | 0.000 | 0.000 | 0.000 | | 1.265 | 0.002 | 0.001 | 0.000 | 0.000 | 0.000 | | |
| | | 0.003 | 0.065 | 0.003 | 0.001 | 0.000 | 0.000 | | 1.265 | 0.002 | 0.001 | 0.000 | 0.000 | 0.000 | 1.339 | |
| | | 0.010 | 0.193 | 0.009 | 0.003 | 0.000 | 0.000 | | 3.777 | 0.006 | 0.002 | 0.000 | 0.000 | 0.000 | | |
| | | 0.005 | 0.096 | 0.006 | 0.002 | 0.000 | 0.000 | | 3.777 | 0.006 | 0.002 | 0.000 | 0.000 | 0.000 | | |
| | | | | | | | | | 0.399 | | | | | | | |
| | | | | | | | 63.694 | | 33.478 | | | | | | | 100.172 |
| | | 0.002 | 0.032 | 0.001 | 0.000 | 0.000 | 0.399 | | 0.466 | 0.002 | 0.001 | 0.000 | 0.000 | 0.000 | | |
| | | 0.003 | 0.065 | 0.003 | 0.001 | 0.000 | 1.196 | | 0.466 | 0.002 | 0.001 | 0.000 | 0.000 | 0.000 | 1.737 | |
| | | 0.008 | 0.149 | 0.007 | 0.002 | 0.000 | 2.755 | | 1.073 | 0.005 | 0.002 | 0.000 | 0.000 | 0.000 | | |
| | | 0.004 | 0.074 | 0.005 | 0.002 | 0.000 | 1.837 | 1.921 | 1.073 | 0.005 | 0.002 | 0.000 | 0.000 | 0.000 | 1.079 | 3.000 |
| | 5 | 0.04 | 1.85 | 0.05 | 0.09 | | | | 89.03 | 0.12 | 0 | 0 | | | 91.19 | |
| | | 0.001 | 0.023 | 0.000 | 0.001 | 0.000 | 0.000 | | 1.239 | 0.002 | 0.000 | 0.000 | 0.000 | 0.000 | | |
| | | 0.001 | 0.046 | 0.001 | 0.002 | 0.000 | 0.000 | | 1.239 | 0.002 | 0.000 | 0.000 | 0.000 | 0.000 | 1.292 | |
| | | 0.004 | 0.143 | 0.005 | 0.006 | 0.000 | 0.000 | | 3.837 | 0.005 | 0.000 | 0.000 | 0.000 | 0.000 | | |
| | | 0.002 | 0.072 | 0.003 | 0.004 | 0.000 | 0.000 | | 3.837 | 0.005 | 0.000 | 0.000 | 0.000 | 0.000 | | |
| | | | | | | | | | 0.397 | | | | | | | |
| | | | | | | | 63.375 | | 31.935 | | | | | | | 97.460 |
| | | 0.001 | 0.023 | 0.000 | 0.001 | 0.000 | 0.397 | | 0.444 | 0.002 | 0.000 | 0.000 | 0.000 | 0.000 | | |
| | | 0.001 | 0.046 | 0.001 | 0.002 | 0.000 | 1.190 | | 0.444 | 0.002 | 0.000 | 0.000 | 0.000 | 0.000 | 1.687 | |
| | | 0.003 | 0.110 | 0.003 | 0.004 | 0.000 | 2.822 | | 1.054 | 0.004 | 0.000 | 0.000 | 0.000 | 0.000 | | |
| | | 0.002 | 0.055 | 0.002 | 0.003 | 0.000 | 1.881 | 1.943 | 1.054 | 0.004 | 0.000 | 0.000 | 0.000 | 0.000 | 1.058 | 3.000 |
| | 7 | 0.04 | 2.85 | 0.07 | 0.09 | | | | 88.35 | 0.16 | 0.02 | 0 | | | 91.58 | |
| | | 0.001 | 0.036 | 0.001 | 0.001 | 0.000 | 0.000 | | 1.230 | 0.002 | 0.000 | 0.000 | 0.000 | 0.000 | | |
| | | 0.001 | 0.071 | 0.002 | 0.002 | 0.000 | 0.000 | | 1.230 | 0.002 | 0.000 | 0.000 | 0.000 | 0.000 | 1.309 | |
| | | 0.004 | 0.218 | 0.006 | 0.005 | 0.000 | 0.000 | | 3.758 | 0.007 | 0.002 | 0.000 | 0.000 | 0.000 | | |
| | | 0.002 | 0.109 | 0.004 | 0.004 | 0.000 | 0.000 | | 3.758 | 0.007 | 0.002 | 0.000 | 0.000 | 0.000 | | |
| | | | | | | | | | 0.386 | | | | | | | |
| | | | | | | | 61.587 | | 32.866 | | | | | | | 97.683 |
| | | 0.001 | 0.036 | 0.001 | 0.001 | 0.000 | 0.386 | | 0.457 | 0.002 | 0.000 | 0.000 | 0.000 | 0.000 | | |
| | | 0.001 | 0.071 | 0.002 | 0.002 | 0.000 | 1.157 | | 0.457 | 0.002 | 0.000 | 0.000 | 0.000 | 0.000 | 1.694 | |
| | | 0.003 | 0.168 | 0.005 | 0.004 | 0.000 | 2.732 | | 1.080 | 0.005 | 0.001 | 0.000 | 0.000 | 0.000 | | |
| | | 0.002 | 0.084 | 0.003 | 0.003 | 0.000 | 1.822 | 1.913 | 1.080 | 0.005 | 0.001 | 0.000 | 0.000 | 0.000 | 1.087 | 3.000 |
| | 10 | 0.22 | 2.35 | 0.39 | 0.06 | | | | 86.15 | 0.16 | 0.24 | 0 | | | 91.8 | |
| | | 0.004 | 0.029 | 0.004 | 0.000 | 0.000 | 0.000 | | 1.199 | 0.002 | 0.006 | 0.000 | 0.000 | 0.000 | | |
| | | 0.007 | 0.059 | 0.011 | 0.001 | 0.000 | 0.000 | | 1.199 | 0.002 | 0.006 | 0.000 | 0.000 | 0.000 | 1.286 | |
| | | 0.023 | 0.183 | 0.036 | 0.004 | 0.000 | 0.000 | | 3.729 | 0.007 | 0.019 | 0.000 | 0.000 | 0.000 | | |
| | | 0.011 | 0.091 | 0.024 | 0.002 | 0.000 | 0.000 | | 3.729 | 0.007 | 0.019 | 0.000 | 0.000 | 0.000 | | |
| | | | | | | | | | 0.379 | | | | | | | |
| | | | | | | | 60.440 | | 31.699 | | | | | | | 95.560 |
| | | 0.004 | 0.029 | 0.004 | 0.000 | 0.000 | 0.378 | | 0.441 | 0.002 | 0.006 | 0.000 | 0.000 | 0.000 | | |
| | | 0.007 | 0.059 | 0.011 | 0.001 | 0.000 | 1.135 | | 0.441 | 0.002 | 0.006 | 0.000 | 0.000 | 0.000 | 1.663 | |
| | | 0.018 | 0.141 | 0.028 | 0.003 | 0.000 | 2.730 | | 1.061 | 0.005 | 0.014 | 0.000 | 0.000 | 0.000 | | |
| | | 0.009 | 0.071 | 0.018 | 0.002 | 0.000 | 1.820 | 1.920 | 1.061 | 0.005 | 0.014 | 0.000 | 0.000 | 0.000 | 1.081 | 3.000 |

# Table A-3. Magnetite analyses

| Sample | Analysis | SiO2 | TiO2 | Al2O3 | Cr2O3 | V2O3 | Fe2O3 | total | FeO | MnO | MgO | CaO | NiO | ZnO | Total | TOTAL |
|---|---|---|---|---|---|---|---|---|---|---|---|---|---|---|---|---|
| MSL-20 | 11 | 0.02 | 2.73 | 0.05 | 0.07 | | | | 89.93 | 0.17 | 0.03 | 0.03 | | | 93.03 | |
| Fe-Ti oxide | | 0.000 | 0.034 | 0.000 | 0.000 | 0.000 | 0.000 | | 1.252 | 0.002 | 0.001 | 0.001 | 0.000 | 0.000 | | |
| | | 0.001 | 0.068 | 0.001 | 0.001 | 0.000 | 0.000 | | 1.252 | 0.002 | 0.001 | 0.001 | 0.000 | 0.000 | 1.327 | |
| | | 0.002 | 0.206 | 0.004 | 0.004 | 0.000 | 0.000 | | 3.772 | 0.007 | 0.002 | 0.002 | 0.000 | 0.000 | | |
| | | 0.001 | 0.103 | 0.003 | 0.003 | 0.000 | 0.000 | | 3.772 | 0.007 | 0.002 | 0.002 | 0.000 | 0.000 | | |
| | | | | | | | | | 0.395 | | | | | | | |
| | | | | | | | 63.018 | | 33.157 | | | | | | | 99.275 |
| | | 0.000 | 0.034 | 0.000 | 0.000 | 0.000 | 0.395 | | 0.461 | 0.002 | 0.001 | 0.001 | 0.000 | 0.000 | | |
| | | 0.001 | 0.068 | 0.001 | 0.001 | 0.000 | 1.184 | | 0.461 | 0.002 | 0.001 | 0.001 | 0.000 | 0.000 | 1.721 | |
| | | 0.002 | 0.159 | 0.003 | 0.003 | 0.000 | 2.752 | | 1.073 | 0.006 | 0.002 | 0.001 | 0.000 | 0.000 | | |
| | | 0.001 | 0.079 | 0.002 | 0.002 | 0.000 | 1.834 | 1.919 | 1.073 | 0.006 | 0.002 | 0.001 | 0.000 | 0.000 | 1.081 | 3.000 |
| | 12 | 0.04 | 3 | 0.08 | 0.07 | | | | 89.04 | 0.18 | 0.05 | 0.03 | | | 92.49 | |
| | | 0.001 | 0.038 | 0.001 | 0.000 | 0.000 | 0.000 | | 1.239 | 0.003 | 0.001 | 0.001 | 0.000 | 0.000 | | |
| | | 0.001 | 0.075 | 0.002 | 0.001 | 0.000 | 0.000 | | 1.239 | 0.003 | 0.001 | 0.001 | 0.000 | 0.000 | 1.324 | |
| | | 0.004 | 0.227 | 0.007 | 0.004 | 0.000 | 0.000 | | 3.745 | 0.008 | 0.004 | 0.002 | 0.000 | 0.000 | | |
| | | 0.002 | 0.113 | 0.005 | 0.003 | 0.000 | 0.000 | | 3.745 | 0.008 | 0.004 | 0.002 | 0.000 | 0.000 | | |
| | | | | | | | | | 0.389 | | | | | | | |
| | | | | | | | 61.983 | | 33.199 | | | | | | | 98.632 |
| | | 0.001 | 0.038 | 0.001 | 0.000 | 0.000 | 0.388 | | 0.462 | 0.003 | 0.001 | 0.001 | 0.000 | 0.000 | | |
| | | 0.001 | 0.075 | 0.002 | 0.001 | 0.000 | 1.164 | | 0.462 | 0.003 | 0.001 | 0.001 | 0.000 | 0.000 | 1.711 | |
| | | 0.003 | 0.176 | 0.006 | 0.003 | 0.000 | 2.722 | | 1.080 | 0.006 | 0.003 | 0.001 | 0.000 | 0.000 | | |
| | | 0.002 | 0.088 | 0.004 | 0.002 | 0.000 | 1.815 | 1.910 | 1.080 | 0.006 | 0.003 | 0.001 | 0.000 | 0.000 | 1.090 | 3.000 |
| MSL-34 | gl,sl | 0.07 | 0.92 | 0.05 | 0.06 | | | | 89.71 | 0.06 | 0 | 0.03 | | | 90.89 | |
| Fe-Ti oxide | | 0.001 | 0.012 | 0.000 | 0.000 | 0.000 | 0.000 | | 1.249 | 0.001 | 0.000 | 0.001 | 0.000 | 0.000 | | |
| | | 0.002 | 0.023 | 0.001 | 0.001 | 0.000 | 0.000 | | 1.249 | 0.001 | 0.000 | 0.001 | 0.000 | 0.000 | 1.278 | |
| | | 0.007 | 0.072 | 0.005 | 0.004 | 0.000 | 0.000 | | 3.908 | 0.003 | 0.000 | 0.002 | 0.000 | 0.000 | | |
| | | 0.004 | 0.036 | 0.003 | 0.002 | 0.000 | 0.000 | | 3.908 | 0.003 | 0.000 | 0.002 | 0.000 | 0.000 | | |
| | | | | | | | | | 0.408 | | | | | | | |
| | | | | | | | 65.057 | | 31.100 | | | | | | | 97.347 |
| | | 0.001 | 0.012 | 0.000 | 0.000 | 0.000 | 0.407 | | 0.433 | 0.001 | 0.000 | 0.001 | 0.000 | 0.000 | | |
| | | 0.002 | 0.023 | 0.001 | 0.001 | 0.000 | 1.222 | | 0.433 | 0.001 | 0.000 | 0.001 | 0.000 | 0.000 | 1.684 | |
| | | 0.006 | 0.055 | 0.003 | 0.003 | 0.000 | 2.902 | | 1.028 | 0.002 | 0.000 | 0.001 | 0.000 | 0.000 | | |
| | | 0.003 | 0.027 | 0.002 | 0.002 | 0.000 | 1.935 | 1.969 | 1.028 | 0.002 | 0.000 | 0.001 | 0.000 | 0.000 | 1.031 | 3.000 |
| | s2 | 0.13 | 0.82 | 0.07 | 0.07 | | | | 90.67 | 0.03 | 0 | 0.04 | | | 91.83 | |
| | | 0.002 | 0.010 | 0.001 | 0.000 | 0.000 | 0.000 | | 1.262 | 0.000 | 0.000 | 0.001 | 0.000 | 0.000 | | |
| | | 0.004 | 0.021 | 0.002 | 0.001 | 0.000 | 0.000 | | 1.262 | 0.000 | 0.000 | 0.001 | 0.000 | 0.000 | 1.291 | |
| | | 0.013 | 0.064 | 0.006 | 0.004 | 0.000 | 0.000 | | 3.909 | 0.001 | 0.000 | 0.002 | 0.000 | 0.000 | | |
| | | 0.007 | 0.032 | 0.004 | 0.003 | 0.000 | 0.000 | | 3.909 | 0.001 | 0.000 | 0.002 | 0.000 | 0.000 | | |
| | | | | | | | | | 0.412 | | | | | | | |
| | | | | | | | 65.767 | | 31.420 | | | | | | | 98.347 |
| | | 0.002 | 0.010 | 0.001 | 0.000 | 0.000 | 0.412 | | 0.437 | 0.000 | 0.000 | 0.001 | 0.000 | 0.000 | | |
| | | 0.004 | 0.021 | 0.002 | 0.001 | 0.000 | 1.235 | | 0.437 | 0.000 | 0.000 | 0.001 | 0.000 | 0.000 | 1.702 | |
| | | 0.010 | 0.048 | 0.005 | 0.003 | 0.000 | 2.903 | | 1.028 | 0.001 | 0.000 | 0.002 | 0.000 | 0.000 | | |
| | | 0.005 | 0.024 | 0.003 | 0.002 | 0.000 | 1.935 | 1.970 | 1.028 | 0.001 | 0.000 | 0.002 | 0.000 | 0.000 | 1.030 | 3.000 |

# Table A-3. Magnetite analyses

| Sample | Analysis | SiO2 | TiO2 | Al2O3 | Cr2O3 | V2O3 | Fe2O3 | total | FeO | MnO | MgO | CaO | NiO | ZnO | Total | TOTAL |
|---|---|---|---|---|---|---|---|---|---|---|---|---|---|---|---|---|
| MSL-20 | g2 | 0.12 | 0.03 | 0.07 | 0.02 | | | | 92.41 | 0.01 | 0.01 | 0.05 | | | 92.75 | |
| Primary | | 0.002 | 0.000 | 0.001 | 0.000 | 0.000 | 0.000 | | 1.286 | 0.000 | 0.000 | 0.001 | 0.000 | 0.000 | | |
| Euhedral | | 0.004 | 0.001 | 0.002 | 0.000 | 0.000 | 0.000 | | 1.286 | 0.000 | 0.000 | 0.001 | 0.000 | 0.000 | 1.295 | |
| Magnetite | | 0.012 | 0.002 | 0.006 | 0.001 | 0.000 | 0.000 | | 3.974 | 0.000 | 0.001 | 0.003 | 0.000 | 0.000 | | |
| | | 0.006 | 0.001 | 0.004 | 0.001 | 0.000 | 0.000 | | 3.974 | 0.000 | 0.001 | 0.003 | 0.000 | 0.000 | | |
| | | | | | | | | | 0.427 | | | | | | | |
| | | | | | | | 68.149 | | 31.015 | | | | | | | 99.473 |
| | | 0.002 | 0.000 | 0.001 | 0.000 | 0.000 | 0.427 | | 0.432 | 0.000 | 0.000 | 0.001 | 0.000 | 0.000 | | |
| | | 0.004 | 0.001 | 0.002 | 0.000 | 0.000 | 1.280 | | 0.432 | 0.000 | 0.000 | 0.001 | 0.000 | 0.000 | 1.720 | |
| | | 0.009 | 0.002 | 0.005 | 0.001 | 0.000 | 2.977 | | 1.004 | 0.000 | 0.001 | 0.002 | 0.000 | 0.000 | | |
| | | 0.005 | 0.001 | 0.003 | 0.001 | 0.000 | 1.984 | 1.994 | 1.004 | 0.000 | 0.001 | 0.002 | 0.000 | 0.000 | 1.007 | 3.000 |
| MSL-34 | g3,1 | 0.1 | 0.57 | 0.07 | 0.02 | | | | 90.71 | 0.05 | 0.06 | 0.03 | | | 91.63 | |
| | | 0.002 | 0.007 | 0.001 | 0.000 | 0.000 | 0.000 | | 1.263 | 0.001 | 0.001 | 0.001 | 0.000 | 0.000 | | |
| | | 0.003 | 0.014 | 0.002 | 0.000 | 0.000 | 0.000 | | 1.263 | 0.001 | 0.001 | 0.001 | 0.000 | 0.000 | 1.285 | |
| | | 0.010 | 0.044 | 0.006 | 0.001 | 0.000 | 0.000 | | 3.929 | 0.002 | 0.005 | 0.002 | 0.000 | 0.000 | | |
| | | 0.005 | 0.022 | 0.004 | 0.001 | 0.000 | 0.000 | | 3.929 | 0.002 | 0.005 | 0.002 | 0.000 | 0.000 | | |
| | | | | | | | | | 0.416 | | | | | | | |
| | | | | | | | 66.285 | | 30.994 | | | | | | | 98.179 |
| | | 0.002 | 0.007 | 0.001 | 0.000 | 0.000 | 0.415 | | 0.431 | 0.001 | 0.001 | 0.001 | 0.000 | 0.000 | | |
| | | 0.003 | 0.014 | 0.002 | 0.000 | 0.000 | 1.245 | | 0.431 | 0.001 | 0.001 | 0.001 | 0.000 | 0.000 | 1.699 | |
| | | 0.008 | 0.034 | 0.005 | 0.001 | 0.000 | 2.931 | | 1.015 | 0.002 | 0.004 | 0.001 | 0.000 | 0.000 | | |
| | | 0.004 | 0.017 | 0.003 | 0.001 | 0.000 | 1.954 | 1.979 | 1.015 | 0.002 | 0.004 | 0.001 | 0.000 | 0.000 | 1.022 | 3.000 |

## Table A-4. Ilmenite analyses

| Sample | Analysis | SiO2 | TiO2 | Al2O3 | Cr2O3 | Fe2O3 | total | FeO | MgO | MnO | CaO | Total | total | mol% ilm | hm | gk | pyr |
|---|---|---|---|---|---|---|---|---|---|---|---|---|---|---|---|---|---|
| MSL-20 | s2 | 0.01 | 51.07 | 0.02 | 0.03 | | | 43.66 | 0.04 | 4.02 | 0.06 | 98.91 | | | | | |
| | | 0.000 | 0.639 | 0.000 | 0.000 | 0.000 | | 0.608 | 0.001 | 0.057 | 0.001 | | | | | | |
| | | 0.000 | 1.278 | 0.001 | 0.001 | 0.000 | | 0.608 | 0.001 | 0.057 | 0.007 | 1.952 | | | | | |
| | | 0.001 | 3.929 | 0.002 | 0.002 | 0.000 | | 1.867 | 0.003 | 0.174 | 0.022 | | | | | | |
| | | 0.001 | 1.964 | 0.001 | 0.001 | 0.000 | | 1.867 | 0.003 | 0.174 | 0.022 | | | | | | |
| | | | | | | | | 0.013 | | | | | | | | | |
| | | | | | | 2.106 | | 41.763 | | | | 99.119 | | | | | |
| | | 0.000 | 0.639 | 0.000 | 0.000 | 0.013 | | 0.581 | 0.001 | 0.057 | 0.001 | | | | | | |
| | | 0.000 | 1.278 | 0.001 | 0.001 | 0.040 | | 0.581 | 0.001 | 0.057 | 0.007 | 1.965 | | | | | |
| | | 0.001 | 3.903 | 0.002 | 0.002 | 0.121 | | 1.775 | 0.003 | 0.173 | 0.022 | | | | | | |
| | | 0.001 | 1.952 | 0.001 | 0.001 | 0.081 | 2.034 | 1.775 | 0.003 | 0.173 | 0.022 | 1.973 | 4.007 | 90.022 | 1.793 | 0.140 | 7.981 |
| | s4 | 0 | 51.19 | 0.02 | 0 | | | 42.99 | 0.03 | 3.94 | 0.03 | 98.2 | | | | | |
| | | 0.000 | 0.641 | 0.000 | 0.000 | 0.000 | | 0.598 | 0.001 | 0.056 | 0.001 | | | | | | |
| | | 0.000 | 1.281 | 0.001 | 0.000 | 0.000 | | 0.598 | 0.001 | 0.056 | 0.004 | 1.940 | | | | | |
| | | 0.000 | 3.963 | 0.002 | 0.000 | 0.000 | | 1.850 | 0.002 | 0.172 | 0.011 | | | | | | |
| | | 0.000 | 1.981 | 0.001 | 0.000 | 0.000 | | 1.850 | 0.002 | 0.172 | 0.011 | | | | | | |
| | | | | | | | | 0.007 | | | | | | | | | |
| | | | | | | 1.137 | | 41.966 | | | | 98.313 | | | | | |
| | | 0.000 | 0.641 | 0.000 | 0.000 | 0.007 | | 0.584 | 0.001 | 0.056 | 0.001 | | | | | | |
| | | 0.000 | 1.281 | 0.001 | 0.000 | 0.021 | | 0.584 | 0.001 | 0.056 | 0.004 | 1.947 | | | | | |
| | | 0.000 | 3.948 | 0.002 | 0.000 | 0.066 | | 1.800 | 0.002 | 0.171 | 0.011 | | | | | | |
| | | 0.000 | 1.974 | 0.001 | 0.000 | 0.044 | 2.019 | 1.800 | 0.002 | 0.171 | 0.011 | 1.984 | 4.003 | 90.995 | 0.992 | 0.106 | 7.888 |
| | s7 | 0.02 | 50.82 | 0.02 | 0 | | | 43.84 | 0.03 | 3.87 | 0.05 | 98.65 | | | | | |
| | | 0.000 | 0.636 | 0.000 | 0.000 | 0.000 | | 0.610 | 0.001 | 0.055 | 0.001 | | | | | | |
| | | 0.001 | 1.272 | 0.001 | 0.000 | 0.000 | | 0.610 | 0.001 | 0.055 | 0.006 | 1.945 | | | | | |
| | | 0.002 | 3.925 | 0.002 | 0.000 | 0.000 | | 1.882 | 0.002 | 0.168 | 0.018 | | | | | | |
| | | 0.001 | 1.962 | 0.001 | 0.000 | 0.000 | | 1.882 | 0.002 | 0.168 | 0.018 | | | | | | |
| | | | | | | | | 0.015 | | | | | | | | | |
| | | | | | | 2.371 | | 41.704 | | | | 98.885 | | | | | |
| | | 0.000 | 0.636 | 0.000 | 0.000 | 0.015 | | 0.580 | 0.001 | 0.055 | 0.001 | | | | | | |
| | | 0.001 | 1.272 | 0.001 | 0.000 | 0.045 | | 0.580 | 0.001 | 0.055 | 0.006 | 1.959 | | | | | |
| | | 0.002 | 3.896 | 0.002 | 0.000 | 0.136 | | 1.778 | 0.002 | 0.167 | 0.018 | | | | | | |
| | | 0.001 | 1.948 | 0.001 | 0.000 | 0.091 | 2.040 | 1.778 | 0.002 | 0.167 | 0.018 | 1.965 | 4.006 | 90.067 | 2.020 | 0.105 | 7.725 |
| | s10 | 0.01 | 50.6 | 0.02 | 0.02 | | | 43.53 | 0.03 | 3.83 | 0.01 | 98.05 | | | | | |
| | | 0.000 | 0.633 | 0.000 | 0.000 | 0.000 | | 0.606 | 0.001 | 0.054 | 0.000 | | | | | | |
| | | 0.000 | 1.267 | 0.001 | 0.000 | 0.000 | | 0.606 | 0.001 | 0.054 | 0.001 | 1.930 | | | | | |
| | | 0.001 | 3.938 | 0.002 | 0.001 | 0.000 | | 1.884 | 0.002 | 0.168 | 0.004 | | | | | | |
| | | 0.001 | 1.969 | 0.001 | 0.001 | 0.000 | | 1.884 | 0.002 | 0.168 | 0.004 | | | | | | |
| | | | | | | | | 0.013 | | | | | | | | | |
| | | | | | | 2.140 | | 41.602 | | | | 98.262 | | | | | |
| | | 0.000 | 0.633 | 0.000 | 0.000 | 0.013 | | 0.579 | 0.001 | 0.054 | 0.000 | | | | | | |
| | | 0.000 | 1.267 | 0.001 | 0.000 | 0.040 | | 0.579 | 0.001 | 0.054 | 0.001 | 1.943 | | | | | |
| | | 0.001 | 3.912 | 0.002 | 0.001 | 0.124 | | 1.788 | 0.002 | 0.167 | 0.004 | | | | | | |
| | | 0.001 | 1.956 | 0.001 | 0.001 | 0.083 | 2.041 | 1.788 | 0.002 | 0.167 | 0.004 | 1.961 | 4.002 | 90.287 | 1.842 | 0.106 | 7.697 |
| MSL-34 | s2 | 0.01 | 51.61 | 0.01 | 0.02 | | | 43.43 | 0.03 | 3.14 | 0.06 | 98.31 | | | | | |
| | | 0.000 | 0.646 | 0.000 | 0.000 | 0.000 | | 0.604 | 0.001 | 0.044 | 0.001 | | | | | | |
| | | 0.000 | 1.292 | 0.000 | 0.000 | 0.000 | | 0.604 | 0.001 | 0.044 | 0.007 | 1.950 | | | | | |
| | | 0.001 | 3.976 | 0.001 | 0.001 | 0.000 | | 1.860 | 0.002 | 0.136 | 0.022 | | | | | | |
| | | 0.001 | 1.988 | 0.001 | 0.001 | 0.000 | | 1.860 | 0.002 | 0.136 | 0.022 | | | | | | |
| | | | | | | | | 0.002 | | | | | | | | | |
| | | | | | | 0.321 | | 43.141 | | | | 98.342 | | | | | |
| | | 0.000 | 0.646 | 0.000 | 0.000 | 0.002 | | 0.600 | 0.001 | 0.044 | 0.001 | | | | | | |
| | | 0.000 | 1.292 | 0.000 | 0.000 | 0.006 | | 0.600 | 0.001 | 0.044 | 0.007 | 1.951 | | | | | |
| | | 0.001 | 3.973 | 0.001 | 0.001 | 0.019 | | 1.846 | 0.002 | 0.136 | 0.022 | | | | | | |
| | | 0.001 | 1.986 | 0.001 | 0.001 | 0.012 | 2.000 | 1.846 | 0.002 | 0.136 | 0.022 | 2.007 | 4.007 | 93.215 | 0.289 | 0.107 | 6.388 |

# Table A-4. Ilmenite analyses

| Sample | Analysis | SiO2 | TiO2 | Al2O3 | Cr2O3 | Fe2O3 | total | FeO | MgO | MnO | CaO | Total | total | mol% ilm | hm | gk | pyr |
|---|---|---|---|---|---|---|---|---|---|---|---|---|---|---|---|---|---|
| MSL-34 | s3 | 0.02 | 50.51 | 0.02 | 0.03 | | | 43.94 | 0.03 | 3.01 | 0.21 | 97.77 | | | | | |
| | | 0.000 | 0.632 | 0.000 | 0.000 | 0.000 | | 0.612 | 0.001 | 0.042 | 0.004 | | | | | | |
| | | 0.001 | 1.264 | 0.001 | 0.001 | 0.000 | | 0.612 | 0.001 | 0.042 | 0.025 | 1.946 | | | | | |
| | | 0.002 | 3.898 | 0.002 | 0.002 | 0.000 | | 1.886 | 0.002 | 0.131 | 0.077 | | | | | | |
| | | 0.001 | 1.949 | 0.001 | 0.001 | 0.000 | | 1.886 | 0.002 | 0.131 | 0.077 | | | | | | |
| | | | | | | | | 0.013 | | | | | | | | | |
| | | | | | | 2.011 | | 42.128 | | | | 97.969 | | | | | |
| | | 0.000 | 0.632 | 0.000 | 0.000 | 0.013 | | 0.586 | 0.001 | 0.042 | 0.004 | | | | | | |
| | | 0.001 | 1.264 | 0.001 | 0.001 | 0.038 | | 0.586 | 0.001 | 0.042 | 0.025 | 1.958 | | | | | |
| | | 0.002 | 3.875 | 0.002 | 0.002 | 0.116 | | 1.797 | 0.002 | 0.130 | 0.077 | | | | | | |
| | | 0.001 | 1.937 | 0.001 | 0.001 | 0.077 | 2.017 | 1.797 | 0.002 | 0.130 | 0.077 | 2.006 | 4.023 | 91.894 | 1.768 | 0.108 | 6.168 |
| | s4 | 0.05 | 50.97 | 0 | 0 | | | 42.81 | 0.03 | 3.24 | 0.49 | 97.68 | | | | | |
| | | 0.001 | 0.638 | 0.000 | 0.000 | 0.000 | | 0.596 | 0.001 | 0.046 | 0.008 | | | | | | |
| | | 0.002 | 1.276 | 0.000 | 0.000 | 0.000 | | 0.596 | 0.001 | 0.046 | 0.058 | 1.978 | | | | | |
| | | 0.005 | 3.870 | 0.000 | 0.000 | 0.000 | | 1.807 | 0.002 | 0.139 | 0.177 | | | | | | |
| | | 0.003 | 1.935 | 0.000 | 0.000 | 0.000 | | 1.807 | 0.002 | 0.139 | 0.177 | | | | | | |
| | | | | | | | | 0.006 | | | | | | | | | |
| | | | | | | 0.944 | | 41.960 | | | | 97.774 | | | | | |
| | | 0.001 | 0.638 | 0.000 | 0.000 | 0.006 | | 0.584 | 0.001 | 0.046 | 0.008 | | | | | | |
| | | 0.002 | 1.276 | 0.000 | 0.000 | 0.018 | | 0.584 | 0.001 | 0.046 | 0.058 | 1.982 | | | | | |
| | | 0.005 | 3.861 | 0.000 | 0.000 | 0.054 | | 1.768 | 0.002 | 0.138 | 0.177 | | | | | | |
| | | 0.003 | 1.931 | 0.000 | 0.000 | 0.036 | 1.967 | 1.768 | 0.002 | 0.138 | 0.177 | 2.085 | 4.051 | 92.419 | 0.843 | 0.108 | 6.617 |
| | s5 | 0.04 | 50.61 | 0 | 0 | | | 44.53 | 0.05 | 3.03 | 0.25 | 98.51 | | | | | |
| | | 0.001 | 0.633 | 0.000 | 0.000 | 0.000 | | 0.620 | 0.001 | 0.043 | 0.004 | | | | | | |
| | | 0.001 | 1.267 | 0.000 | 0.000 | 0.000 | | 0.620 | 0.001 | 0.043 | 0.030 | 1.962 | | | | | |
| | | 0.004 | 3.875 | 0.000 | 0.000 | 0.000 | | 1.896 | 0.004 | 0.131 | 0.091 | | | | | | |
| | | 0.002 | 1.937 | 0.000 | 0.000 | 0.000 | | 1.896 | 0.004 | 0.131 | 0.091 | | | | | | |
| | | | | | | | | 0.017 | | | | | | | | | |
| | | | | | | 2.703 | | 42.095 | | | | 98.778 | | | | | |
| | | 0.001 | 0.633 | 0.000 | 0.000 | 0.017 | | 0.586 | 0.001 | 0.043 | 0.004 | | | | | | |
| | | 0.001 | 1.267 | 0.000 | 0.000 | 0.051 | | 0.586 | 0.001 | 0.043 | 0.030 | 1.977 | | | | | |
| | | 0.004 | 3.844 | 0.000 | 0.000 | 0.154 | | 1.778 | 0.004 | 0.130 | 0.090 | | | | | | |
| | | 0.002 | 1.922 | 0.000 | 0.000 | 0.103 | 2.025 | 1.778 | 0.004 | 0.130 | 0.090 | 2.002 | 4.027 | 91.232 | 2.328 | 0.179 | 6.152 |
| | s7 | 0.04 | 51.08 | 0.01 | 0.01 | | | 42.58 | 0.04 | 3.24 | 0.48 | 97.48 | | | | | |
| | | 0.001 | 0.639 | 0.000 | 0.000 | 0.000 | | 0.593 | 0.001 | 0.046 | 0.008 | | | | | | |
| | | 0.001 | 1.279 | 0.000 | 0.000 | 0.000 | | 0.593 | 0.001 | 0.046 | 0.057 | 1.977 | | | | | |
| | | 0.004 | 3.881 | 0.001 | 0.001 | 0.000 | | 1.799 | 0.003 | 0.139 | 0.174 | | | | | | |
| | | 0.002 | 1.940 | 0.001 | 0.000 | 0.000 | | 1.799 | 0.003 | 0.139 | 0.174 | | | | | | |
| | | | | | | | | 0.004 | | | | | | | | | |
| | | | | | | 0.580 | | 42.058 | | | | 97.537 | | | | | |
| | | 0.001 | 0.639 | 0.000 | 0.000 | 0.004 | | 0.585 | 0.001 | 0.046 | 0.008 | | | | | | |
| | | 0.001 | 1.279 | 0.000 | 0.000 | 0.011 | | 0.585 | 0.001 | 0.046 | 0.057 | 1.979 | | | | | |
| | | 0.004 | 3.876 | 0.001 | 0.001 | 0.033 | | 1.774 | 0.003 | 0.138 | 0.174 | | | | | | |
| | | 0.002 | 1.938 | 0.001 | 0.000 | 0.022 | 1.961 | 1.774 | 0.003 | 0.138 | 0.174 | 2.089 | 4.050 | 92.706 | 0.522 | 0.144 | 6.623 |
| | s9 | 0 | 50.03 | 0.01 | 0.01 | | | 44.71 | 0.04 | 2.93 | 0.13 | 97.86 | | | | | |
| | | 0.000 | 0.626 | 0.000 | 0.000 | 0.000 | | 0.622 | 0.001 | 0.041 | 0.002 | | | | | | |
| | | 0.000 | 1.252 | 0.000 | 0.000 | 0.000 | | 0.622 | 0.001 | 0.041 | 0.016 | 1.933 | | | | | |
| | | 0.000 | 3.887 | 0.001 | 0.001 | 0.000 | | 1.932 | 0.003 | 0.128 | 0.048 | | | | | | |
| | | 0.000 | 1.944 | 0.001 | 0.000 | 0.000 | | 1.932 | 0.003 | 0.128 | 0.048 | | | | | | |
| | | | | | | | | 0.020 | | | | | | | | | |
| | | | | | | 3.221 | | 41.808 | | | | 98.179 | | | | | |
| | | 0.000 | 0.626 | 0.000 | 0.000 | 0.020 | | 0.582 | 0.001 | 0.041 | 0.002 | | | | | | |
| | | 0.000 | 1.252 | 0.000 | 0.000 | 0.061 | | 0.582 | 0.001 | 0.041 | 0.016 | 1.953 | | | | | |
| | | 0.000 | 3.847 | 0.001 | 0.001 | 0.186 | | 1.788 | 0.003 | 0.127 | 0.048 | | | | | | |
| | | 0.000 | 1.924 | 0.001 | 0.000 | 0.124 | 2.049 | 1.788 | 0.003 | 0.127 | 0.048 | 1.965 | 4.014 | 90.929 | 2.771 | 0.144 | 5.998 |

# Table A-4. Ilmenite analyses

| Sample | Analysis | SiO2 | TiO2 | Al2O3 | Cr2O3 | Fe2O3 | total | FeO | MgO | MnO | CaO | Total | total | mol% ilm | hm | gk | pyr |
|---|---|---|---|---|---|---|---|---|---|---|---|---|---|---|---|---|---|
| MSL-34 | s10 | 0 | 50.27 | 0 | 0.02 | | | 43.92 | 0.02 | 3.19 | 0.09 | 97.52 | | | | | |
| | | 0.000 | 0.629 | 0.000 | 0.000 | 0.000 | | 0.611 | 0.000 | 0.045 | 0.002 | | | | | | |
| | | 0.000 | 1.258 | 0.000 | 0.000 | 0.000 | | 0.611 | 0.000 | 0.045 | 0.011 | 1.926 | | | | | |
| | | 0.000 | 3.920 | 0.000 | 0.001 | 0.000 | | 1.904 | 0.002 | 0.140 | 0.033 | | | | | | |
| | | 0.000 | 1.960 | 0.000 | 0.001 | 0.000 | | 1.904 | 0.002 | 0.140 | 0.033 | | | | | | |
| | | | | | | | | 0.014 | | | | | | | | | |
| | | | | | | 2.301 | | 41.847 | | | | 97.748 | | | | | |
| | | 0.000 | 0.629 | 0.000 | 0.000 | 0.014 | | 0.582 | 0.000 | 0.045 | 0.002 | | | | | | |
| | | 0.000 | 1.258 | 0.000 | 0.000 | 0.043 | | 0.582 | 0.000 | 0.045 | 0.011 | 1.941 | | | | | |
| | | 0.000 | 3.891 | 0.000 | 0.001 | 0.134 | | 1.801 | 0.002 | 0.139 | 0.033 | | | | | | |
| | | 0.000 | 1.945 | 0.000 | 0.001 | 0.089 | 2.035 | 1.801 | 0.002 | 0.139 | 0.033 | 1.975 | 4.010 | 91.311 | 2.008 | 0.072 | 6.526 |
| | s11 | 0.01 | 50.27 | 0 | 0.04 | | | 43.63 | 0.03 | 2.93 | 0.06 | 96.9 | | | | | |
| | | 0.000 | 0.629 | 0.000 | 0.000 | 0.000 | | 0.607 | 0.001 | 0.041 | 0.001 | | | | | | |
| | | 0.000 | 1.258 | 0.000 | 0.001 | 0.000 | | 0.607 | 0.001 | 0.041 | 0.007 | 1.916 | | | | | |
| | | 0.001 | 3.941 | 0.000 | 0.002 | 0.000 | | 1.902 | 0.002 | 0.129 | 0.022 | | | | | | |
| | | 0.001 | 1.970 | 0.000 | 0.002 | 0.000 | | 1.902 | 0.002 | 0.129 | 0.022 | | | | | | |
| | | | | | | | | 0.010 | | | | | | | | | |
| | | | | | | 1.631 | | 42.161 | | | | 97.062 | | | | | |
| | | 0.000 | 0.629 | 0.000 | 0.000 | 0.010 | | 0.587 | 0.001 | 0.041 | 0.001 | | | | | | |
| | | 0.000 | 1.258 | 0.000 | 0.001 | 0.031 | | 0.587 | 0.001 | 0.041 | 0.007 | 1.926 | | | | | |
| | | 0.001 | 3.921 | 0.000 | 0.002 | 0.095 | | 1.828 | 0.002 | 0.129 | 0.022 | | | | | | |
| | | 0.001 | 1.960 | 0.000 | 0.002 | 0.064 | 2.026 | 1.828 | 0.002 | 0.129 | 0.022 | 1.982 | 4.007 | 92.331 | 1.457 | 0.109 | 6.061 |
| | s12 | 0.14 | 49.78 | 0.08 | 0.04 | | | 45.17 | 0.05 | 2.93 | 0.04 | 98.22 | | | | | |
| | | 0.002 | 0.623 | 0.001 | 0.000 | 0.000 | | 0.629 | 0.001 | 0.041 | 0.001 | | | | | | |
| | | 0.005 | 1.246 | 0.002 | 0.001 | 0.000 | | 0.629 | 0.001 | 0.041 | 0.005 | 1.930 | | | | | |
| | | 0.014 | 3.874 | 0.007 | 0.002 | 0.000 | | 1.955 | 0.004 | 0.128 | 0.015 | | | | | | |
| | | 0.007 | 1.937 | 0.005 | 0.002 | 0.000 | | 1.955 | 0.004 | 0.128 | 0.015 | | | | | | |
| | | | | | | | | 0.023 | | | | | | | | | |
| | | | | | | 3.607 | | 41.921 | | | | 98.577 | | | | | |
| | | 0.002 | 0.623 | 0.001 | 0.000 | 0.023 | | 0.583 | 0.001 | 0.041 | 0.001 | | | | | | |
| | | 0.005 | 1.246 | 0.002 | 0.001 | 0.068 | | 0.583 | 0.001 | 0.041 | 0.005 | 1.948 | | | | | |
| | | 0.014 | 3.839 | 0.007 | 0.002 | 0.209 | | 1.797 | 0.004 | 0.127 | 0.015 | | | | | | |
| | | 0.007 | 1.919 | 0.005 | 0.002 | 0.139 | 2.065 | 1.797 | 0.004 | 0.127 | 0.015 | 1.943 | 4.008 | 90.536 | 3.085 | 0.180 | 6.002 |
| | s15 | 0.01 | 49.97 | 0 | 0.04 | | | 44.82 | 0.04 | 2.95 | 0.04 | 97.88 | | | | | |
| | | 0.000 | 0.625 | 0.000 | 0.000 | 0.000 | | 0.624 | 0.001 | 0.042 | 0.001 | | | | | | |
| | | 0.000 | 1.251 | 0.000 | 0.001 | 0.000 | | 0.624 | 0.001 | 0.042 | 0.005 | 1.923 | | | | | |
| | | 0.001 | 3.903 | 0.000 | 0.002 | 0.000 | | 1.946 | 0.003 | 0.130 | 0.015 | | | | | | |
| | | 0.001 | 1.951 | 0.000 | 0.002 | 0.000 | | 1.946 | 0.003 | 0.130 | 0.015 | | | | | | |
| | | | | | | | | 0.020 | | | | | | | | | |
| | | | | | | 3.267 | | 41.877 | | | | 98.204 | | | | | |
| | | 0.000 | 0.625 | 0.000 | 0.000 | 0.020 | | 0.583 | 0.001 | 0.042 | 0.001 | | | | | | |
| | | 0.000 | 1.251 | 0.000 | 0.001 | 0.061 | | 0.583 | 0.001 | 0.042 | 0.005 | 1.943 | | | | | |
| | | 0.001 | 3.862 | 0.000 | 0.002 | 0.189 | | 1.800 | 0.003 | 0.128 | 0.015 | | | | | | |
| | | 0.001 | 1.931 | 0.000 | 0.002 | 0.126 | 2.059 | 1.800 | 0.003 | 0.128 | 0.015 | 1.946 | 4.005 | 90.845 | 2.808 | 0.144 | 6.040 |
| | s16 | 0 | 50.84 | 0 | 0 | | | 43.6 | 0.04 | 3.22 | 0.04 | 97.75 | | | | | |
| | | 0.000 | 0.636 | 0.000 | 0.000 | 0.000 | | 0.607 | 0.001 | 0.045 | 0.001 | | | | | | |
| | | 0.000 | 1.273 | 0.000 | 0.000 | 0.000 | | 0.607 | 0.001 | 0.045 | 0.005 | 1.931 | | | | | |
| | | 0.000 | 3.955 | 0.000 | 0.000 | 0.000 | | 1.886 | 0.003 | 0.141 | 0.015 | | | | | | |
| | | 0.000 | 1.978 | 0.000 | 0.000 | 0.000 | | 1.886 | 0.003 | 0.141 | 0.015 | | | | | | |
| | | | | | | | | 0.009 | | | | | | | | | |
| | | | | | | 1.403 | | 42.336 | | | | 97.889 | | | | | |
| | | 0.000 | 0.636 | 0.000 | 0.000 | 0.009 | | 0.589 | 0.001 | 0.045 | 0.001 | | | | | | |
| | | 0.000 | 1.273 | 0.000 | 0.000 | 0.026 | | 0.589 | 0.001 | 0.045 | 0.005 | 1.939 | | | | | |
| | | 0.000 | 3.937 | 0.000 | 0.000 | 0.082 | | 1.823 | 0.003 | 0.140 | 0.015 | | | | | | |
| | | 0.000 | 1.969 | 0.000 | 0.000 | 0.054 | 2.023 | 1.823 | 0.003 | 0.140 | 0.015 | 1.981 | 4.004 | 92.022 | 1.240 | 0.144 | 6.564 |

# Table A-4. Ilmenite analyses

| Sample | Analysis | SiO2 | TiO2 | Al2O3 | Cr2O3 | Fe2O3 | total | FeO | MgO | MnO | CaO | Total | total | mol% ilm | hm | gk | pyr |
|---|---|---|---|---|---|---|---|---|---|---|---|---|---|---|---|---|---|
| MSL-34 | s17 | 0 | 50.15 | 0 | 0.06 | | | 44.43 | 0.03 | 3.22 | 0.08 | 97.97 | | | | | |
| | | 0.000 | 0.628 | 0.000 | 0.000 | 0.000 | | 0.618 | 0.001 | 0.045 | 0.001 | | | | | | |
| | | 0.000 | 1.255 | 0.000 | 0.001 | 0.000 | | 0.618 | 0.001 | 0.045 | 0.010 | 1.931 | | | | | |
| | | 0.000 | 3.901 | 0.000 | 0.004 | 0.000 | | 1.922 | 0.002 | 0.141 | 0.030 | | | | | | |
| | | 0.000 | 1.951 | 0.000 | 0.002 | 0.000 | | 1.922 | 0.002 | 0.141 | 0.030 | | | | | | |
| | | | | | | | | 0.019 | | | | | | | | | |
| | | | | | | 2.984 | | 41.741 | | | | 98.266 | | | | | |
| | | 0.000 | 0.628 | 0.000 | 0.000 | 0.019 | | 0.581 | 0.001 | 0.045 | 0.001 | | | | | | |
| | | 0.000 | 1.255 | 0.000 | 0.001 | 0.056 | | 0.581 | 0.001 | 0.045 | 0.010 | 1.949 | | | | | |
| | | 0.000 | 3.864 | 0.000 | 0.004 | 0.173 | | 1.788 | 0.002 | 0.140 | 0.029 | | | | | | |
| | | 0.000 | 1.932 | 0.000 | 0.002 | 0.115 | 2.050 | 1.788 | 0.002 | 0.140 | 0.029 | 1.960 | 4.009 | 90.639 | 2.563 | 0.108 | 6.555 |
| | s18 | 0 | 50.4 | 0 | 0 | | | 45.02 | 0.03 | 2.94 | 0.11 | 98.5 | | | | | |
| | | 0.000 | 0.631 | 0.000 | 0.000 | 0.000 | | 0.627 | 0.001 | 0.041 | 0.002 | | | | | | |
| | | 0.000 | 1.262 | 0.000 | 0.000 | 0.000 | | 0.627 | 0.001 | 0.041 | 0.013 | 1.943 | | | | | |
| | | 0.000 | 3.895 | 0.000 | 0.000 | 0.000 | | 1.934 | 0.002 | 0.128 | 0.040 | | | | | | |
| | | 0.000 | 1.947 | 0.000 | 0.000 | 0.000 | | 1.934 | 0.002 | 0.128 | 0.040 | | | | | | |
| | | | | | | | | 0.020 | | | | | | | | | |
| | | | | | | 3.179 | | 42.156 | | | | 98.815 | | | | | |
| | | 0.000 | 0.631 | 0.000 | 0.000 | 0.020 | | 0.587 | 0.001 | 0.041 | 0.002 | | | | | | |
| | | 0.000 | 1.262 | 0.000 | 0.000 | 0.060 | | 0.587 | 0.001 | 0.041 | 0.013 | 1.963 | | | | | |
| | | 0.000 | 3.855 | 0.000 | 0.000 | 0.182 | | 1.793 | 0.002 | 0.127 | 0.040 | | | | | | |
| | | 0.000 | 1.928 | 0.000 | 0.000 | 0.122 | 2.049 | 1.793 | 0.002 | 0.127 | 0.040 | 1.962 | 4.011 | 91.039 | 2.719 | 0.107 | 5.981 |
| | s19 | 0 | 50.25 | 0.01 | 0 | | | 43.91 | 0.03 | 3.01 | 0.04 | 97.29 | | | | | |
| | | 0.000 | 0.629 | 0.000 | 0.000 | 0.000 | | 0.611 | 0.001 | 0.042 | 0.001 | | | | | | |
| | | 0.000 | 1.258 | 0.000 | 0.000 | 0.000 | | 0.611 | 0.001 | 0.042 | 0.005 | 1.917 | | | | | |
| | | 0.000 | 3.936 | 0.001 | 0.000 | 0.000 | | 1.913 | 0.002 | 0.133 | 0.015 | | | | | | |
| | | 0.000 | 1.968 | 0.001 | 0.000 | 0.000 | | 1.913 | 0.002 | 0.133 | 0.015 | | | | | | |
| | | | | | | | | 0.013 | | | | | | | | | |
| | | | | | | 2.072 | | 42.043 | | | | 97.495 | | | | | |
| | | 0.000 | 0.629 | 0.000 | 0.000 | 0.013 | | 0.585 | 0.001 | 0.042 | 0.001 | | | | | | |
| | | 0.000 | 1.258 | 0.000 | 0.000 | 0.039 | | 0.585 | 0.001 | 0.042 | 0.005 | 1.930 | | | | | |
| | | 0.000 | 3.910 | 0.001 | 0.000 | 0.121 | | 1.819 | 0.002 | 0.132 | 0.015 | | | | | | |
| | | 0.000 | 1.955 | 0.001 | 0.000 | 0.081 | 2.036 | 1.819 | 0.002 | 0.132 | 0.015 | 1.968 | 4.004 | 91.804 | 1.827 | 0.109 | 6.194 |
| | s22 | 0 | 50.22 | 0 | 0.04 | | | 44.55 | 0.04 | 2.75 | 0.1 | 97.69 | | | | | |
| | | 0.000 | 0.629 | 0.000 | 0.000 | 0.000 | | 0.620 | 0.001 | 0.039 | 0.002 | | | | | | |
| | | 0.000 | 1.257 | 0.000 | 0.001 | 0.000 | | 0.620 | 0.001 | 0.039 | 0.012 | 1.930 | | | | | |
| | | 0.000 | 3.909 | 0.000 | 0.002 | 0.000 | | 1.928 | 0.003 | 0.121 | 0.037 | | | | | | |
| | | 0.000 | 1.954 | 0.000 | 0.002 | 0.000 | | 1.928 | 0.003 | 0.121 | 0 037 | | | | | | |
| | | | | | | | | 0.016 | | | | | | | | | |
| | | | | | | 2.587 | | 42.219 | | | | 97.946 | | | | | |
| | | 0.000 | 0.629 | 0.000 | 0.000 | 0.016 | | 0.588 | 0.001 | 0.039 | 0.002 | | | | | | |
| | | 0.000 | 1.257 | 0.000 | 0.001 | 0.049 | | 0.588 | 0.001 | 0.039 | 0.012 | 1.946 | | | | | |
| | | 0.000 | 3.876 | 0.000 | 0.002 | 0.150 | | 1.812 | 0.003 | 0.120 | 0.037 | | | | | | |
| | | 0.000 | 1.938 | 0.000 | 0.002 | 0.100 | 2.040 | 1.812 | 0.003 | 0.120 | 0.037 | 1.971 | 4.011 | 91.825 | 2.263 | 0.145 | 5.663 |
| | s23 | 0.14 | 50.19 | 0.02 | 0.01 | | | 44.58 | 0.05 | 3.19 | 0.1 | 98.37 | | | | | |
| | | 0.002 | 0.628 | 0.000 | 0.000 | 0.000 | | 0.620 | 0.001 | 0.045 | 0.002 | | | | | | |
| | | 0.005 | 1.256 | 0.001 | 0.000 | 0.000 | | 0.620 | 0.001 | 0.045 | 0.012 | 1.940 | | | | | |
| | | 0.014 | 3.885 | 0.002 | 0.001 | 0.000 | | 1.919 | 0.004 | 0.139 | 0.037 | | | | | | |
| | | 0.007 | 1.942 | 0.001 | 0.000 | 0.000 | | 1.919 | 0.004 | 0.139 | 0.037 | | | | | | |
| | | | | | | | | 0.019 | | | | | | | | | |
| | | | | | | 2.995 | | 41.882 | | | | 98.667 | | | | | |
| | | 0.002 | 0.628 | 0.000 | 0.000 | 0.019 | | 0.583 | 0.001 | 0.045 | 0.002 | | | | | | |
| | | 0.005 | 1.256 | 0.001 | 0.000 | 0.056 | | 0.583 | 0.001 | 0.045 | 0.012 | 1.954 | | | | | |
| | | 0.014 | 3.857 | 0.002 | 0.001 | 0.173 | | 1.790 | 0.004 | 0.138 | 0.037 | | | | | | |
| | | 0.007 | 1.928 | 0.001 | 0.000 | 0.115 | 2.045 | 1.790 | 0.004 | 0.138 | 0.037 | 1.968 | 4.013 | 90.628 | 2.571 | 0.179 | 6.488 |

# Table A-4. Ilmenite analyses

| Sample | Analysis | SiO2 | TiO2 | Al2O3 | Cr2O3 | Fe2O3 | total | FeO | MgO | MnO | CaO | Total | total | mol% ilm | hm | gk | pyr |
|---|---|---|---|---|---|---|---|---|---|---|---|---|---|---|---|---|---|
| MSL-34 | s24 | 0 | 49.43 | 0 | 0.02 | | | 44.57 | 0.06 | 2.98 | 0.13 | 97.19 | | | | | |
| | | 0.000 | 0.619 | 0.000 | 0.000 | 0.000 | | 0.620 | 0.001 | 0.042 | 0.002 | | | | | | |
| | | 0.000 | 1.237 | 0.000 | 0.000 | 0.000 | | 0.620 | 0.001 | 0.042 | 0.016 | 1.917 | | | | | |
| | | 0.000 | 3.873 | 0.000 | 0.001 | 0.000 | | 1.942 | 0.005 | 0.131 | 0.049 | | | | | | |
| | | 0.000 | 1.936 | 0.000 | 0.001 | 0.000 | | 1.942 | 0.005 | 0.131 | 0.049 | | | | | | |
| | | | | | | | | 0.024 | | | | | | | | | |
| | | | | | | 3.758 | | 41.184 | | | | 97.562 | | | | | |
| | | 0.000 | 0.619 | 0.000 | 0.000 | 0.024 | | 0.573 | 0.001 | 0.042 | 0.002 | | | | | | |
| | | 0.000 | 1.237 | 0.000 | 0.000 | 0.071 | | 0.573 | 0.001 | 0.042 | 0.016 | 1.940 | | | | | |
| | | 0.000 | 3.826 | 0.000 | 0.001 | 0.218 | | 1.772 | 0.005 | 0.130 | 0.048 | | | | | | |
| | | 0.000 | 1.913 | 0.000 | 0.001 | 0.146 | 2.059 | 1.772 | 0.005 | 0.130 | 0.048 | 1.955 | 4.014 | 90.225 | 3.218 | 0.217 | 6.126 |

# Table A-5. Broadbeam analyses

| Sample | Analysis | SiO2 | TiO2 | Al2O3 | Cr2O3 | V2O3 | total | Fe2O3 | Fe3+ | total | FeO | MnO | MgO | CaO | NiO | ZnO | Total | TOTAL |
|---|---|---|---|---|---|---|---|---|---|---|---|---|---|---|---|---|---|---|
| MSL-20 | 1 | 0.16 | 15.12 | 0.17 | 0.06 | | | | | | 76.32 | 1.1 | 0.08 | 0.03 | | | 93.05 | |
| | | 0.003 | 0.189 | 0.002 | 0.000 | 0.000 | | 0.000 | | | 1.062 | 0.016 | 0.002 | 0.001 | 0.000 | 0.000 | | |
| | | 0.005 | 0.378 | 0.005 | 0.001 | 0.000 | | 0.000 | | | 1.062 | 0.016 | 0.002 | 0.001 | 0.000 | 0.000 | 1.470 | |
| | | 0.014 | 1.030 | 0.014 | 0.003 | 0.000 | | 0.000 | | | 2.890 | 0.042 | 0.005 | 0.001 | 0.000 | 0.000 | | |
| | | 0.007 | 0.515 | 0.009 | 0.002 | 0.000 | | 0.000 | | | 2.890 | 0.042 | 0.005 | 0.001 | 0.000 | 0.000 | | |
| | | | | | | | | | | | 0.231 | | | | | | | |
| | | | | | | | | 36.916 | | | 43.062 | | | | | | | 96.698 |
| | | 0.003 | 0.189 | 0.002 | 0.000 | 0.000 | | 0.231 | | | 0.599 | 0.016 | 0.002 | 0.001 | 0.000 | 0.000 | | |
| | | 0.005 | 0.378 | 0.005 | 0.001 | 0.000 | | 0.693 | | | 0.599 | 0.016 | 0.002 | 0.001 | 0.000 | 0.000 | 1.701 | |
| | | 0.013 | 0.890 | 0.012 | 0.003 | 0.000 | | 1.631 | | | 1.410 | 0.036 | 0.005 | 0.001 | 0.000 | 0.000 | | |
| | | 0.006 | 0.445 | 0.008 | 0.002 | 0.000 | 0.461 | 1.087 | 0.539 | 1.000 | 1.410 | 0.036 | 0.005 | 0.001 | 0.000 | 0.000 | 2.000 | 3.000 |
| | 3 | 0.14 | 15.18 | 0.24 | 0.08 | | | | | | 77.98 | 1.13 | 0.08 | 0.01 | | | 94.84 | |
| | | 0.002 | 0.190 | 0.002 | 0.001 | 0.000 | | 0.000 | | | 1.085 | 0.016 | 0.002 | 0.000 | 0.000 | 0.000 | | |
| | | 0.005 | 0.380 | 0.007 | 0.002 | 0.000 | | 0.000 | | | 1.085 | 0.016 | 0.002 | 0.000 | 0.000 | 0.000 | 1.497 | |
| | | 0.012 | 1.015 | 0.019 | 0.004 | 0.000 | | 0.000 | | | 2.901 | 0.043 | 0.005 | 0.000 | 0.000 | 0.000 | | |
| | | 0.006 | 0.508 | 0.013 | 0.003 | 0.000 | | 0.000 | | | 2.901 | 0.043 | 0.005 | 0.000 | 0.000 | 0.000 | | |
| | | | | | | | | | | | 0.239 | | | | | | | |
| | | | | | | | | 38.060 | | | 43.692 | | | | | | | 98.612 |
| | | 0.002 | 0.190 | 0.002 | 0.001 | 0.000 | | 0.238 | | | 0.608 | 0.016 | 0.002 | 0.000 | 0.000 | 0.000 | | |
| | | 0.005 | 0.380 | 0.007 | 0.002 | 0.000 | | 0.715 | | | 0.608 | 0.016 | 0.002 | 0.000 | 0.000 | 0.000 | 1.734 | |
| | | 0.011 | 0.876 | 0.016 | 0.004 | 0.000 | | 1.649 | | | 1.402 | 0.037 | 0.005 | 0.000 | 0.000 | 0.000 | | |
| | | 0.005 | 0.438 | 0.011 | 0.002 | 0.000 | 0.457 | 1.099 | 0.543 | 1.000 | 1.402 | 0.037 | 0.005 | 0.000 | 0.000 | 0.000 | 2.000 | 3.000 |
| | 4 | 0.14 | 15.48 | 0.23 | 0.05 | | | | | | 78.1 | 1.24 | 0.07 | 0.03 | | | 95.34 | |
| | | 0.002 | 0.194 | 0.002 | 0.000 | 0.000 | | 0.000 | | | 1.087 | 0.017 | 0.002 | 0.001 | 0.000 | 0.000 | | |
| | | 0.005 | 0.387 | 0.007 | 0.001 | 0.000 | | 0.000 | | | 1.087 | 0.017 | 0.002 | 0.001 | 0.000 | 0.000 | 1.507 | |
| | | 0.012 | 1.029 | 0.018 | 0.003 | 0.000 | | 0.000 | | | 2.886 | 0.046 | 0.005 | 0.001 | 0.000 | 0.000 | | |
| | | 0.006 | 0.514 | 0.012 | 0.002 | 0.000 | | 0.000 | | | 2.886 | 0.046 | 0.005 | 0.001 | 0.000 | 0.000 | | |
| | | | | | | | | | | | 0.237 | | | | | | | |
| | | | | | | | | 37.854 | | | 43.998 | | | | | | | 99.091 |
| | | 0.002 | 0.194 | 0.002 | 0.000 | 0.000 | | 0.237 | | | 0.612 | 0.017 | 0.002 | 0.001 | 0.000 | 0.000 | | |
| | | 0.005 | 0.387 | 0.007 | 0.001 | 0.000 | | 0.711 | | | 0.612 | 0.017 | 0.002 | 0.001 | 0.000 | 0.000 | 1.743 | |
| | | 0.011 | 0.889 | 0.016 | 0.002 | 0.000 | | 1.632 | | | 1.405 | 0.040 | 0.004 | 0.001 | 0.000 | 0.000 | | |
| | | 0.005 | 0.445 | 0.010 | 0.002 | 0.000 | 0.462 | 1.088 | 0.538 | 1.000 | 1.405 | 0.040 | 0.004 | 0.001 | 0.000 | 0.000 | 2.000 | 3.000 |
| | 6 | 0.12 | 14.97 | 0.16 | 0.05 | | | | | | 77.28 | 1.14 | 0.07 | 0.04 | | | 93.84 | |
| | | 0.002 | 0.187 | 0.002 | 0.000 | 0.000 | | 0.000 | | | 1.076 | 0.016 | 0.002 | 0.001 | 0.000 | 0.000 | | |
| | | 0.004 | 0.375 | 0.005 | 0.001 | 0.000 | | 0.000 | | | 1.076 | 0.016 | 0.002 | 0.001 | 0.000 | 0.000 | 1.479 | |
| | | 0.011 | 1.014 | 0.013 | 0.003 | 0.000 | | 0.000 | | | 2.910 | 0.043 | 0.005 | 0.002 | 0.000 | 0.000 | | |
| | | 0.005 | 0.507 | 0.008 | 0.002 | 0.000 | | 0.000 | | | 2.910 | 0.043 | 0.005 | 0.002 | 0.000 | 0.000 | | |
| | | | | | | | | | | | 0.238 | | | | | | | |
| | | | | | | | | 37.932 | | | 43.107 | | | | | | | 97.589 |
| | | 0.002 | 0.187 | 0.002 | 0.000 | 0.000 | | 0.237 | | | 0.600 | 0.016 | 0.002 | 0.001 | 0.000 | 0.000 | | |
| | | 0.004 | 0.375 | 0.005 | 0.001 | 0.000 | | 0.712 | | | 0.600 | 0.016 | 0.002 | 0.001 | 0.000 | 0.000 | 1.715 | |
| | | 0.009 | 0.874 | 0.011 | 0.002 | 0.000 | | 1.661 | | | 1.399 | 0.037 | 0.004 | 0.002 | 0.000 | 0.000 | | |
| | | 0.005 | 0.437 | 0.007 | 0.002 | 0.000 | 0.450 | 1.108 | 0.550 | 1.000 | 1.399 | 0.037 | 0.004 | 0.002 | 0.000 | 0.000 | 2.000 | 3.000 |
| | 7 | 0.13 | 15.24 | 0.19 | 0.07 | | | | | | 76.63 | 1.22 | 0.07 | 0.02 | | | 93.56 | |
| | | 0.002 | 0.191 | 0.002 | 0.000 | 0.000 | | 0.000 | | | 1.067 | 0.017 | 0.002 | 0.000 | 0.000 | 0.000 | | |
| | | 0.004 | 0.381 | 0.006 | 0.001 | 0.000 | | 0.000 | | | 1.067 | 0.017 | 0.002 | 0.000 | 0.000 | 0.000 | 1.479 | |
| | | 0.012 | 1.032 | 0.015 | 0.004 | 0.000 | | 0.000 | | | 2.885 | 0.047 | 0.005 | 0.001 | 0.000 | 0.000 | | |
| | | 0.006 | 0.516 | 0.010 | 0.002 | 0.000 | | 0.000 | | | 2.885 | 0.047 | 0.005 | 0.001 | 0.000 | 0.000 | | |
| | | | | | | | | | | | 0.233 | | | | | | | |
| | | | | | | | | 37.092 | | | 43.213 | | | | | | | 97.246 |
| | | 0.002 | 0.191 | 0.002 | 0.000 | 0.000 | | 0.232 | | | 0.601 | 0.017 | 0.002 | 0.000 | 0.000 | 0.000 | | |
| | | 0.004 | 0.381 | 0.006 | 0.001 | 0.000 | | 0.697 | | | 0.601 | 0.017 | 0.002 | 0.000 | 0.000 | 0.000 | 1.710 | |
| | | 0.010 | 0.892 | 0.013 | 0.003 | 0.000 | | 1.630 | | | 1.407 | 0.040 | 0.004 | 0.001 | 0.000 | 0.000 | | |
| | | 0.005 | 0.446 | 0.009 | 0.002 | 0.000 | 0.462 | 1.086 | 0.538 | 1.000 | 1.407 | 0.040 | 0.004 | 0.001 | 0.000 | 0.000 | 2.000 | 3.000 |

## Table A-5. Broadbeam analyses

| Sample | Analysis | SiO2 | TiO2 | Al2O3 | Cr2O3 | V2O3 | total | Fe2O3 | Fe3+ | total | FeO | MnO | MgO | CaO | NiO | ZnO | Total | TOTAL |
|---|---|---|---|---|---|---|---|---|---|---|---|---|---|---|---|---|---|---|
| | 8 | 0.13 | 14.42 | 0.16 | 0.07 | | | | | | 77.13 | 1.06 | 0.11 | 0.05 | | | 93.13 | |
| | | 0.002 | 0.180 | 0.002 | 0.000 | 0.000 | | 0.000 | | | 1.074 | 0.015 | 0.003 | 0.001 | 0.000 | 0.000 | | |
| | | 0.004 | 0.361 | 0.005 | 0.001 | 0.000 | | 0.000 | | | 1.074 | 0.015 | 0.003 | 0.001 | 0.000 | 0.000 | 1.463 | |
| | | 0.012 | 0.987 | 0.013 | 0.004 | 0.000 | | 0.000 | | | 2.934 | 0.041 | 0.007 | 0.002 | 0.000 | 0.000 | | |
| | | 0.006 | 0.493 | 0.009 | 0.003 | 0.000 | | 0.000 | | | 2.934 | 0.041 | 0.007 | 0.002 | 0.000 | 0.000 | | |
| | | | | | | | | | | | 0.242 | | | | | | | |
| | | | | | | | | 38.530 | | | 42.418 | | | | | | | 96.948 |
| | | 0.002 | 0.180 | 0.002 | 0.000 | 0.000 | | 0.241 | | | 0.590 | 0.015 | 0.003 | 0.001 | 0.000 | 0.000 | | |
| | | 0.004 | 0.361 | 0.005 | 0.001 | 0.000 | | 0.724 | | | 0.590 | 0.015 | 0.003 | 0.001 | 0.000 | 0.000 | 1.704 | |
| | | 0.010 | 0.847 | 0.011 | 0.003 | 0.000 | | 1.699 | | | 1.386 | 0.035 | 0.006 | 0.002 | 0.000 | 0.000 | | |
| | | 0.005 | 0.424 | 0.007 | 0.002 | 0.000 | 0.438 | 1.133 | 0.562 | 1.000 | 1.386 | 0.035 | 0.006 | 0.002 | 0.000 | 0.000 | 2.000 | 3.000 |
| | 9 | 0.12 | 14.53 | 0.14 | 0.06 | | | | | | 76.94 | 1.13 | 0.08 | 0.02 | | | 93.02 | |
| | | 0.002 | 0.182 | 0.001 | 0.000 | 0.000 | | 0.000 | | | 1.071 | 0.016 | 0.002 | 0.000 | 0.000 | 0.000 | | |
| | | 0.004 | 0.364 | 0.004 | 0.001 | 0.000 | | 0.000 | | | 1.071 | 0.016 | 0.002 | 0.000 | 0.000 | 0.000 | 1.462 | |
| | | 0.011 | 0.995 | 0.011 | 0.003 | 0.000 | | 0.000 | | | 2.930 | 0.044 | 0.005 | 0.001 | 0.000 | 0.000 | | |
| | | 0.005 | 0.497 | 0.008 | 0.002 | 0.000 | | 0.000 | | | 2.930 | 0.044 | 0.005 | 0.001 | 0.000 | 0.000 | | |
| | | | | | | | | | | | 0.240 | | | | | | | |
| | | | | | | | | 38.260 | | | 42.472 | | | | | | | 96.811 |
| | | 0.002 | 0.182 | 0.001 | 0.000 | 0.000 | | 0.240 | | | 0.591 | 0.016 | 0.002 | 0.000 | 0.000 | 0.000 | | |
| | | 0.004 | 0.364 | 0.004 | 0.001 | 0.000 | | 0.719 | | | 0.591 | 0.016 | 0.002 | 0.000 | 0.000 | 0.000 | 1.701 | |
| | | 0.009 | 0.855 | 0.010 | 0.003 | 0.000 | | 1.690 | | | 1.390 | 0.037 | 0.005 | 0.001 | 0.000 | 0.000 | | |
| | | 0.005 | 0.428 | 0.006 | 0.002 | 0.000 | 0.441 | 1.127 | 0.559 | 1.000 | 1.390 | 0.037 | 0.005 | 0.001 | 0.000 | 0.000 | 2.000 | 3.000 |
| | 11 | 0.15 | 14.31 | 0.17 | 0.08 | | | | | | 78.38 | 1.06 | 0.06 | 0.04 | | | 94.26 | |
| | | 0.002 | 0.179 | 0.002 | 0.001 | 0.000 | | 0.000 | | | 1.091 | 0.015 | 0.001 | 0.001 | 0.000 | 0.000 | | |
| | | 0.005 | 0.358 | 0.005 | 0.002 | 0.000 | | 0.000 | | | 1.091 | 0.015 | 0.001 | 0.001 | 0.000 | 0.000 | 1.478 | |
| | | 0.014 | 0.970 | 0.014 | 0.004 | 0.000 | | 0.000 | | | 2.953 | 0.040 | 0.004 | 0.002 | 0.000 | 0.000 | | |
| | | 0.007 | 0.485 | 0.009 | 0.003 | 0.000 | | 0.000 | | | 2.953 | 0.040 | 0.004 | 0.002 | 0.000 | 0.000 | | |
| | | | | | | | | | | | 0.248 | | | | | | | |
| | | | | | | | | 39.482 | | | 42.810 | | | | | | | 98.163 |
| | | 0.002 | 0.179 | 0.002 | 0.001 | 0.000 | | 0.247 | | | 0.596 | 0.015 | 0.001 | 0.001 | 0.000 | 0.000 | | |
| | | 0.005 | 0.358 | 0.005 | 0.002 | 0.000 | | 0.742 | | | 0.596 | 0.015 | 0.001 | 0.001 | 0.000 | 0.000 | 1.724 | |
| | | 0.012 | 0.831 | 0.012 | 0.004 | 0.000 | | 1.720 | | | 1.382 | 0.035 | 0.003 | 0.002 | 0.000 | 0.000 | | |
| | | 0.006 | 0.415 | 0.008 | 0.002 | 0.000 | 0.431 | 1.147 | 0.569 | 1.000 | 1.382 | 0.035 | 0.003 | 0.002 | 0.000 | 0.000 | 2.000 | 3.000 |
| | 12 | 0.14 | 14.4 | 0.14 | 0.06 | | | | | | 78.51 | 1.01 | 0.07 | 0 | | | 94.35 | |
| | | 0.002 | 0.180 | 0.001 | 0.000 | 0.000 | | 0.000 | | | 1.093 | 0.014 | 0.002 | 0.000 | 0.000 | 0.000 | | |
| | | 0.005 | 0.360 | 0.004 | 0.001 | 0.000 | | 0.000 | | | 1.093 | 0.014 | 0.002 | 0.000 | 0.000 | 0.000 | 1.479 | |
| | | 0.013 | 0.975 | 0.011 | 0.003 | 0.000 | | 0.000 | | | 2.955 | 0.039 | 0.005 | 0.000 | 0.000 | 0.000 | | |
| | | 0.006 | 0.487 | 0.007 | 0.002 | 0.000 | | 0.000 | | | 2.955 | 0.039 | 0.005 | 0.000 | 0.000 | 0.000 | | |
| | | | | | | | | | | | 0.247 | | | | | | | |
| | | | | | | | | 39.437 | | | 42.981 | | | | | | | 98.238 |
| | | 0.002 | 0.180 | 0.001 | 0.000 | 0.000 | | 0.247 | | | 0.598 | 0.014 | 0.002 | 0.000 | 0.000 | 0.000 | | |
| | | 0.005 | 0.360 | 0.004 | 0.001 | 0.000 | | 0.741 | | | 0.598 | 0.014 | 0.002 | 0.000 | 0.000 | 0.000 | 1.725 | |
| | | 0.011 | 0.836 | 0.010 | 0.003 | 0.000 | | 1.717 | | | 1.387 | 0.033 | 0.004 | 0.000 | 0.000 | 0.000 | | |
| | | 0.005 | 0.418 | 0.006 | 0.002 | 0.000 | 0.431 | 1.145 | 0.569 | 1.000 | 1.387 | 0.033 | 0.004 | 0.000 | 0.000 | 0.000 | 2.000 | 3.000 |
| | 13 | 0.13 | 14.28 | 0.16 | 0.07 | | | | | | 79.43 | 1.03 | 0.07 | 0.01 | | | 95.19 | |
| | | 0.002 | 0.179 | 0.002 | 0.000 | 0.000 | | 0.000 | | | 1.106 | 0.015 | 0.002 | 0.000 | 0.000 | 0.000 | | |
| | | 0.004 | 0.357 | 0.005 | 0.001 | 0.000 | | 0.000 | | | 1.106 | 0.015 | 0.002 | 0.000 | 0.000 | 0.000 | 1.490 | |
| | | 0.012 | 0.960 | 0.013 | 0.004 | 0.000 | | 0.000 | | | 2.968 | 0.039 | 0.005 | 0.000 | 0.000 | 0.000 | | |
| | | 0.006 | 0.480 | 0.008 | 0.002 | 0.000 | | 0.000 | | | 2.968 | 0.039 | 0.005 | 0.000 | 0.000 | 0.000 | | |
| | | | | | | | | | | | 0.253 | | | | | | | |
| | | | | | | | | 40.305 | | | 43.119 | | | | | | | 99.174 |
| | | 0.002 | 0.179 | 0.002 | 0.000 | 0.000 | | 0.252 | | | 0.600 | 0.015 | 0.002 | 0.000 | 0.000 | 0.000 | | |
| | | 0.004 | 0.357 | 0.005 | 0.001 | 0.000 | | 0.757 | | | 0.600 | 0.015 | 0.002 | 0.000 | 0.000 | 0.000 | 1.742 | |
| | | 0.010 | 0.821 | 0.011 | 0.003 | 0.000 | | 1.739 | | | 1.378 | 0.033 | 0.004 | 0.000 | 0.000 | 0.000 | | |
| | | 0.005 | 0.411 | 0.007 | 0.002 | 0.000 | 0.425 | 1.159 | 0.575 | 1.000 | 1.378 | 0.033 | 0.004 | 0.000 | 0.000 | 0.000 | 2.000 | 3.000 |

# Table A-5. Broadbeam analyses

| Sample | Analysis | SiO2 | TiO2 | Al2O3 | Cr2O3 | V2O3 | total | Fe2O3 | Fe3+ | total | FeO | MnO | MgO | CaO | NiO | ZnO | Total | TOTAL |
|---|---|---|---|---|---|---|---|---|---|---|---|---|---|---|---|---|---|---|
| MSL-34 | 4 | 0.11 | 18.91 | 0 | 0.06 | | | | | | 77.08 | 0.86 | 0.05 | 0.09 | | | 92.1 | |
| | | 0.002 | 0.237 | 0.000 | 0.000 | 0.000 | | 0.000 | | | 1.073 | 0.012 | 0.001 | 0.002 | 0.000 | 0.000 | | |
| | | 0.004 | 0.473 | 0.000 | 0.001 | 0.000 | | 0.000 | | | 1.073 | 0.012 | 0.001 | 0.002 | 0.000 | 0.000 | 1.566 | |
| | | 0.009 | 1.209 | 0.000 | 0.003 | 0.000 | | 0.000 | | | 2.740 | 0.031 | 0.003 | 0.004 | 0.000 | 0.000 | | |
| | | 0.005 | 0.605 | 0.000 | 0.002 | 0.000 | | 0.000 | | | 2.740 | 0.031 | 0.003 | 0.004 | 0.000 | 0.000 | | |
| | | | | | | | | | | | 0.203 | | | | | | | |
| | | | | | | | | 32.450 | | | 47.846 | | | | | | | 100.376 |
| | | 0.002 | 0.237 | 0.000 | 0.000 | 0.000 | | 0.203 | | | 0.666 | 0.012 | 0.001 | 0.002 | 0.000 | 0.000 | | |
| | | 0.004 | 0.473 | 0.000 | 0.001 | 0.000 | | 0.610 | | | 0.666 | 0.012 | 0.001 | 0.002 | 0.000 | 0.000 | 1.769 | |
| | | 0.008 | 1.071 | 0.000 | 0.003 | 0.000 | | 1.379 | | | 1.506 | 0.027 | 0.003 | 0.004 | 0.000 | 0.000 | | |
| | | 0.004 | 0.535 | 0.000 | 0.002 | 0.000 | 0.541 | 0.919 | 0.459 | 1.000 | 1.506 | 0.027 | 0.003 | 0.004 | 0.000 | 0.000 | 2.000 | 3.000 |
| | 7 | 0.11 | 20.82 | 0.05 | 0.03 | | | | | | 71.94 | 1.25 | 0.05 | 0.09 | | | 94.33 | |
| | | 0.002 | 0.261 | 0.000 | 0.000 | 0.000 | | 0.000 | | | 1.001 | 0.018 | 0.001 | 0.002 | 0.000 | 0.000 | | |
| | | 0.004 | 0.521 | 0.001 | 0.001 | 0.000 | | 0.000 | | | 1.001 | 0.018 | 0.001 | 0.002 | 0.000 | 0.000 | 1.549 | |
| | | 0.009 | 1.346 | 0.004 | 0.002 | 0.000 | | 0.000 | | | 2.586 | 0.046 | 0.003 | 0.004 | 0.000 | 0.000 | | |
| | | 0.005 | 0.673 | 0.003 | 0.001 | 0.000 | | 0.000 | | | 2.586 | 0.046 | 0.003 | 0.004 | 0.000 | 0.000 | | |
| | | | | | | | | | | | 0.165 | | | | | | | |
| | | | | | | | | 26.382 | | | 48.173 | | | | | | | 96.954 |
| | | 0.002 | 0.261 | 0.000 | 0.000 | 0.000 | | 0.165 | | | 0.670 | 0.018 | 0.001 | 0.002 | 0.000 | 0.000 | | |
| | | 0.004 | 0.521 | 0.001 | 0.001 | 0.000 | | 0.496 | | | 0.670 | 0.018 | 0.001 | 0.002 | 0.000 | 0.000 | 1.713 | |
| | | 0.009 | 1.217 | 0.003 | 0.001 | 0.000 | | 1.157 | | | 1.565 | 0.041 | 0.003 | 0.004 | 0.000 | 0.000 | | |
| | | 0.004 | 0.608 | 0.002 | 0.001 | 0.000 | 0.616 | 0.771 | 0.384 | 1.000 | 1.565 | 0.041 | 0.003 | 0.004 | 0.000 | 0.000 | 2.000 | 3.000 |
| | 17 | 0.22 | 19.52 | 0.11 | 0.02 | | | | | | 73.66 | 1.22 | 0.05 | 0.15 | | | 94.94 | |
| | | 0.004 | 0.244 | 0.001 | 0.000 | 0.000 | | 0.000 | | | 1.025 | 0.017 | 0.001 | 0.003 | 0.000 | 0.000 | | |
| | | 0.007 | 0.489 | 0.003 | 0.000 | 0.000 | | 0.000 | | | 1.025 | 0.017 | 0.001 | 0.003 | 0.000 | 0.000 | 1.546 | |
| | | 0.019 | 1.264 | 0.008 | 0.001 | 0.000 | | 0.000 | | | 2.653 | 0.044 | 0.003 | 0.007 | 0.000 | 0.000 | | |
| | | 0.009 | 0.632 | 0.006 | 0.001 | 0.000 | | 0.000 | | | 2.653 | 0.044 | 0.003 | 0.007 | 0.000 | 0.000 | | |
| | | | | | | | | | | | 0.183 | | | | | | | |
| | | | | | | | | 29.196 | | | 47.357 | | | | | | | 97.843 |
| | | 0.004 | 0.244 | 0.001 | 0.000 | 0.000 | | 0.183 | | | 0.659 | 0.017 | 0.001 | 0.003 | 0.000 | 0.000 | | |
| | | 0.007 | 0.489 | 0.003 | 0.000 | 0.000 | | 0.548 | | | 0.659 | 0.017 | 0.001 | 0.003 | 0.000 | 0.000 | 1.728 | |
| | | 0.017 | 1.131 | 0.007 | 0.001 | 0.000 | | 1.269 | | | 1.526 | 0.040 | 0.003 | 0.006 | 0.000 | 0.000 | | |
| | | 0.008 | 0.565 | 0.005 | 0.001 | 0.000 | 0.580 | 0.846 | 0.420 | 1.000 | 1.526 | 0.040 | 0.003 | 0.006 | 0.000 | 0.000 | 2.000 | 3.000 |
| MSL-58 | g3, #6 | 0.15 | 11.21 | 0.05 | 0.03 | | | | | | 81.04 | 1.07 | 0.07 | 0.06 | | | 93.68 | |
| | | 0.002 | 0.140 | 0.000 | 0.000 | 0.000 | | 0.000 | | | 1.128 | 0.015 | 0.002 | 0.001 | 0.000 | 0.000 | | |
| | | 0.005 | 0.281 | 0.001 | 0.001 | 0.000 | | 0.000 | | | 1.128 | 0.015 | 0.002 | 0.001 | 0.000 | 0.000 | 1.434 | |
| | | 0.014 | 0.783 | 0.004 | 0.002 | 0.000 | | 0.000 | | | 3.147 | 0.042 | 0.005 | 0.003 | 0.000 | 0.000 | | |
| | | 0.007 | 0.391 | 0.003 | 0.001 | 0.000 | | 0.000 | | | 3.147 | 0.042 | 0.005 | 0.003 | 0.000 | 0.000 | | |
| | | | | | | | | | | | 0.286 | | | | | | | |
| | | | | | | | | 45.695 | | | 39.873 | | | | | | | 98.208 |
| | | 0.002 | 0.140 | 0.000 | 0.000 | 0.000 | | 0.286 | | | 0.555 | 0.015 | 0.002 | 0.001 | 0.000 | 0.000 | | |
| | | 0.005 | 0.281 | 0.001 | 0.001 | 0.000 | | 0.858 | | | 0.555 | 0.015 | 0.002 | 0.001 | 0.000 | 0.000 | 1.719 | |
| | | 0.012 | 0.653 | 0.003 | 0.001 | 0.000 | | 1.997 | | | 1.291 | 0.035 | 0.004 | 0.002 | 0.000 | 0.000 | | |
| | | 0.006 | 0.327 | 0.002 | 0.001 | 0.000 | 0.336 | 1.332 | 0.664 | 1.000 | 1.291 | 0.035 | 0.004 | 0.002 | 0.000 | 0.000 | 2.000 | 3.000 |

# APPENDIX B

GEOPHYSICAL DATA:

MAGNETIC DATA (B-1, B-2)
VLF DATA (B-3)
SUSCEPTIBILITY DATA (B-4)

Table B-1. Magnetic readings along lines

| North (m) | East (m) | Reading (nT) | Anomaly (nT) | North (m) | East (m) | Reading (nT) | Anomaly (nT) |
|---|---|---|---|---|---|---|---|
| 0 | 0.0 | 59534.2 | 34.2 | 5 | 0.0 | 59577.4 | 77.4 |
| 0 | 6.0 | 61072.4 | 1572.4 | 5 | 5.0 | 60830.7 | 1330.7 |
| 0 | 7.5 | 63016.1 | 3516.1 | 5 | 10.0 | 66048.5 | 6548.5 |
| 0 | 11.5 | 63614.4 | 4114.4 | 5 | 17.5 | 66693.6 | 7193.6 |
| 0 | 15.0 | 65619.1 | 6119.1 | 5 | 20.0 | 67441.8 | 7941.8 |
| 0 | 17.5 | 66445.0 | 6945.0 | 5 | 22.5 | 67955.2 | 8455.2 |
| 0 | 20.0 | 66140.1 | 6640.1 | 5 | 25.0 | 67952.6 | 8452.6 |
| 0 | 25.0 | 66674.4 | 7174.4 | 5 | 27.5 | 68988.6 | 9488.6 |
| 0 | 30.0 | 68032.0 | 8532.0 | 5 | 30.0 | 67429.2 | 7929.2 |
| 0 | 32.5 | 69876.0 | 10376.0 | 5 | 32.5 | 69372.5 | 9872.5 |
| 0 | 40.0 | 66127.4 | 6627.4 | 5 | 35.0 | 69517.6 | 10017.6 |
| 0 | 42.5 | 64730.2 | 5230.2 | 5 | 37.5 | 68939.9 | 9439.9 |
| 0 | 44.0 | 57363.9 | -2136.1 | 5 | 40.0 | 69255.4 | 9755.4 |
| 0 | 45.0 | 55496.8 | -4003.2 | 5 | 42.5 | 63681.6 | 4181.6 |
| 0 | 47.5 | 55414.2 | -4085.8 | 5 | 45.0 | 56222.3 | -3277.7 |
| 0 | 48.5 | 58642.9 | -857.1 | 5 | 47.5 | 56836.3 | -2663.7 |
| 0 | 51.5 | 59233.9 | -266.1 | 5 | 50.0 | 60969.8 | 1469.8 |
| 0 | 52.5 | 60144.0 | 644.0 | 5 | 52.5 | 62725.8 | 3225.8 |
| 0 | 60.0 | 60701.2 | 1201.2 | 5 | 55.0 | 62506.9 | 3006.9 |
| 0 | 62.5 | 61555.7 | 2055.7 | 5 | 57.5 | 62399.2 | 2899.2 |
| 0 | 65.0 | 61970.4 | 2470.4 | 5 | 60.0 | 62486.4 | 2986.4 |
| 0 | 67.5 | 62228.0 | 2728.0 | 5 | 65.0 | 62433.6 | 2933.6 |
| 0 | 70.0 | 61576.7 | 2076.7 | 5 | 70.0 | 62080.8 | 2580.8 |
| 0 | 72.5 | 60852.6 | 1352.6 | 5 | 72.0 | 61403.5 | 1903.5 |
| 0 | 78.0 | 60030.2 | 530.2 | 5 | 73.0 | 60923.1 | 1423.1 |
| 0 | 81.0 | 59338.6 | -161.4 | 5 | 74.0 | 60456.2 | 956.2 |
| 0 | 82.0 | 59047.9 | -452.1 | 5 | 77.0 | 60014.1 | 514.1 |
| 0 | 83.5 | 58931.8 | -568.2 | 5 | 81.0 | 59870.1 | 370.1 |
| 0 | 85.0 | 58601.3 | -898.7 | 5 | 83.5 | 58975.8 | -524.2 |
| 0 | 90.0 | 58456.0 | -1044.0 | 5 | 89.5 | 58494.8 | -1005.2 |
| 0 | 91.0 | 58293.9 | -1206.1 | 5 | 92.5 | 58314.3 | -1185.7 |
| 0 | 92.0 | 58262.7 | -1237.3 | 5 | 93.5 | 58194.2 | -1305.8 |
| 0 | 93.5 | 58194.2 | -1305.8 | 5 | 95.0 | 58076.0 | -1424.0 |
| 0 | 95.0 | 58112.9 | -1387.1 | 5 | 97.5 | 57992.8 | -1507.2 |
| 0 | 96.0 | 57975.4 | -1524.6 | 5 | 99.0 | 57775.9 | -1724.1 |
| 0 | 97.5 | 57870.0 | -1630.0 | 5 | 100.0 | 57641.0 | -1859.0 |
| 0 | 98.0 | 57840.7 | -1659.3 | 5 | 106.5 | 57405.9 | -2094.1 |
| 0 | 100.0 | 57504.7 | -1995.3 | 5 | 110.0 | 57081.1 | -2418.9 |
| 0 | 107.0 | 57337.1 | -2162.9 | 5 | 111.0 | 57124.3 | -2375.7 |
| 0 | 110.0 | 57173.1 | -2326.9 | 5 | 113.5 | 57196.4 | -2303.6 |
| | | | | 5 | 115.0 | 57254.1 | -2245.9 |

Table B-1. Magnetic data continued

| North (m) | East (m) | Reading (nT) | Anomaly (nT) | North (m) | East (m) | Reading (nT) | Anomaly (nT) |
|---|---|---|---|---|---|---|---|
| 10 | 0.0 | 59479.9 | -20.1 | 15 | 0.0 | 59375.2 | -124.8 |
| 10 | 2.5 | 60019.4 | 519.4 | 15 | 2.5 | 60106.9 | 606.9 |
| 10 | 5.0 | 60663.7 | 1163.7 | 15 | 5.0 | 60626.1 | 1126.1 |
| 10 | 7.5 | 61208.8 | 1708.8 | 15 | 7.5 | 61507.7 | 2007.7 |
| 10 | 10.0 | 63655.3 | 4155.3 | 15 | 10.0 | 64615.6 | 5115.6 |
| 10 | 12.5 | 66768.1 | 7268.1 | 15 | 12.5 | 62250.5 | 2750.5 |
| 10 | 15.0 | 66743.0 | 7243.0 | 15 | 15.0 | 58799.3 | -700.7 |
| 10 | 17.5 | 69800.5 | 10300.5 | 15 | 17.5 | 56161.4 | -3338.6 |
| 10 | 20.0 | 70027.9 | 10527.9 | 15 | 20.0 | 54247.2 | -5252.8 |
| 10 | 22.5 | 68191.3 | 8691.3 | 15 | 22.5 | 53887.4 | -5612.6 |
| 10 | 25.0 | 67793.3 | 8293.3 | 15 | 25.0 | 55331.3 | -4168.7 |
| 10 | 27.5 | 65493.8 | 5993.8 | 15 | 27.5 | 55930.8 | -3569.2 |
| 10 | 30.0 | 66513.2 | 7013.2 | 15 | 30.0 | 56392.3 | -3107.7 |
| 10 | 32.5 | 68977.0 | 9477.0 | 15 | 32.5 | 54713.0 | -4787.0 |
| 10 | 35.0 | 71402.1 | 11902.1 | 15 | 35.0 | 54738.8 | -4761.2 |
| 10 | 37.5 | 71750.5 | 12250.5 | 15 | 37.5 | 53597.8 | -5902.2 |
| 10 | 39.0 | 70538.7 | 11038.7 | 15 | 40.0 | 54392.6 | -5107.4 |
| 10 | 40.0 | 69037.2 | 9537.2 | 15 | 45.5 | 57827.8 | -1672.2 |
| 10 | 42.0 | 69452.4 | 9952.4 | 15 | 47.0 | 59891.9 | 391.9 |
| 10 | 43.0 | 67841.0 | 8341.0 | 15 | 48.0 | 59770.9 | 270.9 |
| 10 | 44.0 | 65281.4 | 5781.4 | 15 | 49.0 | 63878.5 | 4378.5 |
| 10 | 51.5 | 64107.8 | 4607.8 | 15 | 50.0 | 64035.1 | 4535.1 |
| 10 | 55.0 | 64348.5 | 4848.5 | 15 | 51.5 | 64372.9 | 4872.9 |
| 10 | 57.5 | 63532.8 | 4032.8 | 15 | 52.0 | 64894.6 | 5394.6 |
| 10 | 60.0 | 63418.5 | 3918.5 | 15 | 53.0 | 65193.0 | 5693.0 |
| 10 | 62.5 | 63700.0 | 4200.0 | 15 | 54.0 | 64728.6 | 5228.6 |
| 10 | 65.0 | 63319.8 | 3819.8 | 15 | 55.0 | 64634.7 | 5134.7 |
| 10 | 67.5 | 62668.0 | 3168.0 | 15 | 57.0 | 63821.2 | 4321.2 |
| 10 | 72.0 | 61677.2 | 2177.2 | 15 | 65.0 | 63116.0 | 3616.0 |
| 10 | 73.5 | 60482.3 | 982.3 | 15 | 67.5 | 62810.0 | 3310.0 |
| 10 | 77.5 | 59887.7 | 387.7 | 15 | 72.0 | 60655.8 | 1155.8 |
| 10 | 83.5 | 59408.1 | -91.9 | 15 | 75.0 | 60021.8 | 521.8 |
| 10 | 84.0 | 58909.4 | -590.6 | 15 | 81.0 | 59532.7 | 32.7 |
| 10 | 85.0 | 58654.2 | -845.8 | 15 | 83.0 | 58971.2 | -528.8 |
| 10 | 87.5 | 58600.0 | -900.0 | 15 | 85.0 | 58627.3 | -872.7 |
| 10 | 91.0 | 58369.2 | -1130.8 | 15 | 86.0 | 58504.5 | -995.5 |
| 10 | 92.5 | 58150.6 | -1349.4 | 15 | 87.5 | 58457.4 | -1042.6 |
| 10 | 94.0 | 58099.7 | -1400.3 | 15 | 90.0 | 58412.0 | -1088.0 |
| 10 | 97.5 | 57853.8 | -1646.2 | 15 | 95.0 | 58004.2 | -1495.8 |
| 10 | 100.0 | 57596.1 | -1903.9 | 15 | 97.5 | 57863.3 | -1636.7 |
| 10 | 102.5 | 57469.2 | -2030.8 | 15 | 100.0 | 57671.0 | -1829.0 |
| 10 | 105.0 | 57452.9 | -2047.1 | 15 | 102.5 | 57525.6 | -1974.4 |
| 10 | 107.0 | 57410.0 | -2090.0 | 15 | 105.0 | 57477.8 | -2022.2 |
| 10 | 108.0 | 57397.7 | -2102.3 | 15 | 106.5 | 57435.6 | -2064.4 |
| 10 | 110.0 | 57244.7 | -2255.3 | 15 | 111.0 | 57236.7 | -2263.3 |
| 10 | 115.0 | 57274.8 | -2225.2 | 15 | 112.5 | 57181.1 | -2318.9 |
| | | | | 15 | 115.0 | 57179.8 | -2320.2 |

Table B-1. Magnetic data continued

| North (m) | East (m) | Reading (nT) | Anomaly (nT) |
|---|---|---|---|
| 20 | 0.0 | 59446.4 | -53.6 |
| 20 | 2.5 | 60063.7 | 563.7 |
| 20 | 5.0 | 61495.4 | 1995.4 |
| 20 | 7.5 | 62038.4 | 2538.4 |
| 20 | 10.0 | 65022.6 | 5522.6 |
| 20 | 12.5 | 63412.7 | 3912.7 |
| 20 | 15.0 | 58279.9 | -1220.1 |
| 20 | 17.5 | 58432.2 | -1067.8 |
| 20 | 20.0 | 58706.4 | -793.6 |
| 20 | 22.5 | 59870.3 | 370.3 |
| 20 | 25.0 | 64943.4 | 5443.4 |
| 20 | 27.5 | 70285.3 | 10785.3 |
| 20 | 30.0 | 69158.7 | 9658.7 |
| 20 | 32.5 | 67557.3 | 8057.3 |
| 20 | 35.0 | 62633.0 | 3133.0 |
| 20 | 37.5 | 58778.8 | -721.2 |
| 20 | 40.0 | 55398.5 | -4101.5 |
| 20 | 42.5 | 55735.3 | -3764.7 |
| 20 | 45.0 | 55966.3 | -3533.7 |
| 20 | 47.5 | 54177.0 | -5323.0 |
| 20 | 50.0 | 56206.1 | -3293.9 |
| 20 | 52.5 | 57256.0 | -2244.0 |
| 20 | 55.0 | 57623.6 | -1876.4 |
| 20 | 57.5 | 59303.0 | -197.0 |
| 20 | 60.0 | 60233.6 | 733.6 |
| 20 | 62.5 | 61426.2 | 1926.2 |
| 20 | 65.0 | 61632.3 | 2132.3 |
| 20 | 69.5 | 61308.8 | 1808.8 |
| 20 | 72.5 | 60521.7 | 1021.7 |
| 20 | 77.5 | 59817.6 | 317.6 |
| 20 | 80.5 | 59527.0 | 27.0 |
| 20 | 81.0 | 59214.3 | -285.7 |
| 20 | 82.0 | 59128.8 | -371.2 |
| 20 | 83.0 | 58970.2 | -529.8 |
| 20 | 84.0 | 58873.0 | -627.0 |
| 20 | 85.0 | 58638.1 | -861.9 |
| 20 | 87.0 | 58543.6 | -956.4 |
| 20 | 90.0 | 58393.9 | -1106.1 |

Table B-2. Magnetic readings along tie lines

| North (m) | East (m) | Reading (nT) | Anomaly (nT) | North (m) | East (m) | Reading (nT) | Anomaly (nT) |
|---|---|---|---|---|---|---|---|
| 0.0 | 0 | 59457.7 | -42.3 | 0.0 | 30 | 66638.8 | 7138.8 |
| 5.0 | 0 | 59401.5 | -98.5 | 2.5 | 30 | 66709.6 | 7209.6 |
| 7.5 | 0 | 59393.5 | -106.5 | 5.0 | 30 | 67377.8 | 7877.8 |
| 12.5 | 0 | 59526.4 | 26.4 | 7.5 | 30 | 67489.6 | 7989.6 |
| 15.0 | 0 | 59380.5 | -119.5 | 13.0 | 30 | 67032.8 | 7532.8 |
| 17.5 | 0 | 59489.9 | -10.1 | 15.0 | 30 | 64184.7 | 4684.7 |
| 20.0 | 0 | 59664.1 | 164.1 | 17.0 | 30 | 53877.8 | -5622.2 |
| | | | | 18.0 | 30 | 53696.8 | -5803.2 |
| 0.0 | 5 | 61112.7 | 1612.7 | 20.0 | 30 | 60965.2 | 1465.2 |
| 7.5 | 5 | 61134.2 | 1634.2 | | | | |
| 12.5 | 5 | 61114.1 | 1614.1 | 0.0 | 35 | 68351.7 | 8851.7 |
| 15.0 | 5 | 61001.3 | 1501.3 | 2.5 | 35 | 68563.2 | 9063.2 |
| 17.5 | 5 | 61046.2 | 1546.2 | 5.0 | 35 | 68618.8 | 9118.8 |
| 20.0 | 5 | 61744.6 | 2244.6 | 7.5 | 35 | 68675.8 | 9175.8 |
| | | | | 10.0 | 35 | 69629.9 | 10129.9 |
| 2.5 | 10 | 64821.4 | 5321.4 | 16.5 | 35 | 65074.7 | 5574.7 |
| 7.5 | 10 | 65010.2 | 5510.2 | 17.0 | 35 | 58230.7 | -1269.3 |
| 15.0 | 10 | 64274.6 | 4774.6 | 18.5 | 35 | 56678.6 | -2821.4 |
| 17.5 | 10 | 64439.3 | 4939.3 | | | | |
| 20.0 | 10 | 63652.3 | 4152.3 | 0.0 | 40 | 61514.8 | 2014.8 |
| | | | | 2.5 | 40 | 68382.9 | 8882.9 |
| 0.0 | 15 | 66206.3 | 6706.3 | 7.5 | 40 | 71313.8 | 11813.8 |
| 5.0 | 15 | 68062.2 | 8562.2 | 10.0 | 40 | 69585.0 | 10085.0 |
| 7.5 | 15 | 69410.7 | 9910.7 | 12.5 | 40 | 67359.0 | 7859.0 |
| 10.0 | 15 | 67333.6 | 7833.6 | 15.0 | 40 | 65866.7 | 6366.7 |
| 12.5 | 15 | 61638.7 | 2138.7 | 17.5 | 40 | 62305.7 | 2805.7 |
| 16.5 | 15 | 59128.0 | -372.0 | 20.0 | 40 | 60669.5 | 1169.5 |
| 17.5 | 15 | 58011.8 | -1488.2 | | | | |
| 20.0 | 15 | 57575.0 | -1925.0 | 0.0 | 45 | 56957.3 | -2542.7 |
| | | | | 2.5 | 45 | 54041.0 | -5459.0 |
| 0.0 | 20 | 65790.0 | 6290.0 | 7.5 | 45 | 54106.7 | -5393.3 |
| 2.5 | 20 | 66283.7 | 6783.7 | 10.0 | 45 | 57754.5 | -1745.5 |
| 7.5 | 20 | 66911.2 | 7411.2 | 12.5 | 45 | 55447.9 | -4052.1 |
| 13.0 | 20 | 65447.3 | 5947.3 | 15.0 | 45 | 57353.2 | -2146.8 |
| 15.0 | 20 | 65183.0 | 5683.0 | 20.0 | 45 | 56539.7 | -2960.3 |
| 16.0 | 20 | 62431.2 | 2931.2 | | | | |
| 17.5 | 20 | 61865.4 | 2365.4 | 0.0 | 50 | 60925.9 | 1425.9 |
| 20.0 | 20 | 63021.6 | 3521.6 | 5.0 | 50 | 63063.9 | 3563.9 |
| | | | | 7.5 | 50 | 63879.7 | 4379.7 |
| 0.0 | 25 | 66419.5 | 6919.5 | 10.0 | 50 | 65297.7 | 5797.7 |
| 2.5 | 25 | 66719.6 | 7219.6 | 12.5 | 50 | 65842.4 | 6342.4 |
| 5.0 | 25 | 68232.7 | 8732.7 | 20.0 | 50 | 56726.1 | -2773.9 |
| 7.5 | 25 | 68695.6 | 9195.6 | | | | |
| 12.5 | 25 | 67564.6 | 8064.6 | 5.0 | 55 | 62961.3 | 3461.3 |
| 16.0 | 25 | 57427.1 | -2072.9 | 7.5 | 55 | 63217.8 | 3717.8 |
| 17.0 | 25 | 58667.4 | -832.6 | 10.0 | 55 | 63791.5 | 4291.5 |
| 18.5 | 25 | 57613.7 | -1886.3 | 12.5 | 55 | 64947.2 | 5447.2 |
| 20.0 | 25 | 57186.8 | -2313.2 | 15.0 | 55 | 64469.2 | 4969.2 |

Table B-2. Magnetic data continued

| North (m) | East (m) | Reading (nT) | Anomaly (nT) | North (m) | East (m) | Reading (nT) | Anomaly (nT) |
|---|---|---|---|---|---|---|---|
| 0.0 | 60 | 60701.5 | 1201.5 | 0.0 | 95 | 58122.9 | -1377.1 |
| 2.5 | 60 | 61176.7 | 1676.7 | 2.5 | 95 | 58147.7 | -1352.3 |
| 5.0 | 60 | 62007.4 | 2507.4 | 5.0 | 95 | 57997.6 | -1502.4 |
| 7.5 | 60 | 62964.2 | 3464.2 | 7.5 | 95 | 57977.5 | -1522.5 |
| 10.0 | 60 | 63202.7 | 3702.7 | 10.0 | 95 | 58068.8 | -1431.2 |
| 12.5 | 60 | 62918.0 | 3418.0 | 12.5 | 95 | 58035.6 | -1464.4 |
| 17.5 | 60 | 62432.5 | 2932.5 | 15.0 | 95 | 58008.8 | -1491.2 |
| 20.0 | 60 | 60152.7 | 652.7 | 17.5 | 95 | 57969.8 | -1530.2 |
| | | | | 20.0 | 95 | 58067.0 | -1433.0 |
| 0.0 | 65 | 61988.9 | 2488.9 | | | | |
| 2.5 | 65 | 62287.5 | 2787.5 | 0.0 | 100 | 57873.3 | -1626.7 |
| 5.0 | 65 | 62082.1 | 2582.1 | 2.5 | 100 | 57671.0 | -1829.0 |
| 7.5 | 65 | 62447.1 | 2947.1 | 5.0 | 100 | 57570.2 | -1929.8 |
| 10.0 | 65 | 62269.4 | 2769.4 | 7.5 | 100 | 57606.8 | -1893.2 |
| 12.5 | 65 | 61994.4 | 2494.4 | 10.0 | 100 | 57587.8 | -1912.2 |
| 17.5 | 65 | 62521.4 | 3021.4 | 12.5 | 100 | 57616.6 | -1883.4 |
| 20.0 | 65 | 61200.8 | 1700.8 | 15.0 | 100 | 57650.7 | -1849.3 |
| 0.0 | 75 | 60124.8 | 624.8 | 0.0 | 105 | 57808.2 | -1691.8 |
| 2.5 | 75 | 60026.5 | 526.5 | 2.5 | 105 | 57792.2 | -1707.8 |
| 5.0 | 75 | 60343.3 | 843.3 | 5.0 | 105 | 57734.8 | -1765.2 |
| 7.5 | 75 | 59904.1 | 404.1 | 7.5 | 105 | 57493.9 | -2006.1 |
| 12.5 | 75 | 59636.5 | 136.5 | 10.0 | 105 | 57523.5 | -1976.5 |
| 17.5 | 75 | 59705.6 | 205.6 | 12.5 | 105 | 57474.0 | -2026.0 |
| 20.0 | 75 | 59468.1 | -31.9 | 15.0 | 105 | 57483.5 | -2016.5 |
| 0.0 | 80 | 58962.1 | -537.9 | 0.0 | 110 | 57195.0 | -2305.0 |
| 2.5 | 80 | 59128.3 | -371.7 | 2.5 | 110 | 57123.7 | -2376.3 |
| 10.0 | 80 | 59048.9 | -451.1 | 5.0 | 110 | 57293.3 | -2206.7 |
| 15.0 | 80 | 59024.9 | -475.1 | 7.5 | 110 | 57266.9 | -2233.1 |
| 17.5 | 80 | 58966.0 | -534.0 | 10.0 | 110 | 57310.1 | -2189.9 |
| 20.0 | 80 | 59000.6 | -499.4 | 12.5 | 110 | 57319.2 | -2180.8 |
| | | | | 15.0 | 110 | 57327.0 | -2173.0 |
| 0.0 | 85 | 58463.8 | -1036.2 | | | | |
| 2.5 | 85 | 58392.9 | -1107.1 | 0.0 | 115 | 57263.6 | -2236.4 |
| 5.0 | 85 | 58499.2 | -1000.8 | 2.5 | 115 | 57229.7 | -2270.3 |
| 10.0 | 85 | 58608.9 | -891.1 | 5.0 | 115 | 57208.3 | -2291.7 |
| 15.0 | 85 | 58593.2 | -906.8 | 7.5 | 115 | 57252.1 | -2247.9 |
| 17.5 | 85 | 58649.9 | -850.1 | 10.0 | 115 | 57260.9 | -2239.1 |
| 20.0 | 85 | 58597.7 | -902.3 | 12.5 | 115 | 57265.3 | -2234.7 |
| | | | | 15.0 | 115 | 57280.2 | -2219.8 |
| 0.0 | 90 | 58265.4 | -1234.6 | | | | |
| 2.5 | 90 | 58285.8 | -1214.2 | | | | |
| 5.0 | 90 | 58291.7 | -1208.3 | | | | |
| 7.5 | 90 | 58353.9 | -1146.1 | | | | |
| 10.0 | 90 | 58597.5 | -902.5 | | | | |
| 12.5 | 90 | 58593.6 | -906.4 | | | | |
| 15.0 | 90 | 58592.0 | -908.0 | | | | |
| 17.5 | 90 | 58581.7 | -918.3 | | | | |
| 20.0 | 90 | 58565.4 | -934.6 | | | | |

Table B-3. VLF survey results: angle and quadrature

| North (m) | East (m) | Station 1 | | Station 2 | |
|---|---|---|---|---|---|
| | | Angle | Quad | Angle | Quad |
| 0 | 0.0 | -3 | -6 | -21 | 25 |
| 0 | 2.5 | -4 | -4 | -16 | 15 |
| 0 | 5.0 | -8 | -16 | -16 | 17 |
| 0 | 7.5 | -12 | -20 | -17 | 16 |
| 0 | 10.0 | -19 | -14 | -19 | 19 |
| 0 | 12.5 | -20 | -12 | -26 | 20 |
| 0 | 15.0 | -16 | 4 | -21 | 20 |
| 0 | 17.5 | -17 | -1 | -19 | 19 |
| 0 | 20.0 | -15 | -5 | -18 | 18 |
| 0 | 22.5 | -15 | -10 | -17 | 18 |
| 0 | 25.0 | -9 | -10 | -21 | 20 |
| 0 | 27.5 | -10 | 0 | -20 | 16 |
| 0 | 30.0 | -11 | -10 | -21 | 14 |
| 0 | 32.5 | -13 | -16 | -18 | 11 |
| 0 | 35.0 | -13 | -19 | -16 | 11 |
| 0 | 37.5 | -14 | -15 | -13 | 12 |
| 0 | 40.0 | -14 | -17 | -17 | 6 |
| 0 | 42.5 | -12 | -13 | -15 | 7 |
| 0 | 45.0 | -14 | -9 | -17 | 2 |
| 0 | 47.5 | -14 | -10 | -16 | 4 |
| 0 | 50.0 | -12 | 6 | -16 | 0 |
| 0 | 52.5 | -13 | 5 | -19 | -1 |
| 0 | 55.0 | -13 | 0 | -17 | 0 |
| 0 | 57.5 | -15 | 2 | -20 | 4 |
| 0 | 60.0 | -16 | -4 | -19 | -3 |
| 0 | 62.5 | -10 | 2 | -22 | 4 |
| 0 | 65.0 | -10 | -1 | -25 | 3 |
| 0 | 67.5 | -12 | 0 | -20 | 0 |
| 0 | 70.0 | -14 | 5 | -25 | 1 |
| 0 | 72.5 | -12 | 5 | -20 | 1 |
| 0 | 75.0 | -12 | -1 | -22 | 2 |
| 0 | 77.5 | -10 | 3 | -22 | 2 |
| 0 | 80.0 | -12 | -4 | -19 | 1 |
| 0 | 82.5 | -12 | 3 | -20 | -2 |
| 0 | 85.0 | -12 | 4 | -19 | 2 |
| 0 | 87.5 | -11 | 5 | -20 | 1 |
| 0 | 90.0 | -12 | 6 | -20 | -4 |
| 0 | 92.5 | -12 | 0 | -20 | 1 |
| 0 | 95.0 | -11 | 2 | -21 | 2 |
| 0 | 97.5 | -12 | -5 | -20 | 1 |
| 0 | 100.0 | -12 | -2 | -21 | 6 |
| 0 | 102.5 | -15 | -1 | -20 | 10 |
| 0 | 105.0 | -16 | -8 | -20 | 2 |
| 0 | 107.5 | -13 | -8 | -20 | 5 |
| 0 | 110.0 | -14 | -10 | -20 | 1 |
| 0 | 112.5 | -16 | -12 | -19 | 5 |
| 0 | 115.0 | -15 | -4 | -19 | 7 |

Table B-3. VLF data continued

| North (m) | East (m) | Station 1 | | Station 2 | |
|---|---|---|---|---|---|
| | | Angle | Quad | Angle | Quad |
| 5 | 0.0 | -14 | -15 | -18 | 15 |
| 5 | 2.5 | -15 | -19 | -18 | 17 |
| 5 | 5.0 | -14 | -6 | -18 | 14 |
| 5 | 7.5 | -13 | -8 | -19 | 17 |
| 5 | 10.0 | -12 | -6 | -22 | 8 |
| 5 | 12.5 | -15 | -10 | -17 | 15 |
| 5 | 15.0 | -12 | 1 | -17 | 17 |
| 5 | 17.5 | -11 | -1 | -18 | 18 |
| 5 | 20.0 | -12 | 0 | -18 | 15 |
| 5 | 22.5 | -12 | -4 | -18 | 16 |
| 5 | 25.0 | -14 | -8 | -18 | 17 |
| 5 | 27.5 | -14 | -14 | -17 | 16 |
| 5 | 30.0 | -14 | -20 | -18 | 10 |
| 5 | 32.5 | -14 | 2 | -16 | 11 |
| 5 | 35.0 | -14 | -7 | -16 | 10 |
| 5 | 37.5 | -13 | -5 | -15 | 9 |
| 5 | 40.0 | -14 | 2 | -17 | 8 |
| 5 | 42.5 | -15 | 2 | -17 | 4 |
| 5 | 45.0 | -16 | 2 | -19 | 2 |
| 5 | 47.5 | -15 | -1 | -18 | 4 |
| 5 | 50.0 | -12 | 6 | -19 | 2 |
| 5 | 52.5 | -13 | -5 | -20 | 2 |
| 5 | 55.0 | -13 | -6 | -19 | 2 |
| 5 | 57.5 | -13 | 4 | -19 | 5 |
| 5 | 60.0 | -12 | 4 | -20 | 1 |
| 5 | 62.5 | -12 | 4 | -18 | -2 |
| 5 | 65.0 | -12 | -7 | -20 | -1 |
| 5 | 67.5 | -11 | 2 | -19 | -1 |
| 5 | 70.0 | -12 | 4 | -20 | 2 |
| 5 | 72.5 | -12 | 2 | -19 | 1 |
| 5 | 75.0 | -13 | 0 | -20 | 1 |
| 5 | 77.5 | -13 | -3 | -19 | 0 |
| 5 | 80.0 | -14 | 0 | -18 | -2 |
| 5 | 82.5 | -15 | -4 | -18 | 4 |
| 5 | 85.0 | -13 | -5 | -20 | 2 |
| 5 | 87.5 | -13 | -4 | -19 | 2 |
| 5 | 90.0 | -14 | 2 | -20 | 1 |
| 5 | 92.5 | -13 | -1 | -20 | 3 |
| 5 | 95.0 | -12 | 0 | -21 | -4 |
| 5 | 97.5 | -13 | -1 | -20 | -4 |
| 5 | 100.0 | -15 | -4 | -20 | 0 |
| 5 | 102.5 | -14 | 0 | -19 | 1 |
| 5 | 105.0 | -14 | 2 | -19 | 2 |
| 5 | 107.5 | -14 | -4 | -20 | -2 |
| 5 | 110.0 | -15 | 4 | -19 | 0 |
| 5 | 112.5 | -12 | -3 | -19 | 4 |
| 5 | 115.0 | -13 | -4 | -19 | 8 |

Table B-3. VLF data continued

| North (m) | East (m) | Station 1 | | Station 2 | |
|---|---|---|---|---|---|
| | | Angle | Quad | Angle | Quad |
| 10 | 0.0 | -15 | 2 | -12 | 15 |
| 10 | 2.5 | -16 | 0 | -19 | 12 |
| 10 | 5.0 | -16 | -4 | -18 | 16 |
| 10 | 7.5 | -15 | -9 | -19 | 17 |
| 10 | 10.0 | -15 | -9 | -19 | 16 |
| 10 | 12.5 | -14 | -7 | -18 | 17 |
| 10 | 15.0 | -15 | -8 | -18 | 20 |
| 10 | 17.5 | -15 | 0 | -19 | 12 |
| 10 | 20.0 | -15 | -4 | -19 | 20 |
| 10 | 22.5 | -15 | 0 | -20 | 16 |
| 10 | 25.0 | -15 | -2 | -18 | 16 |
| 10 | 27.5 | -14 | -6 | -19 | 13 |
| 10 | 30.0 | -14 | -6 | -18 | 16 |
| 10 | 32.5 | -14 | -8 | -17 | 12 |
| 10 | 35.0 | -15 | -2 | -17 | 16 |
| 10 | 37.5 | -13 | -2 | -17 | 10 |
| 10 | 40.0 | -15 | 0 | -18 | 9 |
| 10 | 42.5 | -13 | 1 | -19 | 8 |
| 10 | 45.0 | -12 | -1 | -19 | 3 |
| 10 | 47.5 | -14 | -1 | -19 | 3 |
| 10 | 50.0 | -14 | 2 | -17 | 0 |
| 10 | 52.5 | -13 | -6 | -18 | 1 |
| 10 | 55.0 | -14 | 4 | -22 | 6 |
| 10 | 57.5 | -14 | -4 | -19 | 0 |
| 10 | 60.0 | -14 | 2 | -22 | 4 |
| 10 | 62.5 | -17 | -2 | -18 | 3 |
| 10 | 65.0 | -14 | 0 | -20 | 2 |
| 10 | 67.5 | -14 | 4 | -19 | 1 |
| 10 | 70.0 | -12 | 0 | -20 | 0 |
| 10 | 72.5 | -14 | -1 | -19 | -2 |
| 10 | 75.0 | -15 | 2 | -19 | -2 |
| 10 | 77.5 | -14 | 2 | -19 | 4 |
| 10 | 80.0 | -14 | 0 | -19 | 2 |
| 10 | 82.5 | -13 | 0 | -19 | -2 |
| 10 | 85.0 | -15 | -2 | -19 | -5 |
| 10 | 87.5 | -15 | -8 | -17 | -2 |
| 10 | 90.0 | -14 | -6 | -20 | -2 |
| 10 | 92.5 | -16 | 4 | -20 | -3 |
| 10 | 95.0 | -14 | -6 | -19 | 0 |
| 10 | 97.5 | -15 | -6 | -18 | 1 |
| 10 | 100.0 | -14 | -4 | -16 | 2 |
| 10 | 102.5 | -15 | 0 | -16 | 2 |
| 10 | 105.0 | -15 | -1 | -15 | -1 |
| 10 | 107.5 | -13 | 0 | -15 | 1 |
| 10 | 110.0 | -15 | -4 | -16 | 3 |
| 10 | 112.5 | -14 | -8 | -15 | 1 |
| 10 | 115.0 | -14 | -6 | -16 | 2 |

Table B-3. VLF data continued

| North (m) | East (m) | Station 1 | | Station 2 | |
|---|---|---|---|---|---|
| | | Angle | Quad | Angle | Quad |
| 15 | 0.0 | -13 | -5 | -18 | 14 |
| 15 | 2.5 | -14 | -4 | -18 | 14 |
| 15 | 5.0 | -15 | -18 | -17 | 20 |
| 15 | 7.5 | -13 | -12 | -17 | 16 |
| 15 | 10.0 | -16 | -11 | -19 | 17 |
| 15 | 12.5 | -16 | -14 | -19 | 13 |
| 15 | 15.0 | -15 | -13 | -19 | 20 |
| 15 | 17.5 | -14 | -12 | -18 | 18 |
| 15 | 20.0 | -14 | -14 | -18 | 19 |
| 15 | 22.5 | -14 | -13 | -18 | 14 |
| 15 | 25.0 | -14 | -9 | -18 | 16 |
| 15 | 27.5 | -15 | -12 | -18 | 17 |
| 15 | 30.0 | -13 | -10 | -18 | 11 |
| 15 | 32.5 | -14 | -12 | -18 | 13 |
| 15 | 35.0 | -14 | -4 | -18 | 10 |
| 15 | 37.5 | -14 | 1 | -18 | 12 |
| 15 | 40.0 | -15 | 2 | -19 | 10 |
| 15 | 42.5 | -14 | 0 | -19 | 6 |
| 15 | 45.0 | -16 | -2 | -19 | 5 |
| 15 | 47.5 | -16 | 2 | -19 | -1 |
| 15 | 50.0 | -15 | 6 | -19 | 1 |
| 15 | 52.5 | -14 | -5 | -19 | -1 |
| 15 | 55.0 | -15 | -4 | -19 | 0 |
| 15 | 57.5 | -16 | -6 | -18 | 3 |
| 15 | 60.0 | -15 | 0 | -20 | -2 |
| 15 | 62.5 | -13 | -8 | -21 | 0 |
| 15 | 65.0 | -15 | -8 | -20 | -1 |
| 15 | 67.5 | -15 | -2 | -19 | -1 |
| 15 | 70.0 | -15 | 1 | -20 | -2 |
| 15 | 72.5 | -13 | 3 | -18 | 0 |
| 15 | 75.0 | -14 | 0 | -18 | 0 |
| 15 | 77.5 | -14 | 3 | -18 | -2 |
| 15 | 80.0 | -11 | 3 | -18 | 0 |
| 15 | 82.5 | -11 | 2 | -16 | 1 |
| 15 | 85.0 | -13 | 4 | -17 | 3 |
| 15 | 87.5 | -14 | -6 | -16 | 2 |
| 15 | 90.0 | -12 | -2 | -17 | 0 |
| 15 | 92.5 | -13 | 0 | -17 | 2 |
| 15 | 95.0 | -14 | 2 | -17 | 6 |
| 15 | 97.5 | -13 | 2 | -17 | 2 |
| 15 | 100.0 | -14 | -4 | -17 | 2 |
| 15 | 102.5 | -14 | -7 | -17 | -1 |
| 15 | 105.0 | -14 | -2 | -16 | 2 |
| 15 | 107.5 | -13 | -4 | -15 | -4 |
| 15 | 110.0 | -14 | -8 | -15 | -2 |
| 15 | 112.5 | -15 | -2 | -15 | -3 |
| 15 | 115.0 | -14 | 2 | -15 | -2 |

Table B-3. VLF data continued

| North (m) | East (m) | Station 1 | | Station 2 | |
|---|---|---|---|---|---|
| | | Angle | Quad | Angle | Quad |
| 20 | 0.0 | -9 | -10 | -17 | 16 |
| 20 | 2.5 | -10 | -10 | -17 | 18 |
| 20 | 5.0 | -10 | -10 | -18 | 18 |
| 20 | 7.5 | -10 | -10 | -19 | 21 |
| 20 | 10.0 | -12 | -12 | -19 | 20 |
| 20 | 12.5 | -12 | -8 | -19 | 18 |
| 20 | 15.0 | -12 | -5 | -19 | 22 |
| 20 | 17.5 | -12 | -11 | -17 | 21 |
| 20 | 20.0 | -12 | -5 | -18 | 21 |
| 20 | 22.5 | -9 | -4 | -17 | 20 |
| 20 | 25.0 | -11 | -2 | -18 | 16 |
| 20 | 27.5 | -11 | -4 | -18 | 16 |
| 20 | 30.0 | -11 | -3 | -19 | 19 |
| 20 | 32.5 | -12 | -10 | -19 | 15 |
| 20 | 35.0 | -11 | -9 | -19 | 10 |
| 20 | 37.5 | -11 | -7 | -19 | 13 |
| 20 | 40.0 | -11 | -4 | -19 | 12 |
| 20 | 42.5 | -11 | 0 | -18 | 9 |
| 20 | 45.0 | -14 | 4 | -19 | 6 |
| 20 | 47.5 | -13 | 0 | -18 | 3 |
| 20 | 50.0 | -14 | 3 | -18 | 1 |
| 20 | 52.5 | -15 | 2 | -19 | 0 |
| 20 | 55.0 | -14 | 1 | -17 | 3 |
| 20 | 57.5 | -14 | 8 | -19 | 2 |
| 20 | 60.0 | -14 | 3 | -19 | 1 |
| 20 | 62.5 | -14 | 3 | -18 | 1 |
| 20 | 65.0 | -14 | 2 | -19 | 3 |
| 20 | 67.5 | -13 | 6 | -19 | 0 |
| 20 | 70.0 | -13 | 5 | -19 | -1 |
| 20 | 72.5 | -15 | 6 | -18 | -1 |
| 20 | 75.0 | -14 | -2 | -18 | 0 |
| 20 | 77.5 | -13 | -3 | -18 | -2 |
| 20 | 80.0 | -14 | 1 | -17 | 2 |
| 20 | 82.5 | -14 | 2 | -18 | 3 |
| 20 | 85.0 | -13 | 3 | -18 | 4 |
| 20 | 87.5 | -14 | -1 | -18 | 1 |
| 20 | 90.0 | -12 | 2 | -19 | 2 |

Station 1 = Seattle, Washington.
Station 2 = Annapolis, Maine.

Table B-4. Susceptibility variation with stratigraphic position

| Sample | Susceptibility x $10^{-6}$ (cgs) | Depth[a] (m) | Rock Type | Rock Layer |
|---|---|---|---|---|
| MSL-61 | 16.33 | -0.5 | t bslt | h bslt |
| MSL-60 | 1458.67 | 0.0 | tmp | spnfx |
| MSL-59 | 3955.00 | 1.0 | s cpy | spnfx |
| MSL-58 | 7332.33 | 2.5 | s cpy | spnfx |
| MSL-57 | 150.33 | 4.9 | s cpy | spnfx |
| MSL-56 | 118.33 | 6.0 | s cpy | spnfx |
| MSL-55 | 105.67 | 7.0 | s cpy | spnfx |
| MSL-54 | 109.67 | 8.5 | s cpy | spnfx |
| MSL-53 | 1328.00 | 10.0 | s cpy | spnfx |
| MSL-52 | 308.00 | 11.0 | s cpy | spnfx |
| MSL-51 | 1067.00 | 12.5 | s cpy | spnfx |
| MSL-50 | 2616.33 | 14.0 | s cpy | spnfx |
| MSL-49 | 6661.33 | 15.0 | s cpy | spnfx |
| MSL-48 | 372.33 | 26.7 | s cpy | spnfx |
| MSL-47 | 3003.00 | 28.2 | s cpy | spnfx |
| MSL-46 | 2626.00 | 30.7 | s cpy | spnfx |
| MSL-45 | 8366.33 | 31.2 | s cpy | spnfx |
| MSL-44 | 129.67 | 31.8 | s cpy | spnfx |
| MSL-43 | 8767.67 | 32.6 | v cpy | gbr |
| MSL-42 | 9761.00 | 33.3 | gbb | gbr |
| MSL-41 | 8635.33 | 35.7 | tmc | gbr |
| MSL-40 | 9752.33 | 37.2 | gbb | gbr |
| MSL-39 | 2963.00 | 38.7 | gbb | gbr |
| MSL-38 | 1847.67 | 39.4 | gbb | gbr |
| MSL-37 | 3794.00 | 39.9 | gbb | gbr |
| MSL-36 | 9726.33 | 41.7 | gbb | gbr |
| MSL-35 | 5334.00 | 41.9 | gbb | gbr |
| MSL-34 | 851.67 | 42.0 | tmc | gbr |
| MSL-33 | 2344.33 | 43.3 | tmc | gbr |
| MSL-32 | 2406.00 | 44.0 | tmc | gbr |
| MSL-31 | 4914.33 | 45.1 | tmc | gbr |
| MSL-30 | 5845.33 | 45.6 | tmc | gbr |
| MSL-29 | 9754.67 | 46.1 | tmc | gbr |
| MSL-28 | 3808.33 | 46.6 | tmc | gbr |
| MSL-27 | 1849.00 | 46.8 | gbb | gbr |
| MSL-26 | 225.67 | 47.3 | gbb | gbr |
| MSL-25 | 831.00 | 47.5 | gbb | gbr |
| MSL-24 | 97.00 | 47.7 | gbb | gbr |
| MSL-23 | 109.33 | 48.0 | gbb | gbr |
| MSL-22 | 2839.00 | 48.1 | cpy | cp cum |
| MSL-21 | 88.33 | 48.4 | cpy | cp cum |
| MSL-20 | 8565.67 | 48.9 | cpy | cp cum |
| MSL-19 | 77.67 | 51.4 | cpy | cp cum |
| MSL-18 | 84.67 | 52.5 | cpy | cp cum |
| MSL-17 | 83.00 | 53.0 | cpy | cp cum |
| MSL-16 | 87.67 | 53.2 | cpy | cp cum |
| MSL-15 | 3312.67 | 56.1 | am prd | ol cum |
| MSL-14 | 3585.33 | 58.7 | am prd | ol cum |

Table B-4. Susceptibility continued

| Sample | Susceptibility x $10^{-6}$ (cgs) | Depth[a] (m) | Rock Type | Rock Layer |
|---|---|---|---|---|
| MSL-13 | 5269.67 | 59.3 | am prd | ol cum |
| MSL-12 | 899.00 | 61.3 | am prd | ol cum |
| MSL-11 | 1906.00 | 62.1 | prd | ol cum |
| MSL-10 | 2331.33 | 62.2 | prd | ol cum |
| MSL-9 | 1980.00 | 63.2 | prd | ol cum |
| MSL-8 | 8706.00 | 67.0 | prd | ol cum |
| MSL-7 | 854.67 | 73.7 | prd | ol cum |
| MSL-6 | 5579.67 | 77.7 | prd | ol cum |
| MSL-5 | 414.00 | 79.7 | prd | ol cum |
| MSL-4 | 2169.67 | 83.6 | prd | ol cum |
| MSL-3 | 73.67 | 88.7 | t bslt | f bslt |
| MSL-2 | 55.33 | 95.7 | t bslt | f bslt |
| MSL-1 | 65.00 | 96.2 | t bslt | f bslt |

[a] Depth from flow top.

Rock type and layer abbreviations are the same as in Table 1.

# APPENDIX C

PALEOMAGNETIC DATA (C-1)

| SAMPLE | Temp | Dec. °N | Inc. °E | Intensity $A/m^2$ | Alpha95 |
|---|---|---|---|---|---|
| MSL-1 | 0 | 242.70 | 57.24 | 2.74E-06 | 19.40 |
| | 250 | 242.96 | 50.55 | 4.35E-06 | 12.69 |
| | 300 | 258.76 | 51.17 | 3.74E-06 | 11.29 |
| | 350 | 226.23 | -47.33 | 7.00E-07 | 42.60 |
| | 400 | 255.98 | -54.91 | 4.40E-07 | 44.94 |
| | 500 | 257.93 | -25.83 | 8.00E-07 | 31.68 |
| | 550 | 43.43 | -40.79 | 1.29E-06 | 24.52 |
| | 560 | 131.13 | -45.78 | 3.54E-06 | 10.19 |
| | 575 | 108.71 | 11.24 | 3.32E-06 | 11.51 |
| | 590 | 138.02 | -51.74 | 5.31E-06 | 6.93 |
| | 600 | 75.16 | 41.10 | 5.69E-06 | 7.81 |
| MSL-2 | 0 | 176.25 | -6.68 | 6.42E-06 | 11.65 |
| | 250 | 173.64 | -6.24 | 5.49E-06 | 13.74 |
| | 300 | 173.97 | -6.97 | 4.60E-06 | 16.25 |
| | 350 | 168.93 | -12.56 | 2.85E-06 | 19.14 |
| | 400 | 176.90 | -11.63 | 3.25E-06 | 15.88 |
| | 500 | 182.86 | -15.49 | 1.22E-06 | 28.27 |
| | 550 | 136.92 | -10.46 | 8.00E-07 | 28.00 |
| | 560 | 198.34 | -51.79 | 2.02E-06 | 16.12 |
| | 575 | 161.50 | 25.65 | 2.06E-06 | 15.95 |
| | 590 | 188.50 | -55.60 | 3.23E-06 | 11.88 |
| | 600 | 148.16 | 25.35 | 1.92E-06 | 14.38 |
| MSL-3 | 0 | 67.41 | -37.36 | 2.88E-04 | 1.69 |
| | 250 | 70.14 | -34.40 | 3.84E-04 | 1.66 |
| | 300 | 65.16 | -32.45 | 3.18E-04 | 1.56 |
| | 350 | 67.95 | -33.23 | 2.79E-04 | 1.82 |
| | 400 | 65.05 | -32.53 | 2.49E-04 | 1.74 |
| | 500 | 62.68 | -32.27 | 1.51E-04 | 2.07 |
| | 550 | 59.22 | -32.51 | 7.28E-05 | 2.96 |
| | 560 | 52.53 | -39.37 | 3.14E-05 | 3.66 |
| | 575 | 47.64 | -30.22 | 2.69E-05 | 3.85 |
| | 590 | 95.05 | -48.18 | 1.06E-05 | 4.37 |
| | 600 | 36.24 | 46.52 | 9.44E-06 | 4.88 |
| MSL-4 | 0 | 145.00 | -1.96 | 1.15E-01 | 0.08 |
| | 250 | 134.66 | -2.55 | 1.55E-01 | 0.73 |
| | 300 | 134.70 | -1.25 | 1.28E-01 | 0.85 |
| | 350 | 128.44 | -2.14 | 6.52E-02 | 0.12 |
| | 400 | 133.13 | -3.88 | 4.63E-02 | 79.99 |
| | 500 | 130.38 | -4.84 | 4.08E-02 | 1.59 |
| | 550 | 114.90 | -6.43 | 1.45E-02 | 2.85 |
| | 560 | 131.59 | -4.85 | 6.53E-03 | 0.35 |
| | 575 | 121.48 | 33.99 | 5.91E-04 | 0.89 |
| | 590 | 155.13 | -9.34 | 2.89E-04 | 1.71 |
| | 600 | 111.50 | 40.09 | 5.98E-04 | 0.84 |

| SAMPLE | Temp | Dec. °N | Inc. °E | Intensity $A/m^2$ | Alpha95 |
|---|---|---|---|---|---|
| MSL-5 | 0 | 213.58 | -26.05 | 5.47E-02 | 0.14 |
| | 250 | 211.58 | -26.82 | 6.39E-02 | 1.47 |
| | 300 | 217.54 | -27.90 | 4.87E-02 | 1.64 |
| | 350 | 217.52 | -29.13 | 2.12E-02 | 0.26 |
| | 400 | 215.28 | -31.67 | 1.56E-02 | 0.15 |
| | 500 | 218.52 | -35.92 | 1.20E-02 | 3.86 |
| | 550 | 212.73 | -41.78 | 6.97E-03 | 1.78 |
| | 560 | 220.46 | -41.73 | 4.41E-03 | 0.67 |
| | 575 | 181.93 | 25.47 | 4.06E-04 | 1.54 |
| | 590 | 237.05 | -43.07 | 2.66E-04 | 1.21 |
| | 600 | 201.51 | 31.13 | 5.39E-04 | 0.7 |
| MSL-6 | 0 | 258.25 | -6.71 | 2.49E-01 | 0.04 |
| | 250 | 254.80 | -2.13 | 1.63E-01 | 2.69 |
| | 300 | 257.87 | 1.44 | 1.53E-01 | 2.77 |
| | 350 | 259.38 | -3.46 | 1.48E-01 | 0.05 |
| | 400 | 250.51 | -2.26 | 1.07E-01 | 0.32 |
| | 500 | 249.21 | -1.72 | 9.76E-02 | 0.77 |
| | 550 | 248.37 | -2.08 | 5.16E-02 | 0.11 |
| | 560 | 249.48 | -2.43 | 3.05E-02 | 0.14 |
| | 575 | 247.28 | 7.25 | 3.16E-03 | 0.41 |
| | 590 | 256.44 | -2.05 | 2.41E-03 | 0.46 |
| | 600 | 239.34 | 30.71 | 1.27E-03 | 2.7 |
| MSL-7 | 0 | 13.69 | 38.02 | 9.82E-03 | 0.12 |
| | 250 | 15.16 | 33.50 | 1.18E-02 | 1.23 |
| | 300 | 13.77 | 28.70 | 1.09E-02 | 1.37 |
| | 350 | 14.30 | 39.48 | 4.32E-03 | 0.26 |
| | 400 | 8.36 | 32.61 | 3.10E-03 | 0.07 |
| | 500 | 351.07 | 25.42 | 2.71E-03 | 3.03 |
| | 550 | 359.49 | 29.22 | 2.38E-03 | 0.87 |
| | 560 | 345.81 | 29.67 | 1.06E-03 | 0.43 |
| | 575 | 46.59 | 36.66 | 1.02E-03 | 0.48 |
| | 590 | 139.19 | -14.33 | 3.70E-04 | 1.00 |
| | 600 | 75.06 | 39.04 | 7.12E-04 | 0.53 |
| MSL-8 | 0 | 30.70 | 25.67 | 1.97E-02 | 0.16 |
| | 250 | 30.38 | 29.61 | 2.84E-02 | 1.19 |
| | 300 | 29.22 | 30.29 | 2.47E-02 | 1.14 |
| | 350 | 27.61 | 33.06 | 1.14E-02 | 0.18 |
| | 400 | 35.02 | 31.99 | 7.82E-03 | 0.22 |
| | 500 | 28.40 | 31.25 | 7.30E-03 | 1.68 |
| | 550 | 20.67 | 30.27 | 5.83E-03 | 0.68 |
| | 560 | 28.81 | 27.48 | 2.54E-03 | 0.39 |
| | 575 | 15.08 | 28.90 | 1.40E-03 | 0.39 |
| | 590 | 73.55 | 6.99 | 5.39E-04 | 0.72 |
| | 600 | 67.66 | 23.98 | 5.99E-04 | 0.72 |

| SAMPLE | Temp | Dec. °N | Inc. °E | Intensity $A/m^2$ | Alpha95 |
|---|---|---|---|---|---|
| MSL-9 | 0 | 8.31 | 33.29 | 1.98E-02 | 0.13 |
| | 250 | 8.61 | 35.90 | 2.61E-02 | 1.02 |
| | 300 | 5.82 | 35.04 | 2.15E-02 | 0.94 |
| | 350 | 13.47 | 37.22 | 9.06E-03 | 0.15 |
| | 400 | 14.97 | 34.08 | 6.15E-03 | 0.20 |
| | 500 | 359.76 | 35.35 | 6.21E-03 | 1.80 |
| | 550 | 9.80 | 29.60 | 5.20E-03 | 0.61 |
| | 560 | 356.58 | 30.68 | 2.39E-03 | 0.31 |
| | 575 | 54.97 | 35.64 | 1.10E-03 | 0.39 |
| | 590 | 6.34 | 0.37 | 3.98E-04 | 0.80 |
| | 600 | 49.08 | 44.33 | 5.82E-04 | 0.59 |
| MSL-10 | 0 | 90.16 | 0.24 | 1.31E-01 | 0.07 |
| | 250 | 86.79 | 0.59 | 1.59E-01 | 0.80 |
| | 300 | 90.55 | 1.82 | 1.21E-01 | 1.21 |
| | 350 | 89.27 | 3.62 | 5.74E-02 | 0.17 |
| | 400 | 87.17 | 2.15 | 3.47E-02 | 0.17 |
| | 500 | 84.36 | 0.61 | 3.15E-02 | 2.35 |
| | 550 | 86.25 | 0.60 | 2.49E-02 | 0.86 |
| | 560 | 63.10 | -16.78 | 8.02E-03 | 1.13 |
| | 575 | 117.40 | 51.28 | 8.70E-04 | 1.33 |
| | 590 | 61.73 | 1.33 | 5.02E-04 | 2.40 |
| | 600 | 178.37 | 68.12 | 4.33E-04 | 1.71 |
| MSL-11 | 0 | 329.99 | 51.70 | 1.51E-02 | 0.19 |
| | 250 | 333.84 | 52.35 | 2.46E-02 | 1.18 |
| | 300 | 326.87 | 52.06 | 2.28E-02 | 1.40 |
| | 350 | 335.08 | 51.86 | 9.86E-03 | 0.17 |
| | 400 | 326.06 | 45.90 | 8.05E-03 | 0.22 |
| | 500 | 328.43 | 43.95 | 7.50E-03 | 1.62 |
| | 550 | 321.68 | 47.80 | 6.22E-03 | 0.75 |
| | 560 | 330.80 | 39.59 | 2.72E-03 | 0.41 |
| | 575 | 264.59 | 61.20 | 9.99E-04 | 0.54 |
| | 590 | 334.10 | 51.75 | 1.12E-03 | 0.53 |
| | 600 | 309.61 | 44.41 | 9.93E-04 | 0.54 |
| MSL-12 | 0 | 353.07 | 32.38 | 2.15E-02 | 0.15 |
| | 250 | 346.93 | 29.67 | 2.71E-02 | 1.31 |
| | 300 | 345.10 | 30.98 | 2.33E-02 | 1.21 |
| | 350 | 343.68 | 38.66 | 8.06E-03 | 0.2 |
| | 400 | 341.38 | 35.68 | 6.80E-03 | 0.22 |
| | 500 | 339.19 | 37.16 | 6.15E-03 | 1.83 |
| | 550 | 331.75 | 46.89 | 4.53E-03 | 0.74 |
| | 560 | 345.66 | 44.70 | 1.89E-03 | 0.49 |
| | 575 | 337.61 | 35.28 | 8.33E-04 | 0.61 |
| | 590 | 10.19 | 30.35 | 9.39E-04 | 0.53 |
| | 600 | 10.70 | 20.51 | 9.85E-04 | 0.66 |

| SAMPLE | Temp | Dec. °N | Inc. °E | Intensity $A/m^2$ | Alpha95 |
|---|---|---|---|---|---|
| MSL-13 | 0 | 305.46 | 50.15 | 2.91E-02 | 0.09 |
| | 250 | 305.26 | 50.10 | 4.06E-02 | 0.78 |
| | 300 | 301.97 | 51.35 | 3.44E-02 | 0.93 |
| | 350 | 303.92 | 49.96 | 1.39E-02 | 0.12 |
| | 400 | 300.10 | 47.56 | 1.14E-02 | 0.2 |
| | 500 | 291.73 | 43.89 | 1.10E-02 | 1.7 |
| | 550 | 303.34 | 56.09 | 8.87E-03 | 0.48 |
| | 560 | 296.78 | 50.69 | 4.46E-03 | 0.27 |
| | 575 | 293.61 | 57.05 | 3.98E-03 | 0.27 |
| | 590 | 290.46 | 48.55 | 2.39E-03 | 0.35 |
| | 600 | 247.40 | 40.45 | 1.90E-03 | 0.45 |
| MSL-14 | 0 | 337.89 | 44.73 | 2.36E-02 | 0.07 |
| | 250 | 340.59 | 48.44 | 3.26E-02 | 0.67 |
| | 300 | 348.76 | 52.90 | 2.72E-02 | 0.67 |
| | 350 | 344.84 | 51.58 | 1.11E-02 | 0.14 |
| | 400 | 348.01 | 51.12 | 8.51E-03 | 0.17 |
| | 500 | 347.61 | 45.34 | 7.48E-03 | 1.27 |
| | 550 | 358.25 | 46.66 | 5.75E-03 | 0.62 |
| | 560 | 340.01 | 40.49 | 2.87E-03 | 0.34 |
| | 575 | 348.24 | 47.15 | 2.55E-03 | 0.33 |
| | 590 | 293.13 | -48.48 | 3.91E-04 | 0.84 |
| | 600 | 206.76 | 46.53 | 1.48E-03 | 0.35 |
| MSL-15 | 0 | 191.68 | 0.16 | 2.17E-01 | 0.06 |
| | 250 | 187.91 | 1.29 | 2.29E-01 | 0.65 |
| | 300 | 184.81 | 1.27 | 2.00E-01 | 0.73 |
| | 350 | 189.64 | 3.91 | 8.94E-02 | 0.09 |
| | 400 | 182.94 | 3.62 | 5.22E-02 | 0.14 |
| | 500 | 186.85 | -2.71 | 3.31E-02 | 1.82 |
| | 550 | 183.60 | 0.82 | 2.72E-02 | 0.66 |
| | 560 | 181.84 | 2.44 | 1.30E-02 | 3.20 |
| | 575 | 197.69 | 9.95 | 2.51E-03 | 0.66 |
| | 590 | 196.11 | -9.41 | 2.20E-03 | 0.69 |
| | 600 | 206.07 | 16.97 | 2.48E-03 | 0.65 |
| MSL-16 | 0 | 242.33 | 41.21 | 1.59E-05 | 7.64 |
| | 250 | 246.35 | 37.35 | 2.28E-05 | 6.28 |
| | 300 | 244.82 | 32.92 | 2.19E-05 | 7.79 |
| | 350 | 248.36 | 31.87 | 1.93E-05 | 7.64 |
| | 400 | 246.35 | 29.05 | 1.53E-05 | 0.14 |
| | 500 | 254.67 | 25.06 | 1.14E-05 | 9.81 |
| | 550 | 247.19 | 17.16 | 1.02E-05 | 13.85 |
| | 560 | 255.20 | 12.25 | 9.20E-06 | 13.29 |
| | 575 | 211.08 | 36.75 | 2.59E-06 | 30.36 |
| | 590 | 254.04 | -55.41 | 3.10E-06 | 21.68 |
| | 600 | 189.34 | 43.87 | 4.34E-06 | 17.43 |

| SAMPLE | Temp | Dec. °N | Inc. °E | Intensity $A/m^2$ | Alpha95 |
|---|---|---|---|---|---|
| MSL-17 | 0 | 299.56 | -23.71 | 1.76E-06 | 21.48 |
| | 250 | 302.09 | -30.30 | 2.31E-06 | 31.66 |
| | 300 | 290.59 | -33.96 | 2.84E-06 | 28.10 |
| | 350 | 299.89 | -35.06 | 2.68E-06 | 30.13 |
| | 400 | 289.66 | -40.99 | 1.91E-06 | 9.92 |
| | 500 | 293.75 | -41.34 | 1.79E-06 | 36.89 |
| | 550 | 272.85 | -24.51 | 9.00E-07 | 55.66 |
| | 560 | 280.20 | -41.18 | 2.06E-06 | 37.86 |
| | 575 | 250.04 | -22.46 | 1.54E-06 | 46.29 |
| | 590 | 289.52 | -39.28 | 1.15E-06 | 45.63 |
| | 600 | 232.21 | 32.22 | 1.45E-06 | 39.39 |
| MSL-18 | 0 | 256.36 | -38.81 | 1.44E-05 | 4.69 |
| | 250 | 261.13 | -44.85 | 2.43E-05 | 3.89 |
| | 300 | 247.10 | -47.23 | 2.32E-05 | 4.69 |
| | 350 | 257.63 | -49.12 | 2.26E-05 | 4.18 |
| | 400 | 260.51 | -50.30 | 1.80E-05 | 35.87 |
| | 500 | 262.62 | -51.71 | 1.61E-05 | 5.09 |
| | 550 | 235.70 | -35.15 | 5.31E-06 | 14.25 |
| | 560 | 257.49 | -48.05 | 4.89E-06 | 16.11 |
| | 575 | 238.27 | -14.29 | 3.96E-06 | 20.77 |
| | 590 | 302.53 | -60.01 | 1.97E-06 | 29.19 |
| | 600 | 247.75 | 26.04 | 3.28E-06 | 21.32 |
| MSL-19 | 0 | 224.64 | 0.89 | 7.93E-06 | 12.1 |
| | 250 | 224.35 | -9.89 | 1.19E-05 | 10.25 |
| | 300 | 229.18 | -10.95 | 1.13E-05 | 10.51 |
| | 350 | 233.12 | -11.94 | 1.06E-05 | 11.32 |
| | 400 | 229.75 | -21.79 | 7.98E-06 | 4.82 |
| | 500 | 239.81 | -21.56 | 7.82E-06 | 11.43 |
| | 550 | 208.85 | 11.67 | 3.10E-06 | 25.15 |
| | 560 | 186.93 | -16.38 | 2.66E-06 | 30.89 |
| | 575 | 76.60 | 36.15 | 2.81E-06 | 27.00 |
| | 590 | 154.19 | -67.53 | 1.75E-06 | 33.05 |
| | 600 | 79.31 | 35.26 | 2.39E-06 | 26.96 |
| MSL-20 | 0 | 145.65 | 44.05 | 8.05E-02 | 0.99 |
| | 250 | 144.55 | 43.73 | 1.82E-01 | 0.69 |
| | 300 | 138.24 | 45.92 | 9.08E-02 | 0.09 |
| | 350 | 135.19 | 46.37 | 7.75E-02 | 0.09 |
| | 400 | 135.64 | 46.55 | 8.94E-02 | 11.65 |
| | 500 | 117.48 | 49.34 | 4.20E-02 | 0.13 |
| | 550 | 137.37 | 45.88 | 4.69E-02 | 1.27 |
| | 560 | 154.56 | 38.81 | 2.72E-02 | 0.18 |
| | 575 | 138.45 | 45.79 | 2.40E-02 | 0.18 |
| | 590 | 229.07 | -13.04 | 1.67E-04 | 1.28 |
| | 600 | 186.28 | 41.37 | 4.32E-04 | 0.98 |

| SAMPLE | Temp | Dec. °N | Inc. °E | Intensity $A/m^2$ | Alpha95 |
|---|---|---|---|---|---|
| MSL-21 | 0 | 158.28 | 25.13 | 1.32E-05 | 9.59 |
| | 250 | 146.32 | 23.81 | 1.78E-05 | 9.19 |
| | 300 | 148.72 | 22.71 | 1.69E-05 | 9.56 |
| | 350 | 145.67 | 17.74 | 1.27E-05 | 12.7 |
| | 400 | 148.88 | 14.18 | 1.01E-05 | 0.98 |
| | 500 | 161.55 | -5.78 | 5.55E-06 | 21.00 |
| | 550 | 126.29 | 50.19 | 1.47E-05 | 7.02 |
| | 560 | 131.98 | 33.42 | 9.91E-06 | 9.77 |
| | 575 | 258.81 | 66.91 | 6.47E-06 | 12.67 |
| | 590 | 230.86 | -56.98 | 7.33E-06 | 10.25 |
| | 600 | 212.00 | 44.62 | 7.95E-06 | 9.41 |
| MSL-22 | 0 | 36.68 | -14.80 | 1.00E-01 | 0.81 |
| | 250 | 44.57 | -11.88 | 2.14E-01 | 0.57 |
| | 300 | 39.95 | -11.69 | 1.03E-01 | 0.08 |
| | 350 | 39.00 | -10.55 | 8.26E-02 | 0.07 |
| | 400 | 42.71 | -11.32 | 9.18E-02 | 13.43 |
| | 500 | 42.37 | -10.30 | 4.72E-02 | 0.11 |
| | 550 | 43.55 | -10.41 | 4.09E-02 | 1.23 |
| | 560 | 40.65 | -11.50 | 2.28E-02 | 0.18 |
| | 575 | 49.17 | -12.04 | 1.43E-02 | 0.20 |
| | 590 | 43.64 | -12.48 | 1.13E-02 | 0.23 |
| | 600 | 327.40 | 54.14 | 4.69E-04 | 1.18 |
| MSL-23 | 0 | 183.47 | -12.73 | 5.89E-05 | 3.82 |
| | 250 | 181.28 | -15.13 | 5.12E-05 | 4.05 |
| | 300 | 182.31 | -13.50 | 5.03E-05 | 4.46 |
| | 350 | 178.87 | -14.59 | 4.37E-05 | 4.36 |
| | 400 | 181.27 | -16.15 | 3.52E-05 | 0.65 |
| | 500 | 179.24 | -16.16 | 2.73E-05 | 5.90 |
| | 550 | 181.52 | -8.47 | 2.18E-05 | 6.76 |
| | 560 | 184.23 | -18.76 | 2.56E-05 | 5.95 |
| | 575 | 289.57 | 35.92 | 5.78E-06 | 13.41 |
| | 590 | 304.08 | -73.11 | 8.44E-06 | 8.57 |
| | 600 | 315.07 | 45.64 | 8.34E-06 | 8.76 |
| MSL-24 | 0 | 45.80 | -4.63 | 5.13E-05 | 5.97 |
| | 250 | 49.01 | -3.72 | 4.34E-05 | 6.26 |
| | 300 | 45.96 | -6.38 | 3.97E-05 | 7.49 |
| | 350 | 50.51 | -1.50 | 3.66E-05 | 7.11 |
| | 400 | 52.39 | -0.82 | 2.61E-05 | 4.92 |
| | 500 | 50.38 | 5.69 | 2.12E-05 | 9.15 |
| | 550 | 48.91 | 17.19 | 1.49E-05 | 10.83 |
| | 560 | 42.62 | 9.22 | 1.20E-05 | 12.53 |
| | 575 | 323.73 | 47.10 | 6.09E-06 | 13.07 |
| | 590 | 257.80 | -62.77 | 8.75E-06 | 8.39 |
| | 600 | 304.68 | 62.01 | 8.62E-06 | 8.85 |

| SAMPLE | Temp | Dec. °N | Inc. °E | Intensity $A/m^2$ | Alpha95 |
|---|---|---|---|---|---|
| MSL-25 | 0 | 202.25 | 3.89 | 3.72E-02 | 1.61 |
| | 250 | 189.22 | 6.90 | 5.79E-02 | 1.24 |
| | 300 | 201.82 | 5.36 | 5.52E-02 | 1.42 |
| | 350 | 194.15 | 4.77 | 4.60E-02 | 1.44 |
| | 400 | 203.83 | 7.18 | 2.73E-02 | 8.40 |
| | 500 | 215.75 | 1.75 | 1.63E-02 | 1.05 |
| | 550 | 198.39 | 5.22 | 1.14E-02 | 1.01 |
| | 560 | 201.02 | 5.73 | 7.22E-03 | 0.41 |
| | 575 | 198.06 | 4.69 | 6.94E-03 | 0.40 |
| | 590 | 329.55 | -47.87 | 1.19E-04 | 1.89 |
| | 600 | 290.27 | 50.14 | 4.11E-04 | 0.76 |
| MSL-26 | 0 | 242.24 | -30.89 | 2.51E-03 | 0.65 |
| | 250 | 241.34 | -28.78 | 1.79E-03 | 0.68 |
| | 300 | 233.12 | -33.32 | 2.58E-03 | 0.82 |
| | 350 | 239.72 | -28.43 | 2.29E-03 | 0.71 |
| | 400 | 240.52 | -27.96 | 1.41E-03 | 0.77 |
| | 500 | 244.47 | -26.85 | 9.30E-04 | 1.09 |
| | 550 | 240.06 | -28.74 | 7.79E-04 | 1.16 |
| | 560 | 235.87 | -28.18 | 6.94E-04 | 1.27 |
| | 575 | 242.16 | -26.37 | 6.76E-04 | 1.26 |
| | 590 | 153.67 | -73.44 | 9.27E-06 | 8.54 |
| | 600 | 170.52 | 35.02 | 1.14E-05 | 6.75 |
| MSL-27 | 0 | 303.17 | -20.00 | 1.22E-02 | 2.70 |
| | 250 | 299.33 | -16.96 | 1.81E-02 | 1.68 |
| | 300 | 298.69 | -16.60 | 1.12E-02 | 0.18 |
| | 350 | 295.25 | -17.85 | 9.02E-03 | 0.20 |
| | 400 | 299.24 | -17.17 | 1.02E-03 | 0.86 |
| | 500 | 296.36 | -17.04 | 4.94E-03 | 0.34 |
| | 550 | 302.46 | -18.60 | 4.55E-03 | 1.15 |
| | 560 | 300.05 | -18.40 | 2.71E-03 | 0.48 |
| | 575 | 296.67 | -18.00 | 9.84E-04 | 0.82 |
| | 590 | 221.33 | 3.44 | 2.25E-05 | 7.00 |
| | 600 | 259.64 | 68.46 | 4.62E-05 | 4.71 |
| MSL-28 | 0 | 57.74 | -3.68 | 1.06E-02 | 1.97 |
| | 250 | 64.22 | -15.61 | 1.52E-02 | 2.44 |
| | 300 | 64.34 | -13.69 | 1.67E-02 | 0.49 |
| | 350 | 67.23 | -17.01 | 7.76E-03 | 0.26 |
| | 400 | 66.46 | -18.10 | 9.03E-03 | 0.62 |
| | 500 | 65.46 | -19.32 | 4.20E-03 | 0.37 |
| | 550 | 65.26 | -18.50 | 2.69E-03 | 0.42 |
| | 560 | 66.29 | -19.80 | 2.34E-03 | 0.48 |
| | 575 | 151.79 | 31.07 | 1.07E-04 | 1.94 |
| | 590 | 235.42 | -32.22 | 5.02E-05 | 3.75 |
| | 600 | 180.58 | 37.70 | 9.97E-05 | 2.34 |

| SAMPLE | Temp | Dec. °N | Inc. °E | Intensity $A/m^2$ | Alpha95 |
|---|---|---|---|---|---|
| MSL-29 | 0 | 78.31 | -2.19 | 6.58E-02 | 1.39 |
| | 250 | 82.65 | -11.70 | 9.44E-02 | 1.11 |
| | 300 | 80.05 | -11.44 | 1.01E-01 | 0.95 |
| | 350 | 79.69 | -13.87 | 8.01E-02 | 1.04 |
| | 400 | 87.66 | -12.91 | 5.68E-02 | 0.83 |
| | 500 | 81.16 | -12.86 | 2.58E-02 | 0.18 |
| | 550 | 79.60 | -11.77 | 2.27E-03 | 0.63 |
| | 560 | 51.99 | -2.86 | 1.32E-03 | 0.75 |
| | 575 | 104.33 | 44.66 | 3.49E-04 | 0.98 |
| | 590 | 224.24 | -12.68 | 1.57E-04 | 1.86 |
| | 600 | 140.51 | 25.42 | 1.83E-04 | 1.11 |
| MSL-30 | 0 | 119.88 | 21.10 | 1.19E-02 | 0.23 |
| | 250 | 120.79 | 19.09 | 5.79E-03 | 0.36 |
| | 300 | 118.88 | 17.36 | 8.40E-03 | 1.03 |
| | 350 | 115.00 | 15.74 | 6.95E-03 | 1.21 |
| | 400 | 115.87 | 13.77 | 4.39E-03 | 1.34 |
| | 500 | 115.17 | 10.17 | 2.76E-03 | 1.76 |
| | 550 | 112.46 | 12.93 | 1.45E-03 | 0.92 |
| | 560 | 95.60 | 3.30 | 9.06E-04 | 0.91 |
| | 575 | 119.55 | 6.73 | 9.73E-04 | 0.92 |
| | 590 | 105.23 | 11.12 | 4.39E-04 | 1.43 |
| | 600 | 174.35 | 55.82 | 1.38E-04 | 1.46 |
| MSL-31 | 0 | 170.39 | 4.90 | 1.84E-03 | 2.12 |
| | 250 | 174.70 | -0.47 | 2.43E-03 | 2.12 |
| | 300 | 88.42 | 21.75 | 2.50E-03 | 0.64 |
| | 350 | 191.39 | -4.29 | 1.86E-03 | 0.79 |
| | 400 | 171.53 | -0.92 | 1.46E-03 | 1.58 |
| | 500 | 172.12 | -2.53 | 9.03E-04 | 1.21 |
| | 550 | 189.30 | -4.84 | 4.59E-03 | 0.49 |
| | 560 | 163.65 | 0.99 | 2.96E-03 | 0.56 |
| | 575 | 82.87 | 57.45 | 2.31E-04 | 1.10 |
| | 590 | 117.40 | -50.19 | 4.65E-05 | 4.50 |
| | 600 | 200.51 | 42.16 | 1.33E-04 | 1.70 |
| MSL-32 | 0 | 37.94 | -36.93 | 2.61E-03 | 2.32 |
| | 250 | 45.83 | -36.88 | 3.12E-03 | 2.01 |
| | 300 | 25.30 | -53.15 | 2.09E-03 | 2.02 |
| | 350 | 41.31 | -36.28 | 2.50E-03 | 0.59 |
| | 400 | 53.09 | -35.96 | 1.73E-03 | 0.98 |
| | 500 | 51.56 | -34.24 | 1.08E-03 | 0.96 |
| | 550 | 52.83 | -34.19 | 5.83E-03 | 0.35 |
| | 560 | 46.67 | -35.75 | 4.72E-03 | 0.47 |
| | 575 | 5.07 | 18.45 | 4.02E-04 | 1.37 |
| | 590 | 74.72 | -65.37 | 1.59E-04 | 2.13 |
| | 600 | 29.33 | 45.62 | 3.62E-04 | 0.91 |

| SAMPLE | Temp | Dec. °N | Inc. °E | Intensity $A/m^2$ | Alpha95 |
|---|---|---|---|---|---|
| MSL-33 | 0 | 51.28 | 1.95 | 2.76E-02 | 0.15 |
| | 250 | 51.61 | 3.73 | 2.33E-02 | 1.74 |
| | 300 | 52.24 | 3.60 | 1.85E-02 | 1.92 |
| | 350 | 57.10 | 4.13 | 7.92E-03 | 0.31 |
| | 400 | 52.42 | 3.94 | 6.14E-03 | 0.72 |
| | 500 | 49.23 | 4.96 | 5.37E-03 | 1.23 |
| | 550 | 52.62 | 6.51 | 2.64E-03 | 0.49 |
| | 560 | 48.37 | 6.61 | 2.26E-03 | 0.62 |
| | 575 | 174.00 | 63.67 | 1.69E-04 | 1.04 |
| | 590 | 289.18 | -82.45 | 3.22E-05 | 8.92 |
| | 600 | 227.83 | 47.16 | 1.75E-04 | 1.07 |
| MSL-34 | 0 | 307.49 | -15.56 | 6.04E-02 | 0.14 |
| | 250 | 314.30 | -13.72 | 7.00E-02 | 1.35 |
| | 300 | 316.82 | -12.01 | 6.28E-02 | 1.32 |
| | 350 | 309.59 | -13.99 | 2.57E-02 | 0.24 |
| | 400 | 309.24 | -16.73 | 2.93E-02 | 0.35 |
| | 500 | 313.91 | -15.16 | 1.43E-02 | 0.28 |
| | 550 | 319.45 | -7.99 | 6.76E-03 | 0.41 |
| | 560 | 336.09 | -14.88 | 1.50E-03 | 0.88 |
| | 575 | 125.08 | 48.15 | 2.39E-04 | 1.18 |
| | 590 | 262.07 | -44.49 | 1.31E-04 | 1.54 |
| | 600 | 154.00 | 55.87 | 3.39E-04 | 0.94 |
| MSL-35 | 0 | 53.78 | -6.01 | 5.32E-02 | 0.10 |
| | 250 | 55.36 | -4.17 | 6.06E-02 | 1.04 |
| | 300 | 51.91 | -3.34 | 5.07E-02 | 1.16 |
| | 350 | 54.30 | -3.05 | 2.44E-02 | 0.16 |
| | 400 | 59.11 | -4.44 | 2.65E-02 | 0.74 |
| | 500 | 67.65 | -8.10 | 1.09E-02 | 0.35 |
| | 550 | 49.99 | -2.31 | 7.95E-03 | 0.29 |
| | 560 | 49.69 | -1.01 | 4.60E-03 | 0.89 |
| | 575 | 106.88 | 43.89 | 1.94E-04 | 1.30 |
| | 590 | 101.37 | 58.87 | 1.17E-04 | 1.73 |
| | 600 | 113.67 | 51.26 | 1.91E-04 | 0.97 |
| MSL-36 | 0 | 111.89 | -21.28 | 8.45E-02 | 0.09 |
| | 250 | 117.63 | -20.92 | 9.21E-02 | 0.88 |
| | 300 | 106.13 | -19.27 | 8.01E-02 | 1.17 |
| | 350 | 110.02 | -19.65 | 3.57E-02 | 0.16 |
| | 400 | 112.43 | -20.04 | 4.11E-02 | 0.57 |
| | 500 | 110.76 | -22.05 | 1.97E-02 | 0.21 |
| | 550 | 112.82 | -21.75 | 1.90E-03 | 0.71 |
| | 560 | 64.54 | -21.92 | 1.33E-03 | 0.42 |
| | 575 | 128.98 | 24.01 | 7.60E-04 | 0.59 |
| | 590 | 312.35 | -74.05 | 6.25E-05 | 3.33 |
| | 600 | 176.01 | 42.09 | 2.96E-04 | 1.01 |

| SAMPLE | Temp | Dec. °N | Inc. °E | Intensity $A/m^2$ | Alpha95 |
|---|---|---|---|---|---|
| MSL-37 | 0 | 69.02 | 28.18 | 5.66E-02 | 0.07 |
| | 250 | 71.68 | 26.98 | 6.65E-02 | 0.77 |
| | 300 | 76.16 | 26.97 | 5.53E-02 | 1.04 |
| | 350 | 75.52 | 27.14 | 2.44E-02 | 0.13 |
| | 400 | 71.78 | 26.57 | 2.96E-02 | 1.46 |
| | 500 | 71.89 | 25.92 | 1.43E-02 | 0.18 |
| | 550 | 68.12 | 25.95 | 1.01E-02 | 0.20 |
| | 560 | 69.54 | 26.45 | 8.53E-03 | 0.19 |
| | 575 | 72.09 | 25.66 | 7.02E-03 | 0.22 |
| | 590 | 22.38 | 36.08 | 2.11E-05 | 7.89 |
| | 600 | 158.04 | 50.04 | 9.46E-04 | 0.54 |
| MSL-38 | 0 | 355.00 | -15.23 | 1.73E-02 | 0.24 |
| | 250 | 349.36 | -12.51 | 1.74E-02 | 2.64 |
| | 300 | 346.64 | -10.32 | 1.50E-02 | 2.71 |
| | 350 | 354.12 | -12.24 | 1.01E-02 | 1.04 |
| | 400 | 359.46 | -15.35 | 5.04E-03 | 0.34 |
| | 500 | 335.77 | -9.55 | 4.53E-03 | 1.50 |
| | 550 | 350.20 | -15.09 | 2.13E-03 | 0.66 |
| | 560 | 335.03 | -26.39 | 2.41E-03 | 1.67 |
| | 575 | 353.44 | -18.56 | 2.90E-03 | 0.60 |
| | 590 | 341.16 | -6.43 | 5.27E-05 | 4.76 |
| | 600 | 140.70 | 42.61 | 7.07E-04 | 0.44 |
| MSL-39 | 0 | 36.74 | -10.73 | 8.22E-03 | 0.40 |
| | 250 | 33.59 | -7.08 | 9.02E-03 | 3.68 |
| | 300 | 38.98 | -7.58 | 7.16E-03 | 3.79 |
| | 350 | 30.42 | -4.77 | 5.57E-03 | 1.44 |
| | 400 | 35.35 | -6.40 | 2.49E-03 | 0.45 |
| | 500 | 48.47 | -8.34 | 2.05E-03 | 2.34 |
| | 550 | 36.97 | -5.43 | 1.17E-03 | 0.95 |
| | 560 | 30.72 | -3.05 | 1.82E-03 | 0.77 |
| | 575 | 46.95 | -5.79 | 1.56E-03 | 0.89 |
| | 590 | 350.09 | -1.80 | 2.06E-05 | 8.71 |
| | 600 | 137.47 | 52.08 | 9.87E-04 | 0.43 |
| MSL-40 | 0 | 332.09 | -31.08 | 5.84E-02 | 0.11 |
| | 250 | 353.02 | -27.21 | 5.75E-02 | 1.27 |
| | 300 | 335.82 | -27.96 | 4.55E-02 | 1.28 |
| | 350 | 340.64 | -28.54 | 1.94E-02 | 0.20 |
| | 400 | 344.71 | -28.29 | 2.23E-02 | 0.68 |
| | 500 | 339.35 | -27.57 | 1.05E-02 | 0.28 |
| | 550 | 331.55 | -30.00 | 6.20E-03 | 0.37 |
| | 560 | 336.84 | -29.46 | 5.23E-03 | 0.42 |
| | 575 | 315.93 | -23.45 | 1.38E-03 | 1.00 |
| | 590 | 119.88 | -9.88 | 4.30E-05 | 3.09 |
| | 600 | 313.30 | 28.00 | 9.88E-04 | 0.53 |

| SAMPLE | Temp | Dec. °N | Inc. °E | Intensity $A/m^2$ | Alpha95 |
|---|---|---|---|---|---|
| MSL-41 | 0 | 156.19 | -41.81 | 4.29E-02 | 0.19 |
| | 250 | 171.70 | -32.33 | 4.66E-02 | 1.75 |
| | 300 | 167.32 | -33.34 | 3.90E-02 | 1.89 |
| | 350 | 176.74 | -29.29 | 1.75E-02 | 0.27 |
| | 400 | 167.05 | -36.65 | 1.99E-02 | 0.61 |
| | 500 | 174.02 | -33.21 | 8.65E-03 | 0.40 |
| | 550 | 166.34 | -41.58 | 5.75E-03 | 0.55 |
| | 560 | 190.52 | -36.10 | 1.72E-03 | 0.93 |
| | 575 | 156.84 | -40.08 | 1.03E-03 | 1.32 |
| | 590 | 346.99 | -1.64 | 2.04E-05 | 8.07 |
| | 600 | 103.17 | 21.70 | 1.22E-03 | 0.56 |
| MSL-42 | 0 | 315.71 | -25.13 | 8.58E-02 | 0.11 |
| | 250 | 319.35 | -21.74 | 8.45E-02 | 1.08 |
| | 300 | 52.69 | -16.58 | 7.04E-02 | 1.24 |
| | 350 | 321.30 | -23.55 | 3.07E-02 | 0.19 |
| | 400 | 320.89 | -22.34 | 3.43E-02 | 0.86 |
| | 500 | 319.91 | -21.26 | 1.48E-02 | 0.25 |
| | 550 | 320.42 | -22.10 | 1.10E-02 | 0.31 |
| | 560 | 147.90 | 23.35 | 2.56E-04 | 1.81 |
| | 575 | 265.24 | -6.39 | 1.33E-04 | 3.00 |
| | 590 | 98.68 | -61.86 | 6.22E-05 | 2.90 |
| | 600 | 245.60 | 36.40 | 2.53E-04 | 0.82 |
| MSL-43 | 0 | 38.37 | -12.52 | 5.50E-02 | 0.13 |
| | 250 | 12.55 | -11.12 | 5.30E-02 | 1.26 |
| | 300 | 16.24 | -10.51 | 4.13E-02 | 1.63 |
| | 350 | 26.41 | -11.19 | 1.96E-02 | 0.24 |
| | 400 | 18.58 | -10.95 | 2.25E-02 | 0.56 |
| | 500 | 22.61 | -10.90 | 9.70E-03 | 0.32 |
| | 550 | 25.29 | -10.58 | 6.63E-03 | 0.41 |
| | 560 | 28.22 | -10.72 | 5.84E-03 | 0.44 |
| | 575 | 220.75 | 56.25 | 3.08E-04 | 1.04 |
| | 590 | 44.08 | -38.58 | 3.30E-05 | 4.68 |
| | 600 | 192.01 | 36.94 | 2.76E-04 | 1.10 |
| MSL-44 | 0 | 242.65 | -25.02 | 2.34E-04 | 1.13 |
| | 250 | 249.85 | -34.55 | 2.58E-04 | 3.66 |
| | 300 | 255.44 | -39.20 | 2.38E-04 | 1.23 |
| | 350 | 254.24 | -45.85 | 1.16E-04 | 2.22 |
| | 400 | 263.34 | -50.87 | 1.57E-04 | 0.69 |
| | 500 | 276.07 | -59.73 | 1.33E-04 | 1.93 |
| | 550 | 280.01 | -60.11 | 1.17E-04 | 2.02 |
| | 560 | 280.13 | -66.18 | 7.05E-05 | 3.09 |
| | 575 | 16.42 | -39.56 | 1.79E-05 | 8.57 |
| | 590 | 49.82 | -42.11 | 4.46E-06 | 9.71 |
| | 600 | 18.16 | 2.00 | 5.55E-06 | 9.52 |

| SAMPLE | Temp | Dec. °N | Inc. °E | Intensity $A/m^2$ | Alpha95 |
|---|---|---|---|---|---|
| MSL-45 | 0 | 326.36 | -31.46 | 1.88E-02 | 0.35 |
| | 250 | 328.43 | -33.23 | 1.80E-02 | 1.23 |
| | 300 | 315.04 | -34.93 | 1.36E-02 | 1.46 |
| | 350 | 324.33 | -36.49 | 6.11E-03 | 0.69 |
| | 400 | 309.33 | -36.86 | 4.70E-03 | 1.69 |
| | 500 | 317.06 | -33.23 | 3.02E-03 | 1.05 |
| | 550 | 314.32 | -36.19 | 2.03E-03 | 1.29 |
| | 560 | 302.15 | -34.85 | 1.70E-03 | 1.34 |
| | 575 | 308.52 | -30.76 | 2.39E-03 | 1.22 |
| | 590 | 80.66 | -75.44 | 1.11E-04 | 2.21 |
| | 600 | 130.51 | 24.86 | 1.19E-04 | 1.23 |
| MSL-46 | 0 | 243.07 | 1.53 | 1.92E-02 | 0.25 |
| | 250 | 241.82 | 0.22 | 2.00E-02 | 0.88 |
| | 300 | 242.29 | 0.85 | 1.58E-02 | 0.99 |
| | 350 | 251.38 | -2.68 | 6.49E-03 | 0.54 |
| | 400 | 244.88 | -1.32 | 5.75E-03 | 0.82 |
| | 500 | 235.34 | 0.74 | 4.63E-03 | 0.55 |
| | 550 | 247.72 | -1.46 | 2.73E-03 | 0.79 |
| | 560 | 238.39 | 1.01 | 2.83E-03 | 0.68 |
| | 575 | 267.19 | -9.92 | 3.15E-04 | 1.76 |
| | 590 | 194.05 | -5.29 | 2.05E-05 | 11.33 |
| | 600 | 291.27 | -10.90 | 6.20E-05 | 3.07 |
| MSL-47 | 0 | 312.05 | -10.30 | 1.88E-02 | 0.26 |
| | 250 | 326.48 | -5.61 | 2.36E-02 | 0.63 |
| | 300 | 326.67 | -5.76 | 1.96E-02 | 0.71 |
| | 350 | 330.10 | -5.49 | 9.17E-03 | 0.30 |
| | 400 | 320.33 | -7.30 | 6.48E-03 | 0.54 |
| | 500 | 324.32 | -6.77 | 4.57E-03 | 0.45 |
| | 550 | 322.70 | -8.58 | 3.52E-03 | 0.51 |
| | 560 | 325.03 | -8.71 | 3.45E-03 | 0.56 |
| | 575 | 199.17 | 44.99 | 1.20E-04 | 2.02 |
| | 590 | 342.48 | 24.68 | 6.56E-05 | 2.35 |
| | 600 | 230.22 | 40.18 | 1.33E-04 | 12.97 |
| MSL-48 | 0 | 357.41 | 11.44 | 3.40E-03 | 0.79 |
| | 250 | 357.85 | 9.42 | 3.93E-03 | 2.50 |
| | 300 | 357.15 | 9.58 | 3.04E-03 | 3.06 |
| | 350 | 356.38 | 7.53 | 1.25E-03 | 1.52 |
| | 400 | 358.98 | 6.16 | 9.18E-04 | 0.41 |
| | 500 | 353.53 | 3.48 | 6.67E-04 | 2.11 |
| | 550 | 354.61 | 1.34 | 4.61E-04 | 2.50 |
| | 560 | 356.84 | 0.86 | 7.61E-04 | 1.90 |
| | 575 | 340.77 | 14.86 | 7.12E-05 | 5.70 |
| | 590 | 30.98 | -42.33 | 2.61E-06 | 37.53 |
| | 600 | 255.87 | 43.94 | 1.74E-05 | 12.11 |

| SAMPLE | Temp | Dec. °N | Inc. °E | Intensity $A/m^2$ | Alpha95 |
|---|---|---|---|---|---|
| MSL-49 | 0 | 91.37 | -5.77 | 8.36E-03 | 0.28 |
| | 250 | 92.39 | -2.14 | 5.64E-03 | 1.18 |
| | 300 | 88.78 | 0.39 | 4.38E-03 | 1.31 |
| | 350 | 98.88 | 0.41 | 1.60E-03 | 0.69 |
| | 400 | 93.25 | 0.03 | 1.09E-03 | 1.80 |
| | 500 | 98.66 | 0.02 | 5.65E-04 | 1.08 |
| | 550 | 95.94 | -2.46 | 4.33E-04 | 1.24 |
| | 560 | 87.28 | 2.66 | 5.85E-04 | 1.18 |
| | 575 | 96.98 | 0.94 | 5.31E-04 | 1.19 |
| | 590 | 289.22 | 5.91 | 1.54E-05 | 7.44 |
| | 600 | 167.15 | 63.04 | 1.55E-04 | 35.52 |
| MSL-50 | 0 | 281.97 | 4.96 | 6.22E-03 | 0.59 |
| | 250 | 293.58 | 11.41 | 5.52E-03 | 2.12 |
| | 300 | 282.88 | 8.83 | 5.34E-03 | 2.33 |
| | 350 | 286.89 | 8.75 | 2.22E-03 | 1.04 |
| | 400 | 288.22 | 9.11 | 1.33E-03 | 0.83 |
| | 500 | 277.89 | 9.96 | 1.00E-03 | 1.68 |
| | 550 | 289.47 | 10.08 | 6.32E-04 | 2.05 |
| | 560 | 283.46 | 8.58 | 1.06E-03 | 1.61 |
| | 575 | 266.28 | 21.68 | 4.43E-04 | 2.80 |
| | 590 | 302.92 | 19.12 | 4.14E-04 | 7.55 |
| | 600 | 358.61 | 45.72 | 2.83E-04 | 32.77 |
| MSL-51 | 0 | 229.03 | 4.87 | 7.71E-04 | 0.94 |
| | 250 | 234.16 | 0.47 | 4.78E-04 | 4.87 |
| | 300 | 224.79 | 4.85 | 4.21E-04 | 1.21 |
| | 350 | 230.96 | 2.79 | 1.33E-04 | 2.60 |
| | 400 | 228.64 | 3.45 | 1.49E-04 | 1.37 |
| | 500 | 228.32 | 4.91 | 9.64E-05 | 2.77 |
| | 550 | 236.90 | 11.31 | 7.65E-05 | 3.19 |
| | 560 | 229.29 | 7.98 | 4.67E-05 | 4.65 |
| | 575 | 90.51 | 53.01 | 4.87E-06 | 25.77 |
| | 590 | 103.88 | 6.38 | 5.92E-06 | 14.58 |
| | 600 | 355.87 | 37.31 | 8.13E-05 | 14.67 |
| MSL-52 | 0 | 270.27 | 4.33 | 3.35E-04 | 2.49 |
| | 250 | 259.80 | 10.22 | 3.01E-04 | 4.40 |
| | 300 | 258.88 | 4.43 | 2.44E-04 | 1.50 |
| | 350 | 259.81 | 4.99 | 9.53E-05 | 2.36 |
| | 400 | 262.72 | 3.99 | 1.09E-04 | 2.41 |
| | 500 | 268.97 | 4.11 | 8.25E-05 | 2.69 |
| | 550 | 264.85 | 4.96 | 4.08E-05 | 3.71 |
| | 560 | 273.57 | 4.40 | 3.63E-05 | 4.27 |
| | 575 | 202.30 | 24.17 | 8.38E-06 | 10.84 |
| | 590 | 333.11 | -2.07 | 1.86E-06 | 25.96 |
| | 600 | 233.37 | 74.75 | 3.92E-06 | 1.44 |

| SAMPLE | Temp | Dec. °N | Inc. °E | Intensity $A/m^2$ | Alpha95 |
|---|---|---|---|---|---|
| MSL-53 | 0 | 34.80 | 2.45 | 3.60E-03 | 0.53 |
| | 250 | 43.93 | 11.30 | 2.91E-03 | 1.79 |
| | 300 | 38.19 | 5.53 | 2.27E-03 | 0.71 |
| | 350 | 41.43 | 11.51 | 7.24E-04 | 1.06 |
| | 400 | 43.04 | 11.77 | 7.28E-04 | 2.24 |
| | 500 | 42.14 | 12.08 | 4.88E-04 | 1.29 |
| | 550 | 43.07 | 10.11 | 2.67E-04 | 1.81 |
| | 560 | 40.18 | 10.65 | 2.95E-04 | 1.81 |
| | 575 | 335.48 | 78.09 | 1.48E-05 | 7.31 |
| | 590 | 11.95 | -23.95 | 7.27E-06 | 13.22 |
| | 600 | 264.11 | 38.98 | 7.96E-06 | 6.58 |
| MSL-54 | 0 | 241.24 | -33.16 | 7.03E-05 | 4.40 |
| | 250 | 237.93 | -38.77 | 6.79E-05 | 14.3 |
| | 300 | 243.71 | -31.74 | 5.35E-05 | 5.16 |
| | 350 | 255.61 | -30.23 | 2.48E-05 | 5.85 |
| | 400 | 241.69 | -35.02 | 2.55E-05 | 1.03 |
| | 500 | 253.18 | -28.20 | 1.58E-05 | 8.06 |
| | 550 | 254.91 | -27.23 | 1.00E-05 | 10.82 |
| | 560 | 295.27 | -55.63 | 3.89E-06 | 23.78 |
| | 575 | 131.28 | 55.20 | 1.54E-06 | 41.63 |
| | 590 | 40.26 | -30.30 | 1.48E-06 | 25.04 |
| | 600 | 37.64 | 14.71 | 9.60E-07 | 1.58 |
| MSL-55 | 0 | 312.60 | -83.03 | 4.83E-05 | 4.69 |
| | 250 | 320.42 | -81.27 | 5.00E-05 | 12.66 |
| | 300 | 292.71 | -75.47 | 4.18E-05 | 5.59 |
| | 350 | 324.91 | -77.20 | 1.86E-05 | 6.55 |
| | 400 | 335.05 | -71.90 | 2.09E-05 | 7.79 |
| | 500 | 6.62 | -61.45 | 1.37E-05 | 6.49 |
| | 550 | 15.77 | -52.26 | 8.95E-06 | 9.29 |
| | 560 | 30.72 | -42.93 | 6.13E-06 | 15.38 |
| | 575 | 30.53 | 17.62 | 2.07E-06 | 33.57 |
| | 590 | 19.85 | -32.79 | 1.58E-06 | 19.90 |
| | 600 | 34.02 | 19.15 | 9.60E-07 | 1.37 |
| MSL-56 | 0 | 209.63 | -22.74 | 7.76E-05 | 4.14 |
| | 250 | 211.37 | -33.35 | 9.96E-05 | 13.34 |
| | 300 | 213.83 | -26.68 | 9.07E-05 | 4.78 |
| | 350 | 214.45 | -31.20 | 4.37E-05 | 6.53 |
| | 400 | 216.63 | -31.60 | 5.63E-05 | 6.93 |
| | 500 | 217.70 | -32.51 | 4.12E-05 | 6.74 |
| | 550 | 217.74 | -32.05 | 1.83E-05 | 10.44 |
| | 560 | 229.68 | -50.83 | 7.38E-06 | 15.21 |
| | 575 | 254.15 | -45.47 | 5.15E-06 | 18.84 |
| | 590 | 260.55 | -69.08 | 1.53E-06 | 21.65 |
| | 600 | 49.12 | 62.46 | 2.15E-06 | 1.68 |

| SAMPLE | Temp | Dec. °N | Inc. °E | Intensity $A/m^2$ | Alpha95 |
|---|---|---|---|---|---|
| MSL-57 | 0 | 202.72 | 10.07 | 2.12E-04 | 2.65 |
| | 250 | 205.90 | 1.40 | 3.01E-04 | 7.79 |
| | 300 | 198.76 | 9.83 | 3.16E-04 | 1.99 |
| | 350 | 206.38 | 2.72 | 1.35E-04 | 3.39 |
| | 400 | 207.41 | -0.63 | 1.79E-04 | 5.85 |
| | 500 | 204.32 | -5.17 | 1.39E-04 | 3.29 |
| | 550 | 220.36 | 13.47 | 7.73E-06 | 13.6 |
| | 560 | 207.29 | -9.42 | 7.70E-06 | 13.94 |
| | 575 | 315.66 | 47.03 | 5.28E-06 | 15.10 |
| | 590 | 216.24 | -75.91 | 2.36E-06 | 12.23 |
| | 600 | 329.85 | 29.44 | 3.39E-06 | 10.47 |
| MSL-58 | 0 | 118.03 | 24.07 | 3.96E-02 | 0.18 |
| | 250 | 124.81 | 24.40 | 2.69E-02 | 0.20 |
| | 300 | 127.28 | 23.85 | 4.15E-02 | 1.61 |
| | 350 | 128.83 | 22.32 | 3.30E-02 | 0.57 |
| | 400 | 133.47 | 21.20 | 1.47E-02 | 3.02 |
| | 500 | 122.82 | 18.32 | 7.82E-03 | 0.47 |
| | 550 | 131.02 | 16.67 | 4.80E-03 | 0.50 |
| | 560 | 136.94 | 25.65 | 1.87E-03 | 0.95 |
| | 575 | 159.40 | 34.19 | 2.84E-04 | 2.92 |
| | 590 | 215.22 | -42.78 | 8.61E-05 | 2.38 |
| | 600 | 257.09 | 16.77 | 7.65E-05 | 2.72 |
| MSL-59 | 0 | 336.58 | 4.64 | 2.71E-02 | 0.20 |
| | 250 | 328.29 | 1.11 | 1.40E-02 | 3.07 |
| | 300 | 330.08 | 6.81 | 1.23E-02 | 3.32 |
| | 350 | 331.68 | 5.69 | 2.31E-02 | 0.69 |
| | 400 | 333.02 | 3.08 | 9.97E-03 | 0.25 |
| | 500 | 333.44 | 0.03 | 7.15E-03 | 0.41 |
| | 550 | 330.34 | -1.71 | 5.09E-03 | 0.49 |
| | 560 | 329.67 | 2.51 | 2.22E-03 | 0.79 |
| | 575 | 24.39 | 18.56 | 2.29E-04 | 1.38 |
| | 590 | 299.82 | -48.76 | 7.04E-05 | 2.56 |
| | 600 | 356.15 | -43.05 | 5.99E-05 | 2.48 |
| MSL-60 | 0 | 174.53 | 2.43 | 1.40E-02 | 0.22 |
| | 250 | 173.13 | -4.19 | 1.65E-02 | 0.67 |
| | 300 | 173.53 | -2.03 | 1.41E-02 | 0.70 |
| | 350 | 168.59 | -2.68 | 1.19E-02 | 0.74 |
| | 400 | 169.48 | -2.24 | 5.05E-03 | 0.33 |
| | 500 | 175.78 | -3.28 | 3.61E-03 | 0.44 |
| | 550 | 176.64 | -4.27 | 2.21E-03 | 0.56 |
| | 560 | 181.40 | -18.52 | 1.08E-03 | 0.81 |
| | 575 | 202.57 | 7.64 | 8.73E-05 | 2.50 |
| | 590 | 200.57 | -28.21 | 2.82E-05 | 5.01 |
| | 600 | 226.98 | -16.80 | 2.85E-05 | 4.86 |

| SAMPLE | Temp | Dec. °N | Inc. °E | Intensity $A/m^2$ | Alpha95 |
|---|---|---|---|---|---|
| MSL-61 | 0 | 60.33 | 15.63 | 1.00E-07 | 82.25 |
| | 250 | 80.71 | 28.67 | 1.30E-07 | 70.15 |
| | 300 | 61.76 | 13.07 | 1.80E-07 | 76.96 |
| | 350 | 115.21 | -10.29 | 1.20E-07 | 78.97 |
| | 400 | 57.43 | -45.46 | 7.00E-08 | 0.38 |
| | 500 | 334.03 | -64.94 | 1.40E-07 | 83.17 |
| | 550 | 335.15 | 18.98 | 1.60E-07 | 75.78 |
| | 560 | 36.69 | 44.94 | 2.00E-07 | 71.15 |
| | 575 | 294.05 | 34.31 | 3.30E-07 | 60.92 |
| | 590 | 259.12 | -85.98 | 2.90E-07 | 63.51 |
| | 600 | 359.99 | 21.00 | 5.60E-07 | 49.47 |

Dec = declination
Inc = Inclination